Elucidating secondary organic aerosol from diesel and gasoline vehicles through detailed characterization of organic carbon emissions

Drew R. Gentner[a], Gabriel Isaacman[b], David R. Worton[b,c], Arthur W. H. Chan[b], Timothy R. Dallmann[a], Laura Davis[a], Shang Liu[d], Douglas A. Day[d,1], Lynn M. Russell[d], Kevin R. Wilson[e], Robin Weber[b], Abhinav Guha[b], Robert A. Harley[a], and Allen H. Goldstein[a,b,2]

[a]Department of Civil and Environmental Engineering, University of California, Berkeley, CA 94720; [b]Department of Environmental Science, Policy and Management, University of California, Berkeley, CA 94720; [c]Aerosol Dynamics, Berkeley, CA 94710; [d]Scripps Institution of Oceanography, University of California at San Diego, La Jolla, CA 92093; and [e]Chemical Sciences Division, Lawrence Berkeley National Laboratory, Berkeley, CA 94720

Edited by Mark H. Thiemens, University of California at San Diego, La Jolla, CA, and approved September 19, 2012 (received for review July 22, 2012)

Emissions from gasoline and diesel vehicles are predominant anthropogenic sources of reactive gas-phase organic carbon and key precursors to secondary organic aerosol (SOA) in urban areas. Their relative importance for aerosol formation is a controversial issue with implications for air quality control policy and public health. We characterize the chemical composition, mass distribution, and organic aerosol formation potential of emissions from gasoline and diesel vehicles, and find diesel exhaust is seven times more efficient at forming aerosol than gasoline exhaust. However, both sources are important for air quality; depending on a region's fuel use, diesel is responsible for 65% to 90% of vehicular-derived SOA, with substantial contributions from aromatic and aliphatic hydrocarbons. Including these insights on source characterization and SOA formation will improve regional pollution control policies, fuel regulations, and methodologies for future measurement, laboratory, and modeling studies.

motor vehicle emission factors | photochemical oxidation | urban air quality | volatile organic compound emissions | petroleum fuel composition

Organic aerosol (OA) in the atmosphere is detrimental to human health and represents a highly uncertain forcing of climate change (1). The use of petroleum-derived fuels is an important source of reactive gas-phase organic carbon that provides key precursors to the formation of secondary OA (SOA) and tropospheric ozone (1). Controlling these emissions from gasoline and diesel vehicles is central to air quality mitigation policies in urban areas (2). Previous work has concluded that further research is necessary to elucidate all organic sources of SOA precursors (3, 4). Significant controversy exists over the contributions of precursors from gasoline and diesel vehicles, and the relative importance of each for SOA formation remains in question, in part because of insufficient chemical characterization of fuels and emissions, and the difficulty of ambient measurements of gas-phase compounds emitted from diesel sources (1, 4–8).

In the United States, diesel fuel accounts for 21% of on-road fuel use (by volume), with off-road sources increasing total use to 28% diesel. In California, the diesel share of on-road use ranges from approximately 10% in coastal cities to more than 30% in agricultural regions (*SI Appendix*, Table S1) (2, 9, 10). Noncombusted hydrocarbons from the fuels are emitted in the exhaust of gasoline and diesel engines, and also via evaporation from gasoline vehicles and service stations. These compounds in unburned gasoline and diesel fuel dominate vehicular emissions of reactive gas-phase carbon that have the potential to form SOA (11, 12). Previous work has shown nontailpipe emissions account for ~30% of gasoline-related emissions in urban regions, but limited work exists constraining the emissions and SOA formation potential of gas-phase organic carbon from gasoline and diesel sources (13). By using extensive fuel analyses and field data from two sites that include many compounds with no previous in situ measurements, we present the most comprehensive data to date on the chemical composition, mass distribution, emissions, and SOA formation potential of nontailpipe gasoline, gasoline exhaust, and diesel exhaust. We determine the relative importance of gasoline and diesel sources for SOA formation in, and downwind of, urban regions. We assess these results in the context of other studies during the past decade and discuss their significant implications for air pollution measurement, modeling, and control.

Results and Discussion

A total of 40 gasoline and 12 diesel fuel samples from California were collected (coincident with field data) and characterized by using several gas-chromatography methods, yielding comprehensive speciation of the "unresolved complex mixture" in diesel fuel. This was accomplished by using soft photoionization techniques, and provides unprecedented detail on the molecular identification and mass distribution of hydrocarbons in diesel fuel (14). Gasoline and diesel fuel, and thus their emissions of unburned hydrocarbons, can be classified by vapor pressure and span the volatile organic compound (VOC) range and the less volatile intermediate-volatility organic compound (IVOC) range (Fig. 1). Gasoline hydrocarbons fall mostly within the VOC range, with some aromatics extending into the IVOC range, whereas only 30% of diesel fuel hydrocarbons are in the VOC range. Diesel fuel is widely distributed across molecules containing 8 to 25 carbon atoms with a peak around 10 to 13 carbon atoms (Fig. 2*A*). This peak is a result of aromatics and cycloalkanes, as straight and branched alkanes are evenly distributed between 10 and 20 carbon atoms. Aromatic and aliphatic hydrocarbons make up 23% and 68% of diesel fuel, respectively. By comparison, gasoline contains ~30% aromatics, with the remainder of the nonethanol fraction dominated by straight and branched alkanes with less than 10 carbon atoms (Table 1 and Fig. 2*A*).

To examine contributions from each source to reactive gas-phase organic carbon in the ambient atmosphere and on-road emissions measured in a roadway tunnel, we used a chemical mass balance model with effective variance weighting on overconstrained

Author contributions: D.R.G. designed research; D.R.G., G.I., D.R.W., A.W.H.C., T.R.D., S.L., D.A.D., R.W., and A.G. performed research; D.R.G., G.I., A.W.H.C., L.M.R., K.R.W., R.A.H., and A.H.G. contributed new reagents/analytic tools; D.R.G., G.I., D.R.W., T.R.D., and L.D. analyzed data; and D.R.G. and G.I. wrote the paper.

The authors declare no conflict of interest.

This article is a PNAS Direct Submission.

[1]Present address: Cooperative Institute for Research in Environmental Studies, University of Colorado, Boulder, CO 80309.

[2]To whom correspondence should be addressed. E-mail: ahg@berkeley.edu.

This article contains supporting information online at www.pnas.org/lookup/suppl/doi:10.1073/pnas.1212272109/-/DCSupplemental.

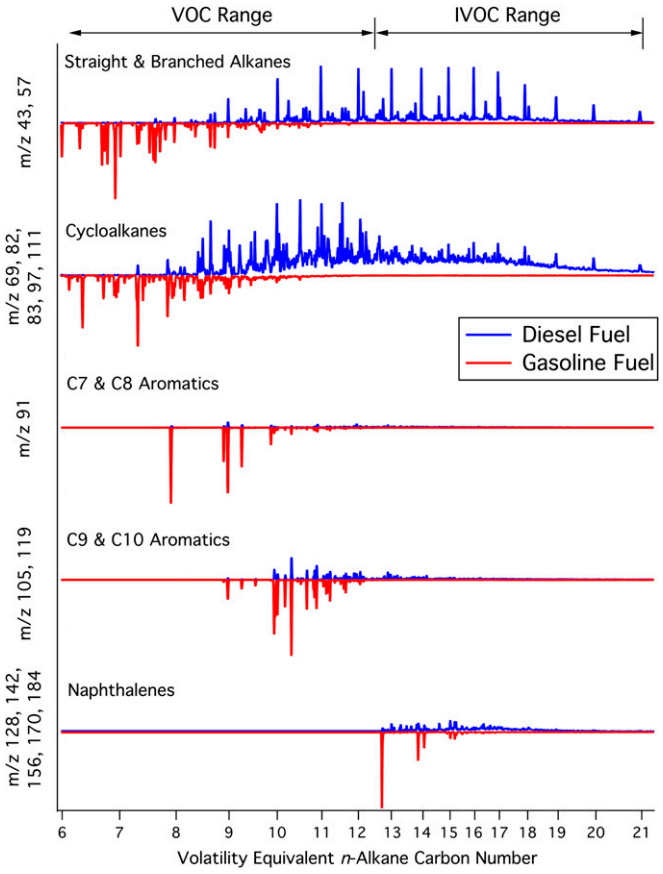

Fig. 1. Distributions of chemical classes for diesel (blue) and gasoline (red) are distinct with some overlap as shown via GC/MS for representative fuel samples. Fuels span both the VOC and IVOC volatility ranges. Chemical classes are represented by their dominant mass fragments and shown as a function of *n*-alkane carbon number.

least-squares regressions (*SI Appendix*) (15). The model uses a subset of measured compounds and capitalizes on differences in the chemical composition of sources to assess the magnitude of total noncombusted hydrocarbon emissions from each source. The source profiles used as a priori information are constructed from liquid fuel data to represent gasoline and diesel exhaust, and vapor-liquid equilibrium calculations to represent nontailpipe gasoline emissions. Equivalent chemical composition in exhaust and liquid fuel has been reported previously for gasoline and is demonstrated in this work for gasoline and diesel at both measurement sites (*SI Appendix*, Fig. S1) (16). Extensive diagnostics were used to assess model performance, including comparisons against independent compounds to confirm the model's ability to predict the behavior of reactive VOCs and IVOCs emitted by gasoline and diesel sources (*SI Appendix*, Figs. S2–S4).

Emission factors for noncombusted gas-phase organic carbon in exhaust were determined to be 0.38 ± 0.11 gC·L^{-1} for gasoline and 0.86 ± 0.25 gC·L^{-1} for diesel vehicles, which are consistent with values calculated by using California's emissions model for the same period (17). With respect to contributions of noncombusted hydrocarbons from gasoline and diesel exhaust, diesel accounted for 24% at the tunnel study in a coastal city, compared with 56% in the urban center of an agricultural region. Accounting for differences in emission factors and fuel densities, this is consistent with on-road fuel sales data in both regions—11% and 33% diesel fuel by volume, respectively (*SI Appendix*, Table S1) (10).

To assess the importance of gasoline and diesel sources for SOA in urban areas, we calculated bulk SOA yields for all three sources and compared them in context of our emission factors and source contributions. Data on SOA yields are limited for many of the hydrocarbons; the mass fraction of diesel, gasoline, and nontailpipe gasoline emissions that have unknown yields are 66%, 25%, and 7%, respectively. Thus, we modeled high-NO_x SOA yields by using published data (where available) and an estimation of yields and uncertainties for unknown values based on best estimates from various plausible scenarios (Fig. 2*B* and *SI Appendix*, Fig. S5).

For the same mass of unburned fuel emissions reacted, diesel exhaust forms 6.7 ± 2.9 times more SOA than gasoline exhaust (bulk SOA yields of 0.15 ± 0.05 and 0.023 ± 0.007 μgSOA·μg^{-1}, respectively). Considering differences in emission factors, diesel exhaust is expected to form 15 times more SOA than gasoline per liter of fuel burned. For populated regions with 10% to 30% diesel fuel use, this implies that diesel exhaust is responsible for two to seven times more SOA than gasoline exhaust (Fig. 3). Nontailpipe gasoline emissions were 39% to 77% lower than gasoline exhaust emissions and produce negligible SOA as a result of a substantially lower yield (0.0024 ± 0.0001).

Our methods also allowed us to examine the most important chemical classes and mass distribution of SOA formation. The vast majority of SOA from gasoline sources is a result of its aromatic content, whereas diesel SOA is predicted to be 47 ± 7% from aliphatics, with the remainder from aromatics (Fig. 2*B* and Table 1).

Regional estimates of daytime SOA concentrations from diesel and gasoline using our model results and calculated SOA yields are consistent with independent positive matrix factor analysis results for aromatic and aliphatic SOA from fossil fuel combustion in the San Joaquin Valley using aerosol MS (AMS) and Fourier transform IR spectroscopy (FTIR) measurements. Based on our model results, we expect an average of 1.3 ± 0.4 μgOA·m^{-3} from motor vehicles compared with average 1.0-μm particulate matter concentrations of 1.8 to 2.1 μg OA·m^{-3} from FTIR and AMS data, respectively (18). These independent data also support the predominance of diesel SOA in the San Joaquin Valley, as young aerosol (O:C ratios of 0.27–0.36) was 58% aliphatic and 42% aromatic (18).

SOA models have made considerable progress by using a parameterization known as the volatility basis set to estimate contributions from unmeasured intermediate and semivolatile compounds (5, 19). Together with traditional explicit models for individual hydrocarbons in the VOC range, models are better able to predict the magnitude of observed SOA, but not all temporal patterns or physical/chemical characteristics (3, 19, 20). Here we evaluate the inclusion of SOA precursors in these models and their distribution in gasoline and diesel exhaust. Aromatics with single or multiple rings have rightfully received considerable attention historically, but their distribution between gasoline and diesel emissions has been relatively unexplored. Gasoline exhaust dominates emissions of C_7 and C_8 aromatics. C_9 aromatic content is four times greater in gasoline than in diesel, and there are nearly equivalent amounts of C_{10} aromatics. For an urban region with 15% diesel fuel use, this implies that gasoline emits more than 90% of the C_9 aromatics and 75% of the C_{10} aromatics. Gasoline SOA from C_9 and C_{10} aromatics represent 26% and 14% of total SOA from gasoline, respectively, and $C_{9–11}$ aromatics represent 5% of SOA from diesel exhaust (Table 1). Emissions of naphthalene and similar small polycyclic aromatic hydrocarbons (PAHs) are shared by gasoline and diesel vehicles, but represent only a minor contribution to potential SOA formation as a result of their minor weight fractions in the fuels (Fig. 2 and *SI Appendix*, Tables S9 and S10).

We examined the compounds included in SOA models and found that 20% to 30% of the SOA formed from gasoline

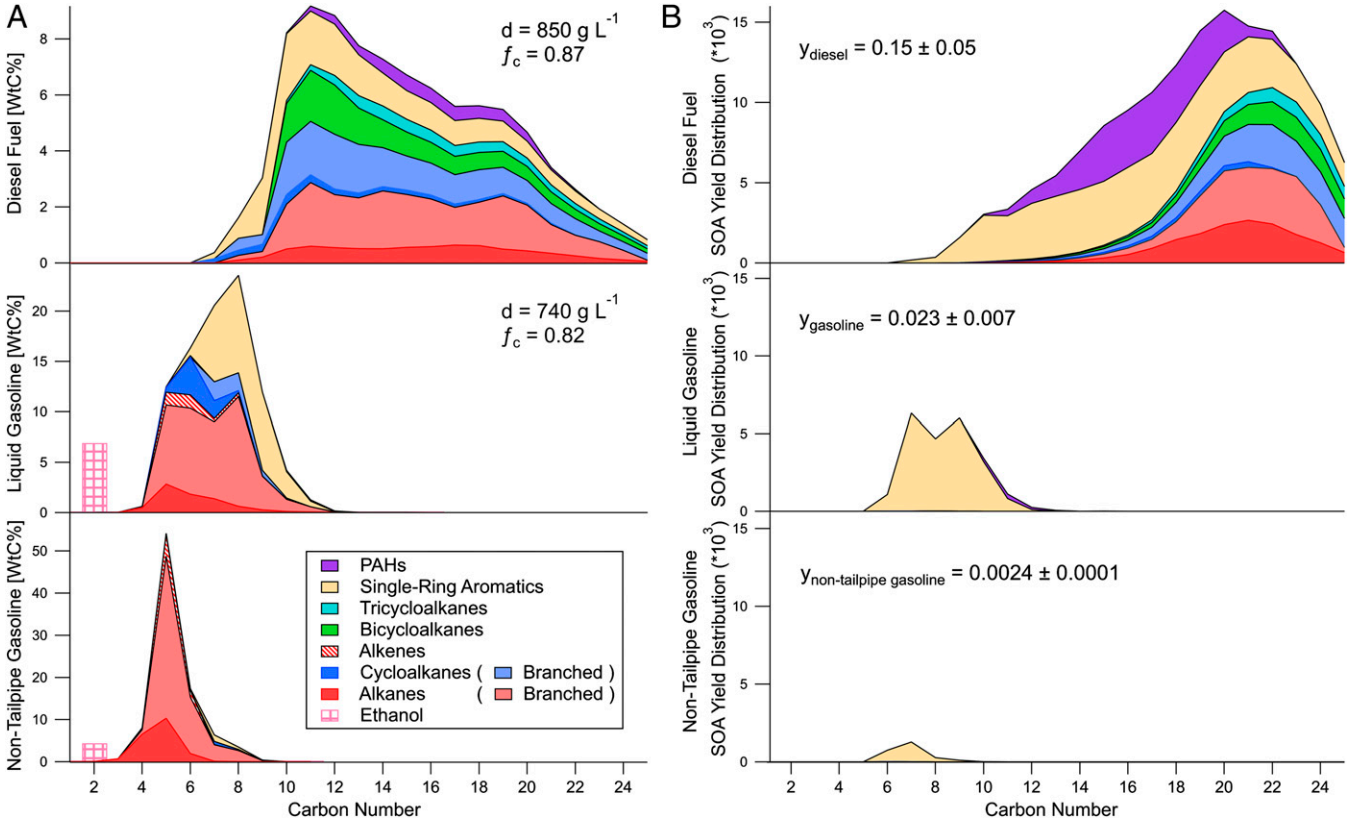

Fig. 2. Distribution of mass (*A*) and SOA formation potential (in μg SOA·μg^{-1}; *B*) in diesel and gasoline fuel (representative of exhaust) and nontailpipe gasoline emissions. Distributions in *A* and *B* are colored by chemical class. Fuel properties (density, carbon fraction) and bulk SOA yields (at an organic particle loading of 10 μg·m^{-3}) are superposed on *A* and *B*, respectively. Predicted SOA from gasoline exhaust is much lower than diesel and dominated solely by aromatic content, whereas diesel SOA is produced from a mix of aromatic and aliphatic compounds. A distribution of the SOA potential uncertainties is provided in *SI Appendix*, Fig. S5.

exhaust was not included in recent urban studies (21–23) (*SI Appendix*). Given the contributions of $C_{9–11}$ aromatics to SOA formation from gasoline and diesel vehicles, it is important that they are better represented in explicit traditional SOA models or the extension of volatility basis set modeling to include the 10^7 and 10^8 μg·m^{-3} effective saturation concentration (C°) bins that fall in the VOC range (*SI Appendix*, Fig. S6) (5, 19, 22). For recent urban studies, we scaled up traditional compound-explicit SOA models (without the volatility basis set) to include the missing 20% to 30% of gasoline SOA and contributions from diesel (assuming 15% diesel fuel use) and calculated a fivefold increase in modeled SOA from vehicular exhaust. Such an inclusion dramatically improves model closure, which has typically underestimated SOA in urban regions by 80% to 90% (19), but additional contributions from other sources of SOA precursors remain critical to model all observed SOA. Further chamber and modeling studies on SOA yields of aromatics with nine or more carbon atoms are important to reduce uncertainties in the SOA-forming potential of gasoline and diesel exhaust emissions and their overall contribution to SOA in urban regions. Additional

Table 1. Distribution of mass and SOA potential by chemical class for diesel exhaust, gasoline exhaust, and nontailpipe gasoline

	Weight by carbon, wtC%			Potential SOA formation, wt%		
Compound class	Diesel exhaust	Gasoline exhaust	Non-tailpipe gasoline	Diesel exhaust	Gasoline exhaust	Non-tailpipe gasoline
Total aliphatic	68 ± 8	58 ± 2	85 ± 4	47 ± 4	0.38 ± 0.07	0.9 ± 0.4
Straight-chain alkanes	7 ± 1	7.7 ± 0.3	20 ± 1	11 ± 2	0.09 ± 0.003	0.02 ± 0.001
Branched alkanes	23 ± 2	40 ± 1	60 ± 3	14 ± 2	0.12 ± 0.003	0.13 ± 0.01
Cycloalkanes (single straight alkyl chain)	2.5 ± 0.2	4.3 ± 0.1	1.03 ± 0.04	1.2 ± 0.3	0.13 ± 0.07	0.7 ± 0.4
Cycloalkanes [branched/multiple alkyl chain(s)]	18 ± 2	6.2 ± 0.3	5.0 ± 0.2	11 ± 2	0.04 ± 0.02	0.05 ± 0.03
Bicycloalkanes	13 ± 1	0	0	6 ± 1	0	0
Tricycloalkanes	4.8 ± 0.6	0	0	4 ± 1	0	0
Single-ring aromatics	19 ± 2	29 ± 1	2.7 ± 0.1	36 ± 9	96 ± 22	99 ± 6
Polycyclic aromatic compounds	4 ± 2	0.32 ± 0.02	0.0003	17 ± 8	3.2 ± 0.9	0.01 ± 0.01
Alkenes (straight, branched, cyclic)	0	3.6 ± 0.1	7.4 ± 0.3	0	0	0
Ethanol	0	6.9 ± 0.5	4.4 ± 0.4	0	0	0

The wt% by total mass for each source can be found in the *SI Appendix*, Table S2.

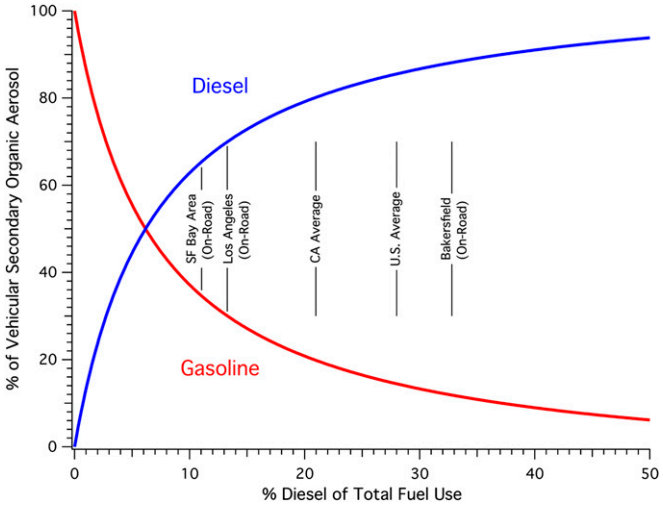

Fig. 3. The percent contribution of gasoline and diesel exhaust to SOA over 0% to 50% diesel fuel use demonstrates the predominance of diesel sources for SOA formation. SOA contributions form the two sources are equivalent at 6% diesel fuel use. The United States and California state averages shown are based on total on- and off-road use. The urban areas in California shown are for on-road fuel use only; off-road contributions will increase the diesel fraction of total use by several percent, but are not available at this scale.

studies on the SOA yields of cyclic alkanes with five- and six-membered rings are also of interest because they are unstudied and represent 37% of diesel and 11% of gasoline fuel.

In 1993, with the goal of mitigating emissions of particulates and nitrogen oxides, California regulated diesel fuel to have less than 10% single-ring aromatics and 1.4% polycyclic aromatic hydrocarbons, but concerns about engine performance and the cost of fuel production led the state to allow higher aromatic levels in diesel fuel (24) (*SI Appendix*). It is evident from our data (Table 1) that the vast majority of diesel fuels sold in California are certified alternative formulations that contain nearly double the aromatic content than initial regulations intended. Although the fuel regulations were designed to help control primary particulate emissions (i.e., black carbon), this enhancement of aromatic content in diesel fuel increases the SOA potential of diesel emissions, especially for hydrocarbons with 9 to 17 carbon atoms. Significant progress is being made to improve heavy-duty diesel engine performance with postcombustion control technology, which may affect emissions of gas-phase organic carbon, but it is clear that attention to gasoline and diesel fuel composition and emissions of reactive organic gases is necessary to control SOA precursor contributions from all vehicle classes. Furthermore, this work has focused on organic carbon emissions originating from fuels, but emissions of unburned motor oil from both gasoline and diesel vehicles represent an additional source of organic carbon. Although total consumption of oil is minor relative to fuel, oil contributes gas and particle-phase compounds with lower volatilities than diesel fuel and should continue to be monitored in field, laboratory, and modeling studies.

Comparing observed concentrations of OA to carbon monoxide has been insightfully used in numerous past studies to examine primary emissions of vehicular (and other anthropogenic) OA and track the formation of SOA in the atmosphere (6, 21, 25–30). ΔOA/ΔCO ratios, and slopes determined from the regression of these values, originate at smaller values following emission before any atmospheric processing. Over the course of 1 to 2 d, ratios change dynamically and increase with the formation of SOA and further atmospheric processing, as the lifetime of CO is relatively long compared with the other processes. A diverse range of ΔOA/ΔCO slopes has been observed across the studies in which this technique has been used (30). In the context of this method, we review data from numerous field campaigns with our observations and SOA yield modeling results to assess the behavior of vehicular OA and the contribution of nonvehicular SOA to total observed OA. We calculate predicted ΔOA/ΔCO ratios from oxidized gasoline and diesel emissions, and the combined effect of emissions from both these sources and photochemical processing in the atmosphere. We also evaluate differences in ΔOA/ΔCO ratios between the week and weekend, and assess the suitability of using solely ΔOA/ΔCO slopes to determine the contributions of gasoline and diesel sources to SOA.

By using derived SOA yields and emission factors for reactive gas-phase organic carbon and CO, we predict ΔOA/ΔCO ratios for a mixture of gasoline and diesel fuel use for comparison with our observations in the San Joaquin Valley (Bakersfield, CA) and other urban studies during the past decade (Fig. 4 and *SI Appendix*). Predicted ΔOA/ΔCO slopes for a range of typical fuel use are consistent with observed ΔOA/ΔCO values in Los Angeles, Tokyo, and Mexico City after initial SOA formation occurring in the first 6 h of processing (Fig. 4*B*) (6, 25, 26). We predict "young" ΔOA/ΔCO ratios well, but as air masses develop from a relatively young photochemical age of ~6 h to ~1 d, ΔOA/ΔCO ratios increase. A three- to fourfold increase was observed in Mexico City, and the effect of increased processing can also be observed in Tokyo, where ΔOA/ΔCO slopes for multiple seasons depict a clear seasonal trend, with the greatest slope occurring in the summer for processed air parcels, whereas less-processed parcels remain consistent with expected ratios for a mix of gasoline and diesel emissions (19, 25, 26).

In the San Joaquin Valley, the increase in ΔOA/ΔCO ratios appears to be coincident with the transition of young semivolatile aerosols to more aged aerosols with lower volatility as shown by the increase in O:C ratios that peaks with ΔOA/ΔCO ratios in the afternoon (Fig. 4) (3, 19, 26). Similarly, a greater fraction of low-volatility OA was observed in the summer in Tokyo (3). Aged ΔOA/ΔCO ratios exceed our predictions despite the consistency demonstrated earlier in this work between average daytime observed vehicular OA concentrations measured by AMS with predicted SOA from motor vehicles. This suggests that the comprehension of all OA transformation processes is incomplete and further work remains to understand the development of low-volatility OA observed in urban plumes globally, a conclusion supported by recent observations and consideration of other mechanisms (3, 20, 31, 32).

Examining differences between weekdays and weekends is another common and insightful metric for assessing emissions and chemical processes. We observed no weekday/weekend difference in the distribution of emissions between gasoline and diesel exhaust in Bakersfield, as daytime values of both decreased by ~40% over the weekend (*SI Appendix*, Fig. S7). However, weekend OA concentrations (total and vehicular) were greater as a result of increased photochemical aging evidenced by higher ΔOA/ΔCO ratios (Fig. 4*C* and *SI Appendix*, Fig. S8). Recent work focused on Los Angeles reported that gasoline is vastly more important than diesel as a source of SOA precursors based on the observation that weekend ΔOA/ΔCO slopes were marginally similar to weekday slopes, with similar photochemical ages despite large differences in diesel activity (6). Similar to Los Angeles, OA concentrations and ΔOA/ΔCO ratios are higher in Bakersfield over the weekend, but this occurs despite no change in the relative use of gasoline and diesel, suggesting that increased OA at both locations over the weekend is a function of decreased diesel NO_x emissions leading to faster photochemical processing, and is independent of changes in the mix of fuel use (33). The ubiquitous increase in ΔOA/ΔCO ratios with increased processing for vehicular and total OA is independent of the mixture of gasoline and diesel, and ΔOA/ΔCO slopes alone are insufficient to

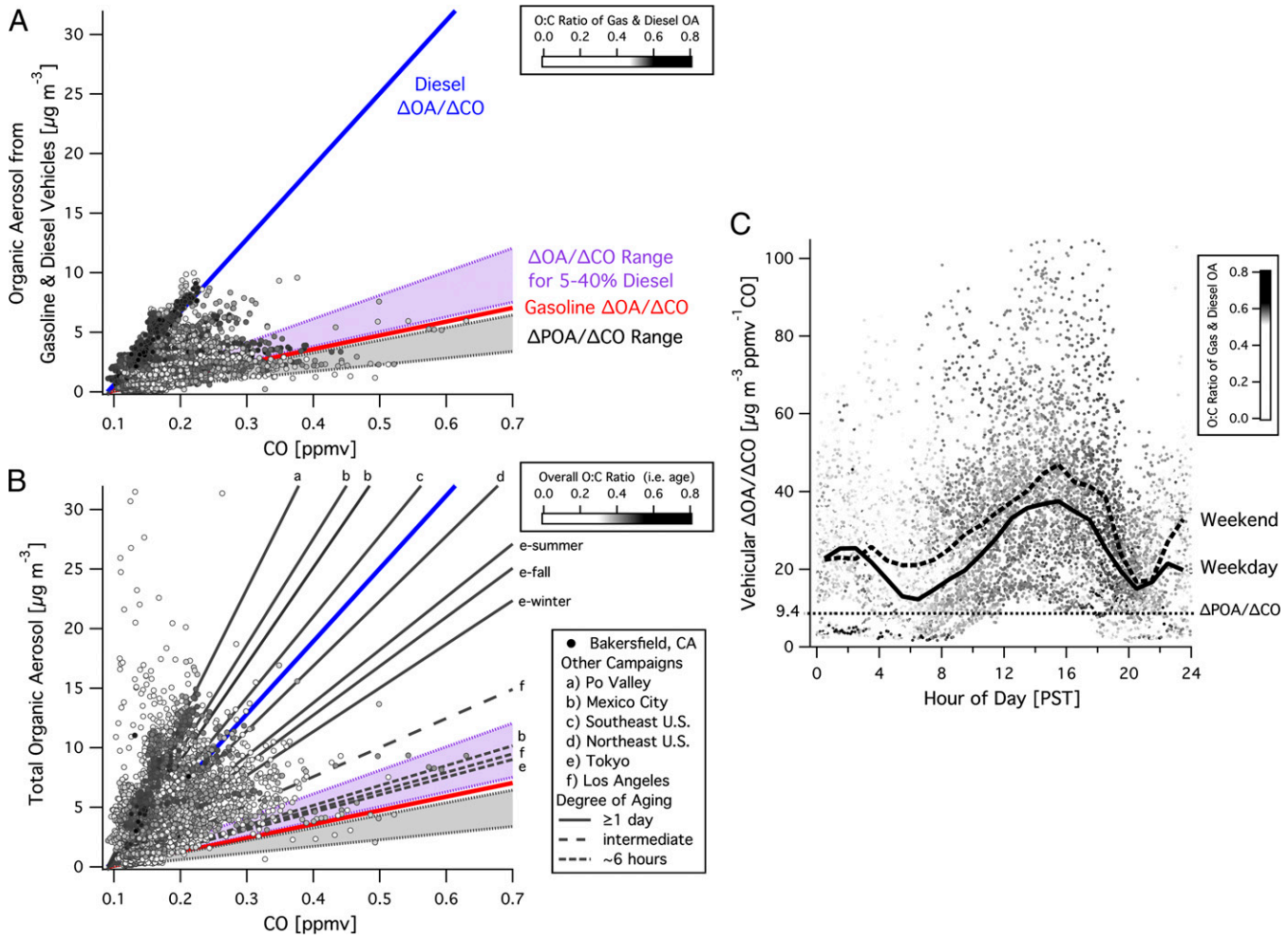

Fig. 4. Comparisons of OA vs. CO show the behavior of primary and secondary OA in the atmosphere and are used to examine vehicular OA and total OA in the San Joaquin Valley (Bakersfield, CA) and numerous other urban sites (6, 18, 21, 25–29). Photochemical aging increases ΔOA/ΔCO ratios and is represented by increased O:C ratios shaded in each panel. (*A*) Best estimates for ΔOA/ΔCO ratios expected for pure gasoline and diesel emissions are added to a ΔPOA/ΔCO value of 9.4 $\mu g \cdot m^{-3} \cdot ppmv^{-1}$ CO to account for primary OA and shown with a range of ΔPOA/ΔCO values (21, 30). Vehicular OA is determined from AMS factor analysis and observations are well constrained at Bakersfield with the exception of the most aged air parcels, whose ΔOA/ΔCO ratios are greater than expected for the mix of gasoline and diesel use. (*B*) Predicted ΔOA/ΔCO slopes for a range of fuel mixtures ranging from 5% to 40% diesel agree with observations of relatively young aerosol in urban areas and vehicular OA at Bakersfield. Observed ΔOA/ΔCO ratios increase with degree of aging and/or the influence of other SOA precursor sources that do not emit CO, which are prominent at Bakersfield and sites a–c. (*C*) Weekday and weekend diurnal averages of vehicular ΔOA/ΔCO show greater ratios in the afternoon and over the weekend as a result of increased photochemical aging. Ratios are calculated with a 90 ppbv CO background, and SDs are shown in *SI Appendix*, Fig. S8.

discern organic SOA precursor contributions from gasoline vs. diesel given the variability in Los Angeles measurements (*SI Appendix*, Fig. S9) (6).

Nonvehicular anthropogenic and biogenic sources also lead to elevated ΔOA/ΔCO ratios with higher slopes occurring in regions with large nonvehicular sources, such as Mexico City, the Southeast United States, and the Po Valley of Italy (Fig. 4*B*). ΔOA/ΔCO ratios in the San Joaquin Valley span a broad range of values observed at other sites and the importance of other SOA sources is supported by elevated ΔOA/ΔCO ratios in aged air masses and episodic contributions of low O:C OA from other sources (Fig. 4*B* and *SI Appendix*, S10) (6, 21, 25–29).

Our expanded measurement capabilities for gasoline and diesel compounds in the liquid fuels and the ambient atmosphere produce a more complete picture of SOA formation from motor vehicles. We provide the ability to predict emissions of SOA precursors and SOA formation that is consistent with fuel use data and ambient measurements. SOA from diesel sources outweighs gasoline contributions, and other sources provide significant precursors in many urban regions. The inclusion of our insights will allow for the development of more effective pollution control policies and inform the design of future studies in the ambient atmosphere, laboratory experiments, and modeling efforts.

Materials and Methods

In situ gas-phase organic carbon measurements were made by using an automated sampling system coupled to a gas chromatograph and mass spectrometer at the Caldecott Tunnel in Oakland, CA, and in Bakersfield, CA, as part of the California at the Nexus of Air Quality and Climate Change (CalNex) campaign. Offline analyses used gas chromatography and MS to analyze the composition of gasoline and diesel fuels. Estimates of bulk SOA yields for each source and SOA yields for precursors without established yields were calculated via a Monte Carlo analysis by using all appropriate laboratory and modeling data. OA in Bakersfield was measured in situ with AMS and offline via FTIR analysis of filter samples. *SI Appendix* provides further detail on the instrumentation, analytical methods, and results presented in this work.

ACKNOWLEDGMENTS. We thank Izadyar Dalvand, Kelsey Boulanger, Brian McDonald, Raymond Lo, and Trevor Ford, as well as staff of the California Air Resources Board, University of California Cooperative Extension (Kern County), and Caldecott Tunnel for their help on various aspects of the data collection and analysis. This work was supported by California Air Resources Board Grant 08-316, US Environmental Protection Agency (EPA) Grant RD834553, EPA Science To Achieve Results Grant FP-91781901-0, US Department of Energy Laboratory-Directed Research and Development Program of Lawrence Berkeley National Laboratory Grant DE-AC02-05CH11231, and National Oceanic and Atmospheric Administration Grant NA10OAR4310104.

1. Hallquist M, et al. (2009) The formation, properties and impact of secondary organic aerosol: Current and emerging issues. *Atmos Chem Phys* 9:5155–5236.
2. US Environmental Protection Agency (2008) *U.S. Clean Air Act*. (And subsequent amendments/rulings). Available at http://www.gpo.gov/fdsys/pkg/USCODE-2008-title42/pdf/USCODE-2008-title42-chap85.pdf.
3. Jimenez JL, et al. (2009) Evolution of organic aerosols in the atmosphere. *Science* 326 (5959):1525–1529.
4. Worton DR, Gentner DR, Isaacman G, Goldstein AH (2012) Embracing complexity: Deciphering origins and transformations of atmospheric organics through speciated measurements. *Environ Sci Technol* 46(10):5265–5266.
5. Robinson AL, et al. (2007) Rethinking organic aerosols: Semivolatile emissions and photochemical aging. *Science* 315(5816):1259–1262.
6. Bahreini R, et al. (2012) Gasoline emissions dominate over diesel in formation of secondary organic aerosol mass. *Geophys Res Lett* 39:L06805.
7. Weitkamp EA, Lambe AT, Donahue NM, Robinson AL (2008) Laboratory measurements of the heterogeneous oxidation of condensed-phase organic molecular makers for motor vehicle exhaust. *Environ Sci Technol* 42(21):7950–7956.
8. Pye HOT, Pouliot GA (2012) Modeling the role of alkanes, polycyclic aromatic hydrocarbons, and their oligomers in secondary organic aerosol formation. *Environ Sci Technol* 46(11):6041–6047.
9. US Energy Information Administration (2010) *Prime Supplier Sales Volumes*. Available at http://www.eia.gov/dnav/pet/pet_cons_prim_dcu_nus_a.htm. Accessed May 2012.
10. California Department of Transportation (2008) *California Motor Vehicle Stock Travel, and Fuel Forecast (MVSTAFF) 2008 Report*. Available at http://www.dot.ca.gov/hq/tsip/otfa/tab/documents/mvstaff/mvstaff08.pdf. Accessed April 2012.
11. Kirchstetter TW, Singer BC, Harley RA (1996) Impact of oxygenated gasoline use on california light-duty vehicle emissions. *Environ Sci Technol* 30:661–670.
12. Schauer JJ, Kleeman MJ, Cass GR, Simoneit BRT (1999) Measurement of emissions from air pollution sources. 2. C1 through C30 organic compounds from medium duty diesel trucks. *Environ Sci Technol* 33:1578–1587.
13. Gentner DR, Harley RA, Miller AM, Goldstein AH (2009) Diurnal and seasonal variability of gasoline-related volatile organic compound emissions in Riverside, California. *Environ Sci Technol* 43(12):4247–4252.
14. Isaacman G, et al. (2012) Improved resolution of hydrocarbon structures and constitutional isomers in complex mixtures using gas chromatography-vacuum ultraviolet-mass spectrometry. *Anal Chem* 84(5):2335–2342.
15. Watson JG, Cooper JA, Huntzicker JJ (1984) The effective variance weighting for least squares calculations applied to the mass balance receptor model. *Atmos Environ* 18: 1347–1355.
16. Leppard WR, et al. (1992) *Effects of Gasoline Composition on Vehicle Engine-Out and Tailpipe Hydrocarbon Emissions. Technical Paper Series no. 920329* (Society of Automotive Engineers, Warrendale, PA).
17. California Air Resources Board (2011) *Motor Vehicle Emission Factor/Emission Inventory Model - EMFAC* 2011. Available at http://www.arb.ca.gov/msei/msei.htm. Accessed April 2012.
18. Liu S, et al. (2012) Secondary organic aerosol formation from fossil fuel sources contribute majority of summertime organic mass at Bakersfield. *J Geophys Res*.
19. Hodzic A, et al. (2010) Modeling organic aerosols in a megacity: Potential contribution of semi-volatile and intermediate volatility primary organic compounds to secondary organic aerosol formation. *Atmos Chem Phys* 10:5491–5514.
20. Cappa CD, Wilson KR (2012) Multi-generation gas-phase oxidation, equilibrium partitioning, and the formation and evolution of secondary organic aerosol. *Atmos Chem Phys Discuss* 12:3295–3356.
21. de Gouw JA, et al. (2008) Sources of particulate matter in the northeastern United States: 1. Direct emissions and secondary formation of organic matter in urban plumes. *J Geophys Res* 113:D08301.
22. Dzepina K, et al. (2011) Modeling the multiday evolution and aging of secondary organic aerosol during MILAGRO 2006. *Environ Sci Technol* 45(8):3496–3503.
23. Johnson D, et al. (2006) Simulating regional scale secondary organic aerosol formation during the TORCH 2003 campaign in the southern UK. *Atmos Chem Phys* 6:403–418.
24. California Air Resources Board *California Diesel Fuel and Reformulated Gasoline Regulations*. [with subsequent amendments (2004, 2008) and certified alternative diesel formulations (1993)]. Available at http://www.arb.ca.gov/fuels/diesel/081404dslregs.pdf, http://www.arb.ca.gov/fuels/gasoline/082908CaRFG_regs.pdf, http://www.arb.ca.gov/fuels/diesel/diesel_alt.htm. Accessed April 2012.
25. Takegawa N, et al. (2006) Seasonal and diurnal variations of submicron organic aerosol in Tokyo observed using the Aerodyne aerosol mass spectrometer. *J Geophys Res* 111:D11206.
26. Kleinman KI, et al. (2008) The time evolution of aerosol composition over the Mexico City plateau. *Atmos Chem Phys* 8:1559–1575.
27. Weber RJ, et al. (2007) A study of secondary organic aerosol formation in the anthropogenic-influenced southeastern United States. *J Geophys Res* 112:D13302.
28. DeCarlo PF, et al. (2008) Fast airborne aerosol size and chemistry measurements above Mexico City and central Mexico during the MILAGRO Campaign. *Atmos Chem Phys* 8:4027–4048.
29. Crosier J, et al. (2007) Chemical composition of summertime aerosol in the Po Valley (Italy), northern Adriatic and Black Sea. *Q J R Meteorol Soc* 113:61–75.
30. de Gouw JA, Jimenez JL (2009) Organic aerosols in the Earth's atmosphere. *Environ Sci Technol* 43(20):7614–7618.
31. Ervens B, Turpin BJ, Weber RJ (2011) Secondary organic aerosol formation in cloud droplets and aqueous particles (aqSOA): A review of laboratory, field and model studies. *Atmos Chem Phys* 11:11069–11102.
32. Rollins AW, et al. (2012) Nighttime growth of particulate organic nitrates: A significant source of atmospheric secondary organic aerosols. *Science* 337(6099):1210–1212.
33. Russell AR, Valin LC, Bucsela EJ, Wenig MO, Cohen RC (2010) Space-based constraints on spatial and temporal patterns of NO(x) emissions in California, 2005-2008. *Environ Sci Technol* 44(9):3608–3615.

Supplementary Material for:

Elucidating secondary organic aerosol from diesel and gasoline vehicles through detailed characterization of organic carbon emissions

Drew R. Gentner[1], Gabriel Isaacman[2], David R. Worton[2,3], Arthur W.H. Chan[2], Timothy R. Dallmann[1], Laura Davis[1], Shang Liu[4], Douglas A. Day[4,5], Lynn M. Russell[4], Kevin R. Wilson[6], Robin Weber[2], Abhinav Guha[2], Robert A. Harley[1], and Allen H. Goldstein[1,2]*

[1] Department of Civil and Environmental Engineering, University of California, Berkeley, CA 94720, USA.
[2] Department of Environmental Science, Policy and Management, University of California, Berkeley, CA, 94720, USA.
[3] Aerosol Dynamics Inc., Berkeley, CA, 94710, USA.
[4] Scripps Institution of Oceanography, University of California, San Diego, La Jolla, CA, 92093, USA.
[5] now at: Cooperative Institute for Research in Environmental Studies, University of Colorado, Boulder, CO, 80309, USA.
[6] Chemical Sciences Division, Lawrence Berkeley National Laboratory, Berkeley, CA, 94720, USA.
* Corresponding author: ahg@berkeley.edu

Contents of supplementary material:

1. **Materials and methods**
2. **Supporting results**
3. **References**
4. **Supplementary figures S1-11**
5. **Supplementary tables S1-11**

1. Materials and methods

1.1 Site descriptions

Two sets of *in situ* VOC data are presented in this work: on-road measurements of motor vehicle exhaust sampled from the Caldecott tunnel in Oakland, CA and ambient measurements made in Bakersfield, CA at the CalNex (California Research at the Nexus of Air Quality and Climate Change) supersite.

Emissions from gasoline and diesel vehicles were measured as part of a field sampling campaign to characterize on-road mobile sources. Measurements were made July 13-29, 2010 at the Caldecott tunnel, on Highway 24 in Oakland, CA. The site has been used previously for on-road emission studies (*9*). The tunnel is 1 km in length and consists of three 2-lane traffic bores, which have a 4% grade. Sampling for the data presented here was taken in the uphill eastbound traffic bore with all vehicle types and traffic rates of approximately 2,000 light-duty vehicles and 30-140 medium and heavy-duty trucks per hour running on a mixture of gasoline and diesel fuel. Sample inlets were located in a ventilation aperture in the tunnel roof approximately 50 m prior to the tunnel exit and extended ~0.1 m into the tunnel traffic bore.

The CalNex supersite (35.3463° N, 118.9654° W) was located in southeast Bakersfield, a city in the southern San Joaquin Valley whose total metropolitan population is roughly 800,000.

The measurement site was typically downwind of the urban core and the nearby (<0.5 mile) intrastate highway 58 that is used by both gasoline and diesel vehicles, including substantial use for long-haul trucking routes both during the night and over the weekend. Sampling of gas-phase organics and supporting gas measurements took place May 18 - June 30, 2010 from the top of an 18 m tower.

1.2 *In situ* gas-phase organic carbon measurements

At both the tunnel and ambient measurement sites, chemical speciation of gas-phase organic carbon was achieved using a gas chromatograph (Hewlett Packard 5890 Series II) that was equipped with a quadrapole mass selective detector (Hewlett Packard 5971) and a flame ionization detector. The instrument was operated *in situ* with a custom system that automated the collection and analysis of samples. Ambient and on-road samples were collected for the first 30 minutes of every hour. At CalNex, the inlet was located at the top of the 18 m tower with the instrument located in a temperature-controlled trailer at ground level. To prevent line losses and accurately preserve compounds, ozone and particulate matter were removed at the inlet using 47 mm glass fiber filters (Pall, type A/E) that were coated in sodium thiosulfate according to the method vetted by Pollmann et al. (*1*). At the Caldecott tunnel, a longer inlet was used for multiple instruments that could not be operated in the ventilation duct. This 45 m shared inlet was constructed of aluminum and was 6" in diameter. Laminar flow was maintained with a volumetric flow rate of 200 L min^{-1}. For the VOC/IVOC measurements presented in this paper, a subsample was taken from the flow centerline, and particles were removed using the same filters used in the CalNex set-up. At both campaigns, filters were changed daily in the morning to reduce any potential artifacts. After ozone and particulate removal, the sample traveled at ~1 L min^{-1} down a 1/4" insulated Silcosteel line heated to >80°C to a preconcentration system, where two separate channels sampled off the main flow, each at ~20 mL min^{-1}. Ozone removal was confirmed by measuring the remainder of the main flow with a spectroscopic ozone analyzer (Dasibi model 1008-AH). During the tunnel study, minor losses of oxygenated and intermediate-volatility hydrocarbons occurred due to adsorption in the shared 6" inlet owing to its lack of passivation and heating. Due to this potential bias, these compounds were not used in the CMB modeling.

This instrument, similar to one used previously by Millet et al. (*2*), was equipped with two independent measurement channels sampling from the same inlet line. Channel 1 focused on a broad range of VOCs including those with lower volatilities (ranging from isopentane to tetradecane). Channel 2 measured more volatile, low-molecular weight compounds (e.g. propene – isopentane). At CalNex, prior to subsampling from the inlet line for the 2 channels, an internal standard (n-octane, 5.0 ppm) was constantly added to the sample flow at 2 mL/min, such that after the dynamic dilution its concentration was ~2 ppb. The internal standard was used to correct for any drift in the sensitivity of the mass selective detector and to assess overall instrument analytical stability. The entire main sampling line and all other elements of the sampling/preconcentration system that pertain to Channel 1 were constructed with passivated steel or other highly inert materials that were heated to constant temperatures at or above 90°C using resistive heaters. This was done to minimize losses of any VOC due to adsorption, absorption, or condensation, especially for compounds with lower volatility.

The Channel 2 sub-sample went through a custom-made water trap to remove water that could adsorb onto the channel 2 adsorbent trap. This was accomplished by passing the Channel 2

Teflon sample line through an aluminum block that was cooled to 0°C and routinely heated and purged between samples.

Ambient samples for both channels were concentrated on custom-made multilayer adsorbent traps using a system of three 12-port rotary valves (Valco, Valcon E) to automate sampling and injection. Adsorbent traps were constructed out of 1/8" Sulfinert steel tubing and contained the following sequences of adsorbent materials secured by glass wool at each end; Channel 1: 60 mg glass beads (Alltech, 60/80 mesh, DCMS-treated), 20 mg Tenax TA (Supelco, 60/80 mesh), 30 mg Carbopak B (Supelco, 60/80 mesh), and 40 mg Carbopak X (Supelco, 60/80 mesh); Channel 2: 60 mg glass beads, 30 mg Carbopak B, 40 mg Carbopak X, and 40 mg Carboxen 1000 (Supelco, 60/80 mesh). During sample collection adsorbent traps were thermoelectrically cooled to a constant 15°C and 5°C for channel 1 and 2, respectively. Following the preconcentration of ~1 L on each adsorbent trap, analytes were thermally desorbed at 320°C with a reverse flow of helium and injected directly onto their respective capillary columns where chromatographic separation was assisted by a ramped temperature program in the GC oven. The effluent from the traps was injected onto a DB-624 capillary column (60 m × 0.32 mm × 1.8 μm) and a HP-Plot-Q capillary column (30 m × 0.32 mm × 20.0 μm) for channel 1 and 2, respectively.

All flows were measured and controlled using mass-flow controllers (MKS Instruments), and system temperatures were monitored using T-type thermocouples (Thermo Scientific). All system data were recorded on a data-logging system (Campbell-Scientific).

The instrument was calibrated for more than 100 individual VOCs using a combination of standard gas mixtures and liquid standards. Three gas standard cylinders with ppm concentrations (Apel-Riemer, Scotty Gas) were dynamically diluted into a ~1 L min^{-1} flow of pure air supplied from a zero air generator (Aadco Inc.) to get pptv to ppbv-level concentrations. At CalNex, liquid standards were introduced into the system at the top of the tower to account for any losses in the sample lines or preconcentration system. Multi-point calibrations were run at the beginning and end of the measurement campaign, and daily single-point standards were run to verify the calibrations. Pure air from the zero air generator was also used to run daily blank runs to check for any artifacts or biases in the system. For identified compounds without standards, their response factors on the MSD were determined by multiplying the fraction of the quantifying ion in a representative mass spectrum by the total ion response factor calculated from known compounds of similar chemical classes. This method, while approximate, provides concentration data with a reasonable amount of uncertainty when standards are not available for relatively unstable hydrocarbons.

We quantified hourly concentrations for ~200 VOCs, including linear alkanes, branched alkanes, cyclic alkanes, alkenes, aromatics, Polycyclic Aromatic Hydrocarbons (PAHs), terpenoids, halogenated compounds, species containing sulfur, oxygenates, and alcohols. Detection limits for most compounds were at or near 1 pptv with accuracies determined by standards (±5%) and MKS flow controllers (±5%). Numerous compounds reported have limited or no prior *in situ* ambient measurements. This includes compounds in the intermediate-volatility range (IVOCs), such as the methylnaphthalenes and dimethylnaphthalenes. Some compounds are reported together as groups because it was infeasible to accurately separate them on the chromatographic column used while measuring such a wide range of compounds.

1.3 Supporting *in situ* measurements

An extensive suite of instrumentation was deployed to both field studies to characterize gas and particle species. In the Caldecott tunnel, Black Carbon (BC), carbon monoxide (CO), and carbon dioxide (CO_2) were measured at inlets co-located with gas-phase organic sampling. After passing through a 2.5 μm cyclone (URG Corporation, model 2000-30EN), BC was measured using an aethalometer (McGee Sci. model AE-16) and post-processed as described elsewhere (*3*). CO and CO_2 were measured via an infrared spectrometer (TECO Inc. Model 48) and non-dispersive infrared absorption (LI-COR, Lincoln, NE; model LI-820), respectively, with twice daily zero and calibration checks. Uncertainties are estimated to be ± 3 and 2%, respectively. Raw data were recorded at high-time resolution, but was averaged for this analysis to 30-min periods coincident with the VOC measurements.

At CalNex-Bakersfield, aerosol measurements were made using an Aerosol Mass Spectrometer (AMS) and Fourier Transform Infrared spectroscopy (FTIR) analysis of filters to assess $PM_{1.0}$ and $PM_{2.5}$ concentrations and composition; methods have been described elsewhere (*4*). Carbon monoxide was measured from the top of the tower using a gas filter correlation infrared spectrometer (Teledyne, API M300EU2). Comparisons of Organic Aerosol (OA) to CO were done at 5-min time resolution with a $PM_{1.0}$ cutpoint. Vehicular OA, as presented in the paper, was determined as the sum of the 4 vehicular aerosol factors from the positive matrix factorization analysis of the AMS data: low O:C alkane, low O:C aromatic, high O:C alkane, and high O:C aromatic (*4*).

1.4 Fuel characterization

Forty samples of regular and premium grade gasoline, and twelve samples of diesel fuel were collected from service stations during summer 2010 (coincident with the field studies) in 4 California locations (Bakersfield, Pasadena, Sacramento, and Berkeley). Gasoline samples were analyzed at Chevron laboratories (Richmond, CA) by gas chromatography with dual flame ionization detectors. Additional analyses were performed to resolve co-eluting peaks. Over 400 compounds were quantified in the fuel samples via this method. Compositional averages for the state and each location were calculated assuming a 80:20 regular to premium usage.

To characterize the full range of compounds in diesel fuel, samples were analyzed by 2 methods. Samples were analyzed via direct injection on a traditional 1-dimensional gas chromatograph (HP 5890 Series II) with a quadrapole mass selective detector (HP 5971) on a DB-624 column (60 m × 0.32 mm × 1.8 μm). Where available, liquid standards were used to calibrate traditionally-characterized components. Nine of the twelve diesel fuel samples were additionally run on a Rxi-5Sil MS column (60 m × 0.25 mm × 0.5 μm; Restek) coupled to a time-of-flight mass spectrometer (TOFMS; HTOF model, Tofwerk) with a custom modification to allow single-photon ionization. Effluent from the column was ionized using 10.5 eV vacuum-ultraviolet photons generated by synchrotron radiation at the Chemical Dynamics Beamline of the Advanced Light Source (ALS) at Lawrence Berkeley National Lab. Analysis of this data was performed following methods described previously (*5*), with improved quantification owing to the use of a more extensive suite of structurally-relevant standards.

Vapor-liquid equilibrium calculations were performed for each liquid gasoline sample to predict gasoline vapor composition, which were then averaged statewide and at each location using the same methodology as the liquid fuel. A detailed description of the non-ideal solution equilibrium calculations for gasoline has been published previously (*6, 7*). Uncertainties

presented with all fuel data in this work have been propagated to reflect all variability in fuel samples.

1.5 Comparison of fuels to ambient and tunnel measurements

In order to compare expected versus measured source profiles for gas-phase organics, we compare gasoline and diesel fuel to both tunnel and ambient VOC/IVOC measurements. Isooctane and *n*-dodecane are selected as tracers for gasoline and diesel exhaust, respectively. Isooctane represents a good tracer for gasoline exhaust since it is a trimethylpentane that is intentionally produced during the refining process and added to gasoline to comprise 3.6 ± 0.3 wt% of California gasoline (Summer 2010). Additionally, it will only be present as a minor component of evaporative gasoline emissions and diesel exhaust. *n*-dodecane represents a good tracer for diesel exhaust since it is prevalent in diesel fuel and will be emitted only as a non-combusted hydrocarbon, while it makes up only 0.01% of gasoline fuel and diesel emissions will greatly exceed any other minor urban VOC source of *n*-dodecane. From the fuels, expected ratios to tracers are derived by dividing the concentration (i.e. mol%) of a given compound by that of either isooctane or *n*-dodecane. For the tunnel and ambient data we performed linear regressions using a trust-region Levenberg-Marquardt least orthogonal distance method to account for uncertainties in both the compound measurements.

1.6 Chemical mass balance source receptor modeling and emission factor calculations

Previous work gives detailed descriptions of source receptor modeling and chemical mass balance methods (*6, 8*). For each hourly sample in the Caldecott tunnel (N=114) and at CalNex-Bakersfield (N=487), an over-constrained matrix system was constructed with 6 to 10 compounds to represent the source profiles of the 3 sources. For each site, several confirmation model runs with different sets of compounds were used in the model to assess sensitivity of results. A summary of compounds used for modeling can be found in Tables S3-4. All compounds used in the model have authentic standards.

The gas-phase organic carbon data have numerous VOCs and IVOCs that act as source tracers either independently or in tandem with other compounds. With regards to gasoline and diesel emissions, emissions of most observed tracer compounds had not undergone significant photochemistry that could bias the model over the timescales observed between emission and measurement at either field site. This is evidenced by roughly identical ratios for gasoline-related compounds in the ambient measurements compared to liquid gasoline collected in Bakersfield during the campaign (Fig. S1). If considerable aging with the ability to bias our model had occurred, these comparisons would be poor for compounds that have differences in OH reaction constants. Chemical losses were only really a concern at the Bakersfield site since the on-road emissions study was in close proximity to the source. At Bakersfield, evidence of chemical losses in the fresh emissions can occasionally be seen in comparisons of model results to independent compounds that are highly reactive, which is only an issue with the most reactive compounds that are not used in modeling for that reason. This lack of observable photochemical processing of the primary emissions used in the model allows us to effectively assess emissions from gasoline and diesel sources. Additionally, any minor biases that could be introduced due to chemical losses are minimized by selecting compounds for the model that have relatively similar reaction rates with OH and negligible reaction rates with ozone.

The source profiles used as inputs in the model were derived from the compound-specific fuel profiles presented in this work, with liquid fuels representing exhaust profiles and vapor-

liquid equilibrium calculations determining the non-tailpipe profile. Previous work has shown compositional consistency for non-combusted gas-phase organics in liquid gasoline and gasoline exhaust (*10*). In addition to confirming this finding for gasoline, we also demonstrate compositional consistency for diesel fuel and exhaust (Fig. S1).

For Bakersfield, a fourth source representing fugitive light hydrocarbon ($C_{1\text{-}7}$) emissions from petroleum extraction and refining was necessary to properly model non-tailpipe gasoline emissions; data for this source came from U.S. geological surveys. Additionally, given the low volatility of hydrocarbons in diesel fuel, evaporative contributions of diesel fuel are expected to be negligible compared to exhaust emissions. Using IGOR Pro 6.22, a least-squares solution was determined for each over-constrained system to determine each hourly source contribution in ppbC using effective variance weighting methods described by Watson *et al.* and used by the U.S. EPA in their CMBv8.2 modeling platform (*8, 11*). To assess model performance, we calculated normalized biases and root mean squared errors for each compound used in the model and each independent compound. We also calculated the reduced chi-squared test and model R-squared for each hourly sample; results can be seen in Fig. S4. We verified the predictive capability of all compounds to independent compounds to confirm the ability of the model to predict the behavior of reactive VOCs and IVOCs that are emitted by both gasoline and diesel at both measurement sites. For brevity's sake a selection of these compounds are shown in Figs. S2-3. Minor inconsistencies observed in a few of the panels are due to a combination of oxidation losses during the most photochemically-active periods of the day, other non-vehicular sources, and, in the case of IVOCs in the tunnel study, adsorptive losses on walls of the shared inlet.

Emission factors for non-combusted gas-phase organic carbon (expressed as GPOC in equations) were calculated using the modeling results and supporting in-situ measurements from the Caldecott tunnel study. The gasoline emission factor was determined using methods similar to previous studies (*9*). First, by taking the average of hourly emission factors, calculated as the source contribution ($SC_{t,gasoline}$) over total carbon ($\Delta Total\ C_t$) during the weekend when diesel traffic and thus contributions to total carbon were negligible. The source contribution is the concentration of non-combusted gas-phase organic carbon from gasoline and the total carbon is used to determine the total amount of fuel burned by adjusting for fuel density and carbon content (Eqn. S1). Uncertainty is determined from the standard deviation of the emission factor.

$$EF_{GPOC,gasoline\ exhaust} = \frac{1}{N}\sum_{t=0}^{N}\left[\frac{SC_{t,gasoline}}{\Delta Total\ C_t}\right] f_{c,gasoline} d_{gasoline} \quad \text{(S1)}$$

$$\Delta Total\ C_t = [CO_2]_{t,tunnel} + [CO]_{t,tunnel} - [CO_2]_{t,ambient} - [CO]_{t,ambient} \quad \text{(S2)}$$

$$where:$$

$$SC_{t,gasoline}\ [=]\ \text{gC GPOC m}^{-3}\ (@25°C)$$

$$\Delta Total\ C_t\ and\ concentrations\ [=]\ \text{kgC m}^{-3}$$

$$N : number\ of\ samples$$

$$f_{c,gasoline} : carbon\ fraction\ of\ gasoline\ [=]\ \text{kgC kg}^{-1}$$

$$d_{gasoline} : liquid\ density\ of\ gasoline\ [=]\ \text{kg L}^{-1}\ (@25°C)$$

$$Assumption: SC_{t,gasoline,tunnel} \gg SC_{t,gasoline,ambient}$$

The results of this method were compared to a regression method where the slope of the source contribution vs. total carbon is used to calculate the emission factor and the uncertainty is determined from the standard deviation of the slope. This is similar to the previous method except that the slope of the regression is used in place of the average and provides a slightly different estimation of uncertainty.

$$EF_{GPOC,gasoline\ exhaust} = \left[\frac{SC_{t,gasoline}}{Total\ C_t}\right]_{slope} f_{c,gasoline} d_{gasoline} \quad \text{(S3)}$$

The diesel emission factor is calculated similarly, but since the total carbon signal is dominated by gasoline in the tunnel, Black Carbon (BC) is used in its place since BC is largely from diesel. To correct for BC contributions from gasoline, BC measurements are adjusted to isolate the diesel signature using the gasoline source contribution and emission factors for non-combusted gas-phase organic carbon and BC from gasoline derived in this work and elsewhere (*3*). The slope of the diesel gas-phase organic carbon concentration to BC is then multiplied by the diesel BC emission factor and the diesel fuel density to get the diesel emission factor in gC GPOC m^{-3}. Data from weekdays and weekends are used in the regression.

$$EF_{GPOC,diesel\ exhaust} = \left[\frac{SC_{t,diesel}}{BC_{t,diesel}}\right]_{slope} EF_{BC,diesel\ exhaust} d_{diesel} \quad \text{(S4)}$$

$$BC_{t,diesel} = BC_{t,observed} - \frac{SC_{t,gasoline} EF_{BC,gasoline\ exhaust}}{EF_{GPOC,gasoline\ exhaust}} \quad \text{(S5)}$$

where:

$EF_{BC,gasoline} = 0.020 \pm 0.003\ gBC\ kg^{-1}$ (Caldecott Tunnel Study)

$EF_{BC,diesel} = 0.54 \pm 0.07\ gBC\ kg^{-1}$ (Dallmann et al. (*3*))

Emission factors are compared to those from the California emission factor model (EMFAC2011); determined from statewide summer 2010 data for running emissions and weighted for all vehicle models using vehicle miles traveled (VMT) (*12*). The resulting emission factor is in gC GPOC L^{-1} and must be multiplied by ~0.73 to compare to the derived emission factors for non-combusted gas-phase organic carbon as 27% of reactive organic gas (ROG) emissions from gasoline are products of incomplete combustion (*9*). The exact ratio of products of incomplete combustion to total ROG emissions will vary depending on fuel type, oxygenate level and driving conditions. The value presented here is intended to check consistency with outside measurements and is not used in any of our calculations.

$$EF_{GPOC,gasoline} = \frac{\frac{\sum\left[EF_{ROG,vehicle\ type} VMT_{vehicle\ type}\right]}{\sum\left[VMT_{vehicle\ type}\right]} f_{c,gasoline} d_{gasoline}}{\frac{\sum\left[\left(EF_{CO,vehicle\ type}\frac{MW_C}{MW_{CO}} + EF_{CO2,vehicle\ type}\frac{MW_C}{MW_{CO2}}\right) VMT_{vehicle\ type}\right]}{\sum\left[VMT_{vehicle\ type}\right]}} \quad \text{(S6)}$$

$$EF_{CO,gasoline} = \frac{\frac{\sum\left[EF_{CO,vehicle\ type} VMT_{vehicle\ type}\right]}{\sum\left[VMT_{vehicle\ type}\right]} f_{c,gasoline} d_{gasoline}}{\frac{\sum\left[\left(EF_{CO,vehicle\ type}\frac{MW_C}{MW_{CO}} + EF_{CO2,vehicle\ type}\frac{MW_C}{MW_{CO2}}\right) VMT_{vehicle\ type}\right]}{\sum\left[VMT_{vehicle\ type}\right]}} \quad \text{(S7)}$$

Calculations to determine diesel emission factors for gas-phase organic carbon and CO are the same as for gasoline while using the diesel fuel properties.

1.7 Secondary organic aerosol yield determination methodology and associated calculations

To determine overall SOA yields for each source and the distribution of SOA formation from each source across molecular sizes and chemical classes, we first determined the distribution of mass in each source's emissions and organized it into 25 x 8 matrices ($W_{ij,source}$). The rows of the matrix represent carbon number (i) and the columns, chemical class (j) as shown in Tables S5-7. With the objective of determining average high-NO_x yields for the subset of isomers in each point in this matrix, we determined which values were well-known in the literature from chamber or modeling data, and which had insufficient data.

For all compounds, high-NO_x SOA yields for known and estimated compounds are calculated or modeled assuming an average organic particle concentration of 10 μg m^{-3}. This organic particle loading was used as a value relevant to chamber studies, urban areas, and downwind urban areas (*13-14*). As the organic loading decreases the yields of IVOCs will also decrease slightly due to changes in partitioning of the reaction products. While the effect of partitioning due to particle loading is relatively well parameterized for some studied hydrocarbons, the effect on other compounds characterized in the fuels is less constrained. If the organic particle loading is decreased from 10 to 5 μg m^{-3} under high-NO_x conditions, the SOA yields of straight and branched alkanes will decrease by an average of 30% in the range of 16-22 carbon atoms, and C_{6-8} aromatics will decrease by ~25%. Thus, significant changes in the relative contributions of gasoline and diesel sources are not expected under high-NO_x conditions, but future work remains using our framework to constrain the sensitivity of the bulk SOA yields and the partitioning of oxidation products from compounds without established yields.

Straight and branched alkanes were considered to have known yields. Yields for *n*-alkanes were calculated using the model reported by Jordan *et al.* (*15*) and the product yields provided therein. The volatilities of those reaction products are assumed to decrease by a multiplicative factor of 0.35 per carbon number (*16*). Yields for branched alkanes were calculated using the same model assuming an average 30% alkoxy radical decomposition (*17*), yielding a product with the volatility of a ketone with 3/4 of the original carbon atoms. For all compounds, volatility was calculated using SIMPOL as described by Pankow *et al.* (*18*). We assumed branched aliphatic compounds have volatilities similar to an *n*-alkane with similar gas chromatographic retention times, which is a reasonable proxy for volatility within a compound class (*19, 20*). Modeled SOA yields for straight-chain and branched alkanes are shown in Table S8.

Estimates for SOA yields of other compound classes (straight-chain cycloalkanes (e.g. decylcyclohexane), branched cycloalkanes, bicycloalkanes, tricycloalkanes, aromatics, and PAHs) were estimated via a Monte Carlo analysis (discussed below) by combining various scenarios constrained by literature and model data. All unknown compounds are treated as branched. For all compound classes, one possible scenario posits an SOA yield of the *n*-alkane of a similar volatility, similar to the use of a volatility basis set model using *n*-alkanes as surrogate

compounds, such as the analysis of Mexico City aerosol performed by Lee-Taylor *et al.* (*21*). Similarly, branched alkanes can be expected to be a reasonable surrogate for all branched aliphatic compounds, providing an alternate scenario. Furthermore, several additional schemes are available for estimating yields of cyclic aliphatic compounds based on the small amount of laboratory data available on cyclic alkanes (*17*). Most of these scenarios provide similar estimated SOA yields.

Small aromatic compounds are somewhat better constrained by laboratory data, though data for larger aromatics and PAHs are scarce. Small aromatics (C_6 through C_8) are assumed to be known and have the yields of benzene, toluene, and *m*-xylene found in the literature (*22, 23*). C_9 and larger aromatics can be estimated using extrapolations of the two-product models of toluene and *m*-xylene, assuming the products decrease in volatility using the carbon number multiplicative factor described above. These models provide conservative estimates as the yield for even the largest aromatics does not exceed 0.17 using these models. The literature model for naphthalene (*13*) provides yields closer to those expected based on volatility, so is used as an estimate for aromatics and PAHs. Alternate PAH scenarios assume C_{10} - C_{12} PAHs to have SOA yields of naphthalene, methylnaphthalene, and dimethylnaphthalene, based on literature values (*13*). Yields for larger PAHs are based on the extrapolation of these models. Extrapolations of models provide conservative upper and lower bounds for the least volatile aromatic compounds: 0.10 to 1.28 for C_{19}-C_{25} aromatics, 0.31 to 1.28 for C_{19}-C_{25} PAHs.

The Monte Carlo estimation does not give preference to any of the scenarios. For clarity, we provide a summary of the scenarios used to model unknown yields. Scenarios 3-6 for the cycloalkanes and scenarios 3-4 for the multi-ring cycloalkanes are based on laboratory data for three measured cyclohexanes (*17*).

Cycloalkanes:

1) Yields of *n*-alkanes of similar volatility (*15*)
2) Yields of branched alkanes of similar volatility
3) Yields of branched alkanes with 2 more carbon atoms
4) Yields of branched alkanes with 1 less carbon atom
5) $C_{5\text{-}10}$ have yields of branched alkanes with 2 more carbon atoms, while C_{16} and larger have yields with 1 less carbon atom. Yields for $C_{11\text{-}15}$ are interpolated
6) Yields extrapolated from C_6 (branched alkane with 2 more carbon atoms) and C_{16} (branched alkane with 1 less carbon atom)

Bicycloalkanes & Tricycloalkanes:

1) Yields of *n*-alkanes of similar volatility (*15*)
2) Yields of branched alkanes of similar volatility
3) $C_{5\text{-}10}$ have yields of branched alkanes with 2 more carbon atoms, while C_{16} and larger have yields with 1 less carbon atom. Yields for $C_{11\text{-}15}$ are interpolated
4) Yields extrapolated from C_6 (branched alkane with 2 more carbon atoms) and C_{16} (branched alkane with 1 less carbon atom)

Aromatics (C_9 and larger):

1) Yields of *n*-alkanes of similar volatility (*15*)
2) Yields extrapolated from toluene two-product model (*22*)
3) All yields are 0.10 based on Chan *et al.* (*13*)
4) Yields extrapolated from naphthalene two-product model (*13*)

PAHs:

1) Yields of *n*-alkanes of similar volatility (*15*)
2) Yields extrapolated from naphthalene two-product model (*13*)
3) Yields for C_{12} and larger extrapolated from methylnaphthalene two-product model with $C_{10\text{-}11}$ having known yields (*13*)
4) Yields for C_{12} and larger assumed to be that of dimethylnaphthalene with $C_{10\text{-}11}$ having known yields (*13*)

We performed a Monte Carlo analysis to determine both bulk yields for each source and the distribution of those yields in each source to determine the most important compounds for SOA formation. If the yield for a given carbon number and chemical class point in the matrix was well-known, then the known yield did not change and no uncertainty is reported (Table S8). For unknown or understudied yields, for each iteration we randomly selected a scenario (*k*) from the constructed scenarios and added up to ±10% Gaussian-distributed noise (represented as $Y_{estimate,ijk}$*$gnoise(0.1)$ in Equation S8). Each iteration of known and randomly selected unknown yield values (Y'_{ij}) is multiplied by the known and constant weight percent matrix from each source ($W_{ij,source}$). The average of 10,000 iterations provides the distribution of SOA formation across each source ($Y_{ij,source}$) weighted by the chemical composition of the source. Uncertainties for all points in the matrices ($\sigma_{Yij,source}$) are determined by assessing the deviation of values across the 10,000 simulations (M=10000).

$$Y'_{ij} = \begin{cases} Y_{known,ij}, & if\ known\ value\ exists \\ Y_{estimate,ijk} + Y_{estimate,ijk} * gnoise(0.1), & if\ no\ known\ value\ exists \end{cases} \quad \text{(S8)}$$

$$where\ k\ is\ selected\ by\ a\ random\ number\ generator$$

$$Y_{ij,source} = \frac{1}{M}\sum^{M}\left[W_{ij,source} * Y'_{ij}\right]\frac{1}{100} \quad \text{(S9)}$$

$$\sigma_{ij,Y_{source}} = \sqrt{\frac{1}{M}\left(\sum^{M}\left[Y^2_{ij,source}\right] - M\bar{Y}^2_{ij,source}\right)} \quad \text{(S10)}$$

The bulk SOA yield for a source (y_{source}) is calculated by summing the distribution of SOA yields from the entire matrix to provide a value that can be multiplied by total non-combusted organic carbon from a source to determine the predicted SOA. The uncertainty of the bulk yield value ($\sigma_{y,source}$) is determined by assessing the deviation of all values in the simulations and is shown in Fig. S5.

$$y_{source} = \sum_i \sum_j Y_{ij,source} \quad \text{(S11)}$$

$$\sigma_{y_{source}} = \sum_i \sum_j \sqrt{\frac{1}{M}\left(\sum^{M}[y^2_{source}] - M\bar{y}^2_{source}\right)} \quad \text{(S12)}$$

Uncertainties presented in Table 1 and throughout the analyses have been propagated to reflect all uncertainties associated with the calculation and comparison of values.

The estimation of expected total SOA from gasoline and diesel presented in the paper (1.3 ± 0.4 μgOA m^{-3}) for comparison to AMS data was calculated by taking the daytime (8:00-19:30 PST) average of source contributions from gasoline and diesel (13.5 ± 9.3 and 9.8 ± 7.1

ppbC, respectively (N=270)) and determining the predicted SOA from both using the derived bulk SOA yields. Our CMB modeling method allows us to assess emissions from gasoline and diesel sources within several hours of transport to the site, and compare them to SOA production from a slightly larger scale of regional emissions and photochemistry as measured by the AMS. While, this does not act as a direct comparison since the observed SOA by the AMS is somewhat decoupled from the fresh emissions used to calculate the expected SOA, it does provide supporting evidence for the consistency of our calculations with observations. There were no significant multi-day OA events with accumulation of precursors or aerosol since concentrations decreased substantially on a daily basis due to meteorology. Dry-deposition of $PM_{1.0}$ OA would not have been a significant loss process, nor would coagulation of particles given particle number concentrations.

In the paper we examine the inclusion of SOA formation from gasoline in several traditional SOA modeling studies (MILAGRO, TORCH, NEAQS) and find that 20% of the SOA from gasoline is missing in the compound explicit models used at the TORCH and NEAQS campaigns, and 30% at the MILAGRO/MCMA studies (*24-26*). This was determined using the published list of compounds included in their models with our average liquid gasoline profile and determined SOA yields shown in Tables S6 and S8.

1.8 Calculation of ΔOA/ΔCO slopes

For the purposes of comparison to a broad set of urban studies, we estimate ΔOA/ΔCO slopes using derived bulk SOA yields and emission factors for non-combusted gas-phase organic carbon and CO:

$$\left[\frac{\Delta OA}{\Delta CO}\right]_{Predicted} = \left[\frac{\Delta POA}{\Delta CO}\right] + \frac{y_{gasoline} EF_{GPOC,gasoline} V_{gasoline} + y_{diesel} EF_{GPOC,diesel} V_{diesel}}{EF_{CO,gasoline} V_{gasoline} + EF_{CO,diesel} V_{diesel}} \quad \text{(S13)}$$

where $V_{gasoline}$ and V_{diesel} are the fraction of gasoline and diesel sold by volume and:

$$V_{gasoline} + V_{diesel} = 1 \quad \text{(S14)}$$

The emission factors for non-combusted gas-phase organic carbon and CO were:

$EF_{VOC,gasoline} = 0.45\ gGPOC\ L^{-1}$ (from this work, consistent with EMFAC2011 (*12*))

$EF_{VOC,diesel} = 1.01\ gGPOC\ L^{-1}$ (from this work, consistent with EMFAC2011 (*12*))

$EF_{CO,gasoline} = 12750\ ppmv\ L^{-1}$ (from EMFAC2011 (*12*))

$EF_{CO,diesel} = 3890\ ppmv\ L^{-1}$ (from EMFAC2011 (*12*))

The [ΔPOA/ΔCO] constant is the average observed slope reported previously (9.4 μg m^{-3} $ppmv^{-1}$ CO) and is similar for most urban studies (*24, 27*).

Additional derivations of the OA/ΔCO equation that include non-tailpipe gasoline VOC emissions with no associated CO emissions have a negligible effect on predicted ΔOA/ΔCO values. Similarly, including cold start emissions, which has a slightly different ΔOA/ΔCO ratio than the running emission factors used (i.e. more CO in cold start emissions), does not have a

substantial effect on the predicted ratio. Therefore, the simplified version (Equation S13) was used to calculate ΔOA/ΔCO ratios.

2. Supporting results

2.1 Characterization of gasoline and diesel fuel

We present the most comprehensive chemical speciation of diesel fuel to date with over 90% mass closure as part of an overall assessment of gasoline and diesel fuel. In this work, we supply unprecedented detail on both the overall mass and chemical distribution of both fuels and in-depth compound specific speciation data for use in future analyses and models such as those presented in this work. Composition data for hundreds of individual hydrocarbons in both fuels are shown in Tables S9-11 with average values for the state of California and site-specific data for the 4 regions from which fuel was collected. Ten gasoline samples and three diesel samples were analyzed for each location and standard deviations represent the variability between fuel samples. Gasoline, with 10 wt% ethanol additive, had an average density of 740 ± 7 g L^{-1}, and a carbon fraction of 0.824. Diesel fuel had an average density of 852 ± 10 g L^{-1} and a carbon fraction of 0.866. Gasoline composition was relatively homogeneous across the state in terms of mass distribution and percentages of chemical classes with minor differences in concentrations of individual compounds. Diesel fuel showed some heterogeneity with a few samples being slightly shifted in mass distribution. Overall, the composition was similar, but not as homogeneous as gasoline likely due to differences in regulations between gasoline and diesel fuel. The standard deviations in Tables 1 and S2 reflect this variability. Future work with the supplied data must recognize that both regional and seasonal differences in fuel can significantly affect the ratios of specific compounds and caution should be taken when extrapolating detailed data outside of the timeframe and locations presented here.

The volatility basis set defines VOCs as compounds with saturation concentrations (C°) > 10^6 μg m^{-3}, IVOCs as $C^\circ = 10^3$-10^6 μg m^{-3}, and a third class Semi-Volatile Organic Compounds (SVOCs) as C° = 1–100 μg m^{-3} (*28*). A small fraction (~5%) of diesel fuel extends into the SVOC range (Fig. S6). For the purposes of comparison to *a priori* information used in SOA models to represent diesel POA, IVOCs, and SVOCs, we present the composition of diesel fuel in terms of the volatility basis set used in many SOA models (Fig. S6) (*25-26, 28-29*).

Following the U.S. Clean Air Act of 1990, gasoline composition was reformulated numerous times over the following 2 decades. Currently, California reformulated gasoline, similar to U.S. reformulated gasoline, is regulated to contain less than 25% aromatics and 6% alkenes (by volume) largely due to their ozone formation potential (*30*). Across our 4 locations we measured a range of 24-29 wt% aromatics and 2-5 wt% olefins. During the summer, vapor pressure is also regulated to reduce non-tailpipe evaporative emissions. All of California is required to use reformulated gasoline and most U.S. regions that fail to meet air quality standards are required to use U.S. reformulated gasoline. Across the whole U.S., about a third of the gasoline sold is reformulated (*31*). Conventional gasoline, compared to reformulated gasoline can contain greater amounts of aromatics and olefins, which are likely to increase its reactivity and SOA formation potential (*32*).

Diesel fuel has been regulated nationally for sulfur content, but only in California has the organic composition been regulated. Starting in 1993, diesel fuels distributed in California have been regulated to contain less than 10% aromatics by volume and 1.4% PAHs by weight (*30*). A provision contained within the regulations allows for producers and importers of diesel fuel to sell an alternative diesel formulation if they can prove that emissions from a heavy-duty diesel

engine using their fuel are similar or lower for nitrogen oxides, particulate matter, and soluble organic fraction of particulate matter. Such "Certified Diesel Fuel Formulations" contain 15 to 25% aromatics and 2 to 5% PAHs (*30*).

2.2 CMB analysis results and comparison of emission factors to EMFAC2011

Over a mix of weekdays and weekends, diesel exhaust constituted 24 ± 14% of gas-phase organic carbon from motor vehicle exhaust emissions at the Caldecott tunnel, and 56 ± 18% of total exhaust at the Bakersfield supersite in the San Joaquin Valley. Diesel fuel sales data are consistent with model results at both sites when accounting for differences in emission factors since 11% and 33% of on-road fuel use is diesel in the San Francisco bay area and Kern county, respectively (*33*). It is important to note that off-road use of diesel represents a non-negligible amount of diesel fuel use and will increase total diesel fuel use by a few percent on a state and national level. On-road diesel use is 4-6x greater than off-road on these scales, but county-level data do not exist at this time.

The contributions of non-tailpipe gasoline (i.e. evaporative) emissions were slightly different than previous work showing that non-tailpipe gasoline was responsible for ~30% of gasoline-related VOC emissions in the South Coast Air Basin (*6*). 17 ± 9% of gasoline-related emissions were from non-tailpipe sources in the Caldecott tunnel, which is not unexpected since emissions from service stations and resting emissions from vehicles would not play a role in the tunnel environment. In Bakersfield, non-tailpipe gasoline was 38 ± 21 % of emissions from gasoline vehicles—slightly higher than previous work.

In terms of the overall contribution to non-combusted gas-phase organic carbon emissions at Bakersfield, diesel exhaust, gasoline exhaust, and non-tailpipe gasoline comprised 44 ± 16%, 35 ± 13%, and 21 ± 12% of motor vehicle emissions, respectively. At the Caldecott tunnel, diesel exhaust, gasoline exhaust, and non-tailpipe gasoline comprised 20 ± 12%, 66 ± 13%, and 14 ± 7% of motor vehicle emissions, respectively.

Atypical of many urban areas, weekday/weekend differences were not strong in Bakersfield with regard to the distribution of emissions between gasoline and diesel exhaust as daytime values of both decreased by ~40% on the weekends (Fig. S7).

From the tunnel study, emissions of non-combusted gas-phase organic carbon were determined to be 0.38 ± 0.11 gC L^{-1} for gasoline exhaust and 0.86 ± 0.25 gC L^{-1} for diesel exhaust. Values calculated using California's emissions model for the same period (*12*) are 0.36 gC L^{-1} and 0.75 gC L^{-1} before adjusting for products of incomplete combustion for gasoline and diesel, respectively. The gasoline emission factor is close to gasoline emission factors calculated by both methods (0.30 ± 0.11 gC L^{-1} using the regression method), but diesel is somewhat different with our value being slightly higher. Differences in gasoline and diesel fleet distribution across varying vehicle classes, ages, and levels of maintenance in the tunnel versus that of EMFAC may be responsible for these differences, as "high-emitters" are sometimes self-selected out of dynamometer testing.

Calculated exhaust emission factors are lower bounds since they do not include products of incomplete combustion or cold start emissions. The calculated values are focused on unburned hydrocarbons, which are considerably more important for SOA formation. While many products of incomplete combustion are highly reactive and important for overall OH reactivity, ozone formation and may have indirect effects on SOA; most of them are not currently expected to form SOA directly with the exception of larger carbonyls that make up a minor fraction of

emissions (*9, 34*). Continued work is necessary to understand their emissions, but for these reasons they are not included in the emission factors derived and used in this study.

The methods applied in this work include the ability to examine emissions and concentrations of individual compounds in addition to overall source contributions. Emission factors for any individual compound in gasoline and/or diesel fuel (or set of compounds) can be estimated by adjusting the reported emission factors for non-combusted gas-phase organic carbon by the compound's compositional fraction in the fuel (e.g. $EF_{n\text{-}dodecane,diesel} = EF_{GPOC,diesel} * WtC\%_{n\text{-}dodecane,diesel}$ /100). Similarly, the ambient concentration of any compound can be estimated by multiplying the source contributions (ppbC) by the compound's composition (WtC%) in the sources and summing the terms. Additionally, estimates of SOA from each source can be obtained my multiplying emission factors or calculated emissions by bulk SOA yields.

2.3 ΔOA/ΔCO ratios

Emissions of SOA precursors are dominated by diesel, whereas CO emissions are dominated by gasoline, so ΔOA/ΔCO ratios are sensitive to changes in fuel use. In urban areas which have a mixture of diesel and gasoline use, gasoline CO overwhelms the ΔOA/ΔCO relationship as gasoline mobile sources are responsible for 30x more CO than diesel (*35*). In urban regions such as the South Coast Air Basin, 90% of CO emissions are from mobile sources versus 65% statewide (*12, 35*). The ΔOA/ΔCO ratio presented for gasoline is an upper bound given the relatively slow reaction rates for benzene and toluene.

In previous work that reported the predominance of gasoline sources for SOA formation, weekday values in Los Angeles were centered on 14 μg m^{-3} $ppmv^{-1}$ CO and we predict a very similar value of 13 μg m^{-3} $ppmv^{-1}$ CO for a reported 17% diesel fraction of total fuel use cited in the study (*36*). Photochemical ages reported in Los Angeles during the weekend are greater due to faster photochemical processing likely associated with lower NO_x emissions from diesel sources (*36, 37*). Adjusting observed weekend ΔOA/ΔCO values from Los Angeles for photochemical aging results in a ΔOA/ΔCO slope very similar to that expected from a gasoline-dominated fleet (*36*). Based on previous work, a 3-4x increase in the ΔOA/ΔCO slope occurs from photochemical ages of ~6 hours to 1 day at a roughly linear rate (*29, 38*). Thus, ages of 12 and 24 hours should correspond to increases of 2x and 4x, respectively. Observed weekend ratios ranged from 22 to 70 μg m^{-3} $ppmv^{-1}$ CO (Figure S9) (*36*). The corresponding range of photochemical ages shown over the weekend extend from 12 hours to just over 24 hours as determined by toluene/benzene ratios of 2.0 through 1.0 (*36, 39*). Adjusting the observed ΔOA/ΔCO values of 22 to 70 μg m^{-3} $ppmv^{-1}$ CO, by factors of 2 to 4, respectively, produces ΔOA/ΔCO values around 11 to 17 μg m^{-3} $ppmv^{-1}$ CO at ~6 hours of photochemical processing, and does not consider the influence of other sources of SOA precursors. Similarly, in Figure S9, we estimate aged weekend ΔOA/ΔCO values based on a fuel mixture of 5-10% diesel and see general agreement with reported measurements. We contend that ΔOA/ΔCO slopes alone are not sensitive enough to effectively discern the contributions of gasoline vs. diesel, and given the variability in data from the Los Angeles study, it is difficult to separate the effects of changes in SOA precursor emissions, CO emissions, and increased photochemical processing.

Non-vehicular anthropogenic and biogenic sources contribute SOA precursors without CO and will vary depending on the characteristics of an urban region as shown by enhanced ΔOA/ΔCO slopes in Mexico City, the Southeast U.S., and the Po Valley (despite outlier filtering for major non-vehicular events in some studies) (*38, 39-41*).

Our derived SOA yields are intended to model the first several generations of photochemical oxidation, which corresponds to the extent of oxidation effectively constrained by experimental measurements. It is highly plausible that the continued increase in ΔOA/ΔCO ratios beyond our predictions is caused by the continued oxidation of multi-generation oxidation products in the gas-phase. In this study, we have refrained from estimating SOA yields for these highly-aged air masses as doing so would require excessive extrapolation with high uncertainties. A re-evaluation of gasoline and diesel SOA yields is encouraged once these data become available.

References

1 Pollmann J, Ortega J, Helmig D (2005) Analysis of atmospheric sesquiterpenes: Sampling losses and mitigation of ozone interferences, *Environ. Sci. Technol*., 39:9620-9629.

2 Millet DB *et al.* (2005) Atmospheric volatile organic compound measurements during the Pittsburgh Air Quality Study: Results, interpretations, and quantification of primary and secondary contributions. *J. Geophys. Res.* 110:D07S07.

3 Dallmann TR *et al*. (2012) On-Road Measurement of Gas and Particle Phase Pollutant Emission Factors for Individual Heavy-Duty Diesel Trucks. *Environ. Sci. Technol.* 46:8511-8518.

4 Liu S *et al*. (2012) Secondary organic aerosol formation from fossil fuel sources contribute majority of summertime organic mass at Bakersfield. *J. Geophys. Res.* in review.

5 Isaacman G *et al.* (2012) Improved resolution of hydrocarbon structures and constitutional isomers in complex mixtures using gas chromatography-vacuum ultraviolet-mass spectrometry. *Anal. Chem.* 84:2335-2342.

6 Gentner DR, Harley RA, Miller AM, Goldstein AH (2009) Diurnal and Seasonal Variability of Gasoline-Related Volatile Organic Compound Emissions in Riverside, California. *Environ. Sci. Technol.* 43:4247-4252.

7 Harley RA, Coulter-Burke SC, Yeung TS (2000) Relating liquid fuel and headspace vapor composition in California reformulated gasoline samples containing ethanol. *Environ. Sci. Technol.* 34:4088-4094.

8 Watson JG, Cooper JA, Huntzicker JJ (1984) The effective variance weighting for least squares calculations applied to the mass balance receptor model. *Atmos. Env.* 18:1347-1355.

9 Kirchstetter TW, Singer BC, Harley RA (1996) Impact of Oxygenated Gasoline Use on California Light-Duty Vehicle Emissions. *Environ. Sci. Technol.* 30:661-670.

10 Leppard WR *et al.* (1992) Effects of gasoline composition on vehicle engineout and tailpipe hydrocarbon emissions. *SAE Tech. Pap. Ser.* No. 920329.

11 U.S. Environmental Protection Agency, *EPA-CMB8.2* (http://www.epa.gov/scram001/receptor_cmb.htm)

12 California Air Resources Board, *Motor Vehicle Emission Factor/Emission Inventory Model - EMFAC 2011* (http://www.arb.ca.gov/msei/msei.htm)

13 Chan AWH *et al.* (2009) Secondary organic aerosol formation from photooxidation of naphthalene and alkylnaphthalenes: implications for oxidation of intermediate volatility organic compounds (IVOCs). *Atmos. Chem. Phys*. 9:3049-3060.

14 Zhang Q R *et al*. (2007) Ubiquity and dominance of oxygenated species in organic aerosols in anthropogenically-influenced Northern Hemisphere midlatitudes. *Geophys. Res. Lett.* 34:L13801
15 Jordan CE *et al*. (2008) Modeling SOA formation from OH reactions with C8–C17 n-alkanes. *Atmos. Environ.* 42:8015-8026.
16 Kroll JH, Seinfeld JH (2008) Chemistry of secondary organic aerosol: Formation and evolution of low-volatility organics in the atmosphere. *Atmos. Environ.* 42:3593-3624.
17 Lim YB, Ziemann PJ (2009) Effects of molecular structure on aerosol yields from OH radical-initiated reactions of linear, branched, and cyclic alkanes in the presence of NOx. *Environ. Sci. Technol.* 43:2328-2334.
18 Pankow JF, Asher WE (2008) SIMPOL.1: a simple group contribution method for predicting vapor pressures and enthalpies of vaporization of multifunctional organic compounds. *Atmos. Chem. Phys*., 8:2773-2796.
19 Isaacman G *et al.*, (2011) Understanding evolution of product composition and volatility distribution through in-situ GC × GC analysis: a case study of longifolene ozonolysis. *Atmos. Chem. Phys*., 11:5335-5346.
20 Hinckley DA, Bidleman TF, Foreman WT, Tuschall JR (1990) Determination of Vapor Pressures for Nonpolar and Semipolar Organic Compounds from Gas Chromatographic Retention Data. *J. Chem. Eng. Data* 35:232-237.
21 Lee-Taylor J *et al.* (2011) Explicit modeling of organic chemistry and secondary organic aerosol partitioning for Mexico City and its outflow plume. *Atmos. Chem. Phys*., 11:13219-13241.
22 Ng NL *et al*. (2007) Secondary organic aerosol formation from *m*-xylene, toluene, and benzene. *Atmos. Chem. Phys.* 7:3909-3922.
23 Wyche KP *et al.* (2009) Gas phase precursors to anthropogenic secondary organic aerosol: detailed observations of 1,3,5-trimethylbenzene photooxidation, *Atmos. Chem. Phys.*, 9:635-665.
24 de Gouw JA *et al.* (2008) Sources of particulate matter in the northeastern United States: 1. Direct emissions and secondary formation of organic matter in urban plumes. *J. Geophys. Res.* 113:D08301.
25 Dzepina K *et al.* (2011) Modeling the Multiday Evolution and Aging of Secondary Organic Aerosol During MILAGRO 2006. *Environ. Sci. Technol.* 45:3496-3503.
26 Johnson D *et al*. (2006) Simulating regional scale secondary organic aerosol formation during the TORCH 2003 campaign in the southern UK. *Atmos. Chem. Phys.* 6:403-418.
27 de Gouw JA, Jimenez JL (2009) Organic aerosols in the Earth's atmosphere. *Environ. Sci. Technol.* 43:7614-7618.
28 Robinson AL *et al*. (2007) Rethinking organic aerosols: Semivolatile emissions and photochemical aging. *Science* 315:1259-1262.
29 Hodzic A *et al.* (2010) Modeling organic aerosols in a megacity: potential contribution of semi-volatile and intermediate volatility primary organic compounds to secondary organic aerosol formation. *Atmos. Chem. Phys.* 10:5491-5514.
30 California Air Resources Board, *California Diesel Fuel and Reformulated Gasoline Regulations (with subsequent amendments)* (http://www.arb.ca.gov/fuels/fuels.htm)
31 U.S. Energy Information Administration, *National fuel sales data* (2010 data, http://www.eia.gov/dnav/pet/pet_cons_prim_dcu_nus_a.htm)

32 U.S. Environmental Protection Agency, *U.S. Clean Air Act (and subsequent amendments/rulings)* (http://www.epa.gov/air/caa/)
33 California Department of Transportation, *California Motor Vehicle Stock Travel, and Fuel Forecast (MVSTAFF) 2008 Report* (http://www.dot.ca.gov/hq/tsip/smb/documents/mvstaff/mvstaff08.pdf)
34 Schauer JJ, Kleeman MJ, Cass GR, Simoneit BRT (1999) Measurement of Emissions from Air Pollution Sources. 2. C1 through C30 Organic Compounds from Medium Duty Diesel Trucks. *Environ. Sci. Technol.* 33:1578-1587.
35 California Air Resources Board, *Estimated annual average emissions, 2010*. (http://www.arb.ca.gov/ei/emsmain/emsmain.htm).
36 Bahreini R *et al*. (2012) Gasoline emissions dominate over diesel in formation of secondary organic aerosol mass. *Geophys. Res. Lett.* 39:L06805.
37 Russell AR, Valin LC, Bucsela EJ, Wenig MO, Cohen RC (2010) Space-based Constraints on Spatial and Temporal Patterns of NO*x* Emissions in California, 2005-2008. *Environ. Sci. Technol.* 44:3608-3615.
38 Kleinman KI *et al.* (2008) The time evolution of aerosol composition over the Mexico City plateau. *Atmos. Chem. Phys.* 8:1559-1575.
39 Weber RJ *et al.* (2007) A study of secondary organic aerosol formation in the anthropogenic-influenced southeastern United States. *J. Geophys. Res.* 112:D13302.
40 DeCarlo PF *et al.* (2008) Fast airborne aerosol size and chemistry measurements above Mexico City and Central Mexico during the MILAGRO Campaign. *Atmos. Chem. Phys.* 8:4027-4048.
41 Crosier J *et al.* (2007) Chemical composition of summertime aerosol in the Po Valley (Italy), northern Adriatic and Black Sea. *Q. J. R. Meteorol. Soc.* 113:61-75.

Supplementary Figures

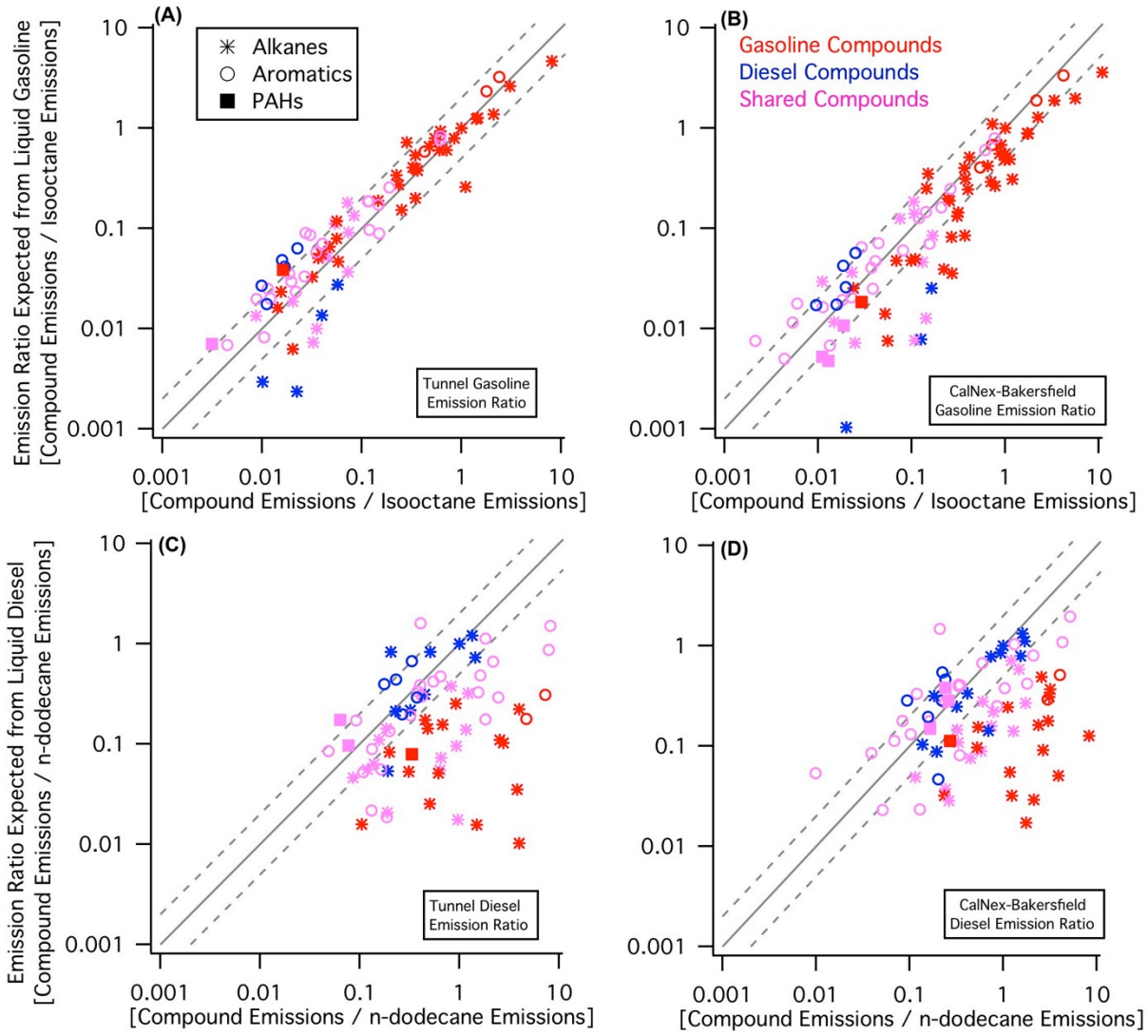

Figure S1: Demonstration of compositional consistency between gasoline and diesel fuel to gasoline and diesel exhaust, respectively, at both **(A, C)** the Caldecott tunnel and Bakersfield **(B, D)** using regressions to gasoline (isooctane) and diesel (n-dodecane) tracers. Similar to Fig. 1, compounds dominated by gasoline (red) are most consistent with the liquid gasoline profile. Conversely, those dominated by diesel (blue) agree most with diesel fuel. Compounds shared by gasoline and diesel (pink) vary in degree of covariance with each source depending on relative content in each fuel and relative magnitude of each source at each field site.

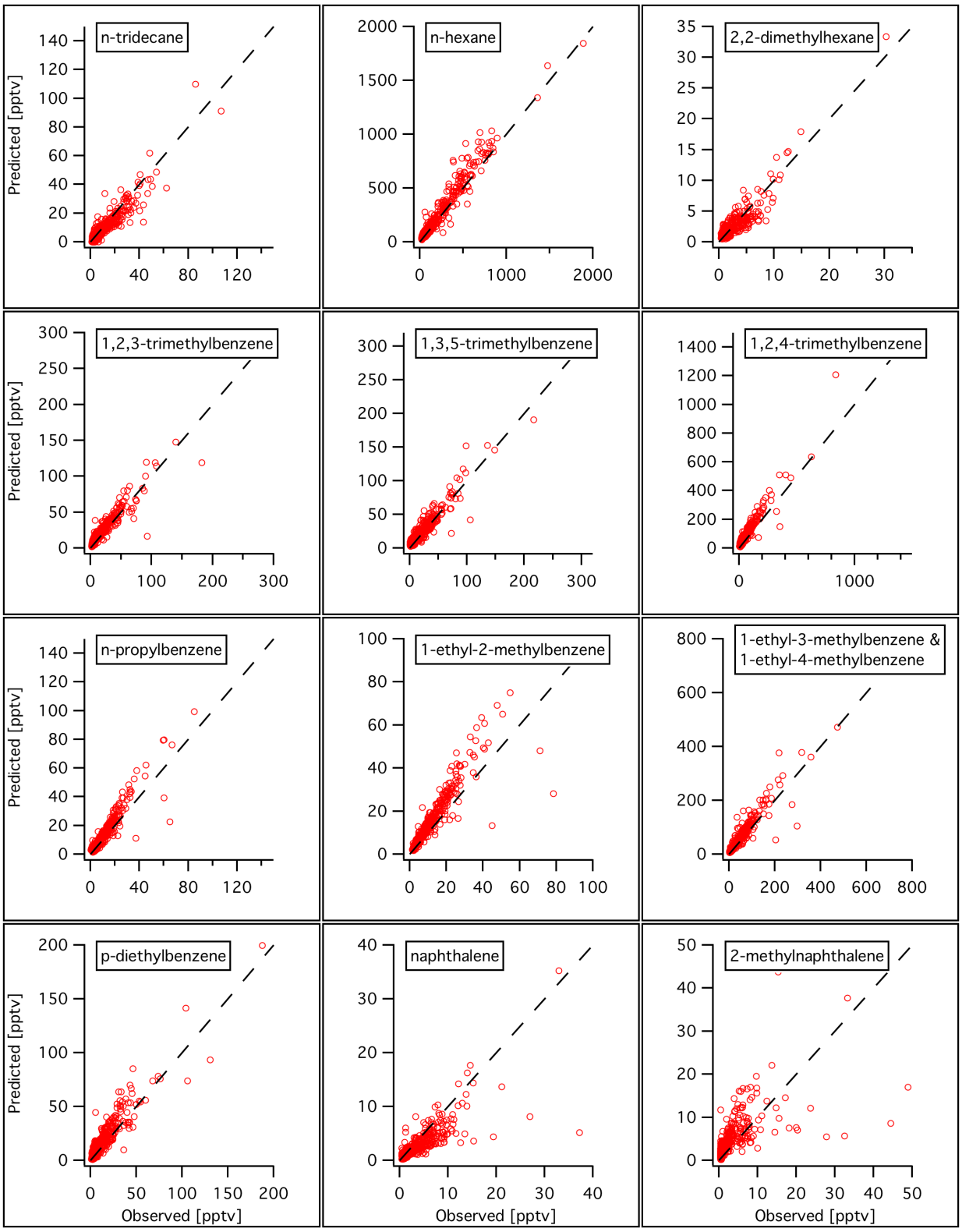

Figure S2: Verification of model perfomance at CalNex-Bakersfield by comparing predicted compound concentrations with observations of independent compounds not included in model. The 1:1 line is shown in each panel as a dashed line.

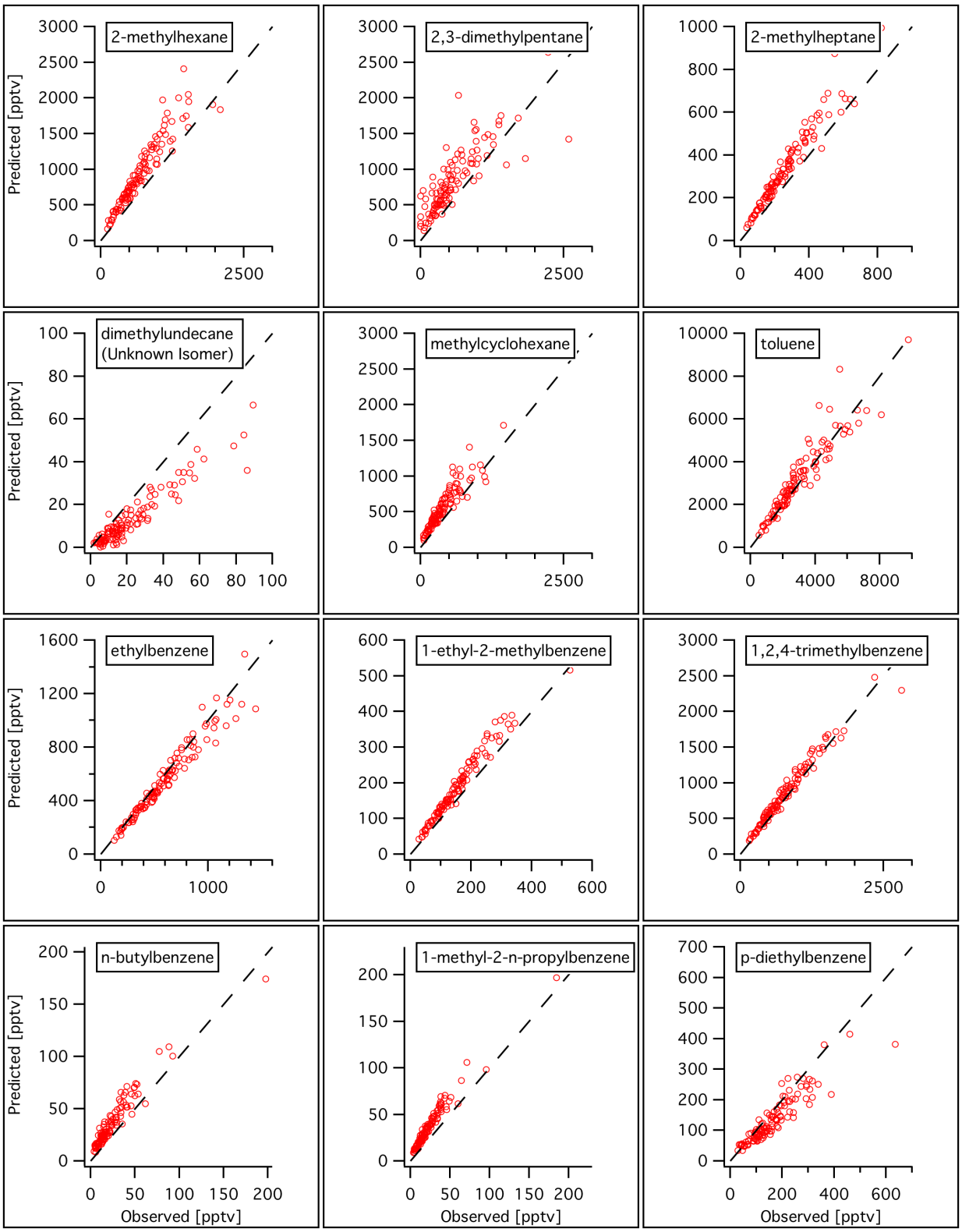

Figure S3: Verification of model perfomance at the Caldecott Tunnel (Oakland, CA) by comparing predicted compound concentrations with observations of independent compounds not included in model. The 1:1 line is shown in each panel as a dashed line.

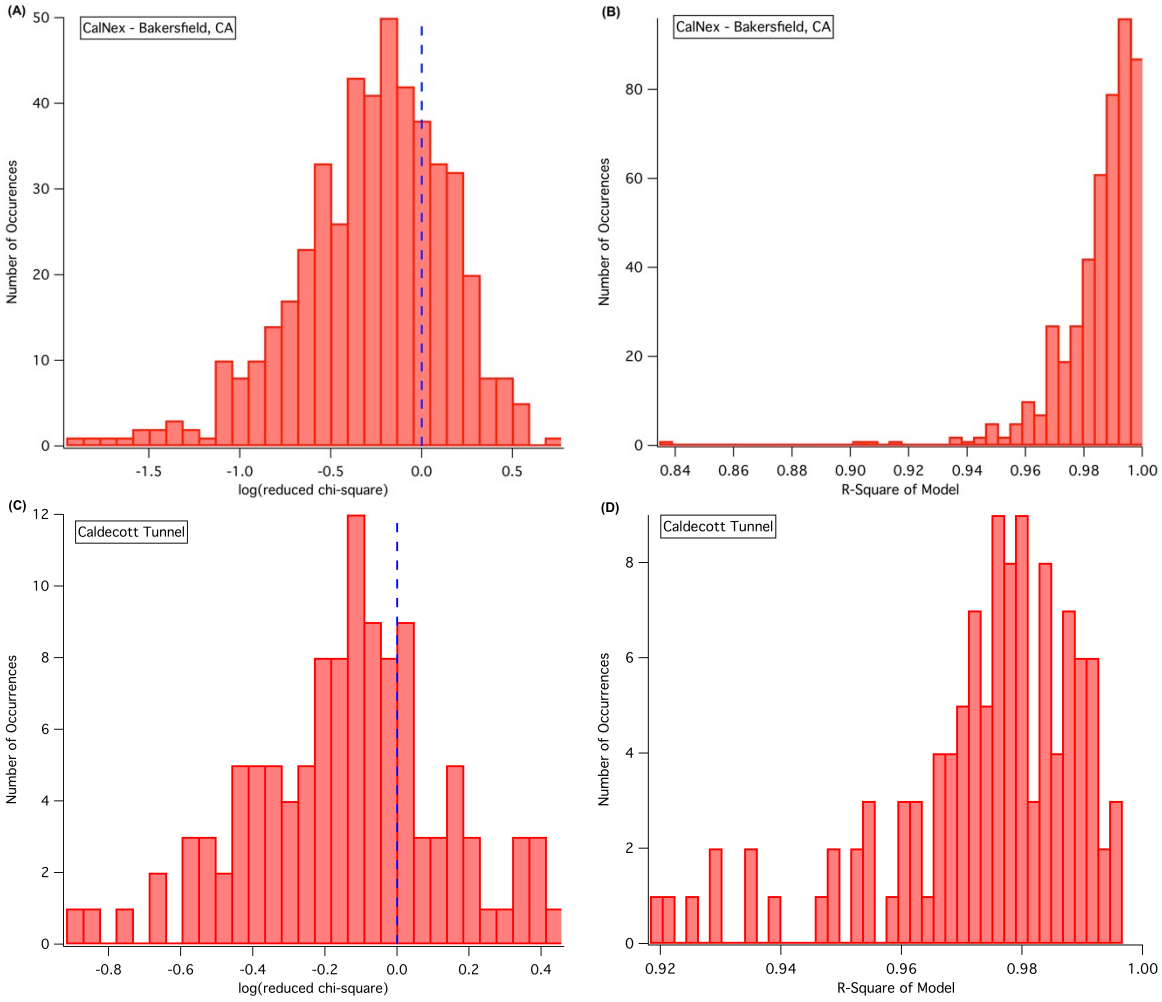

Figure S4: Internal model diagnotics for **(A-B)** CalNex-Bakersfield site (N=487) and **(C-D)** the Caldecott tunnel (N=114). Panels A & C shows the log of the reduced chi-square test where ≤ 0 indicates a good fit of model data. Similarly, Panels B & D shows the overall coefficient of determination (r^2) of compounds used in the model and values close to 1.0 indicate robust model performance.

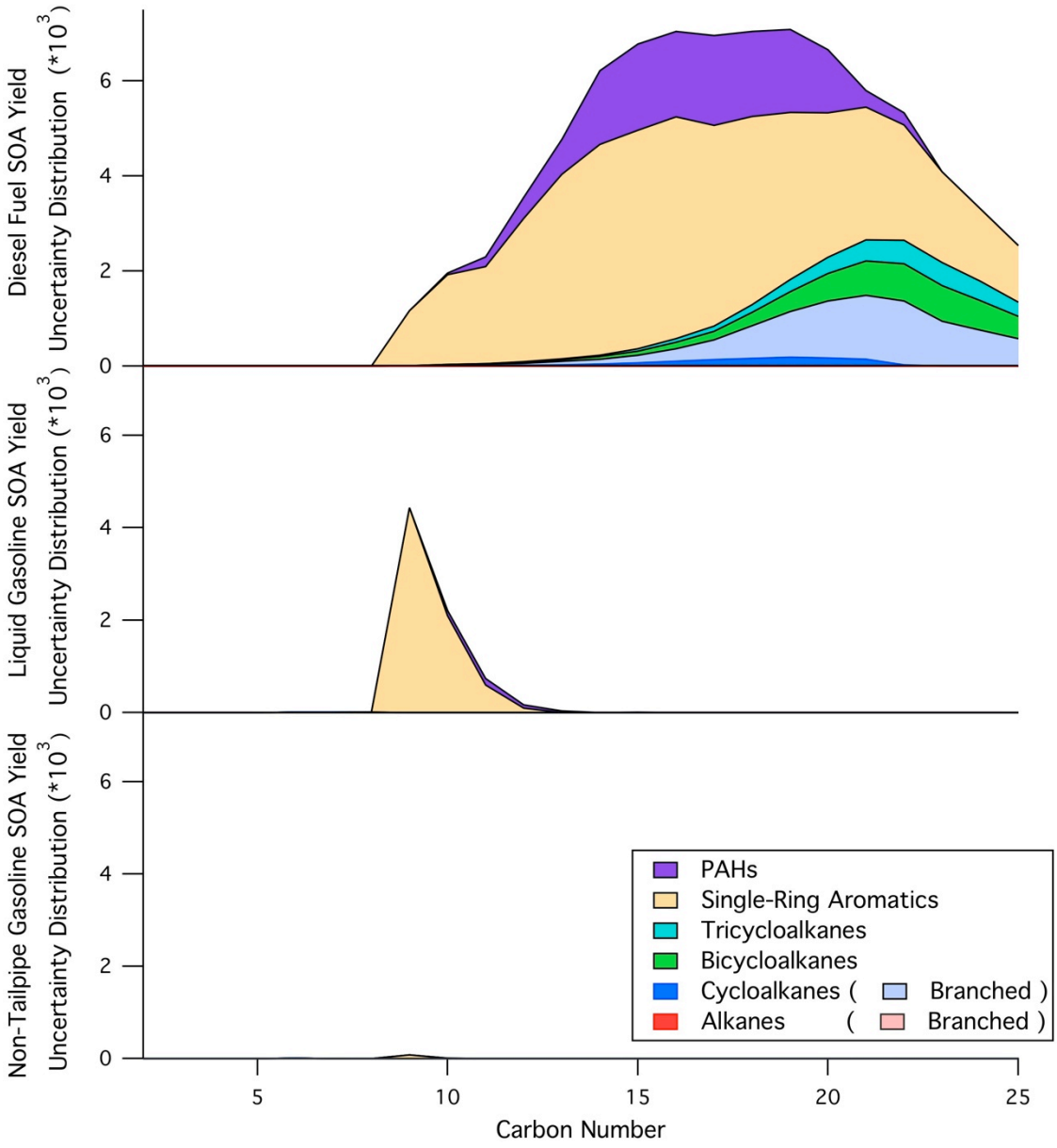

Figure S5: Distibutions of SOA yield uncertainties [μgSOA μg^{-1}] from each source where uncertainties are based on Monte Carlo anlaysis. Diesel exhasut has greatest uncertainty due to insufficent studies on intermediate volatility compounds likely to form SOA, with the exception of straight and branched alkanes.

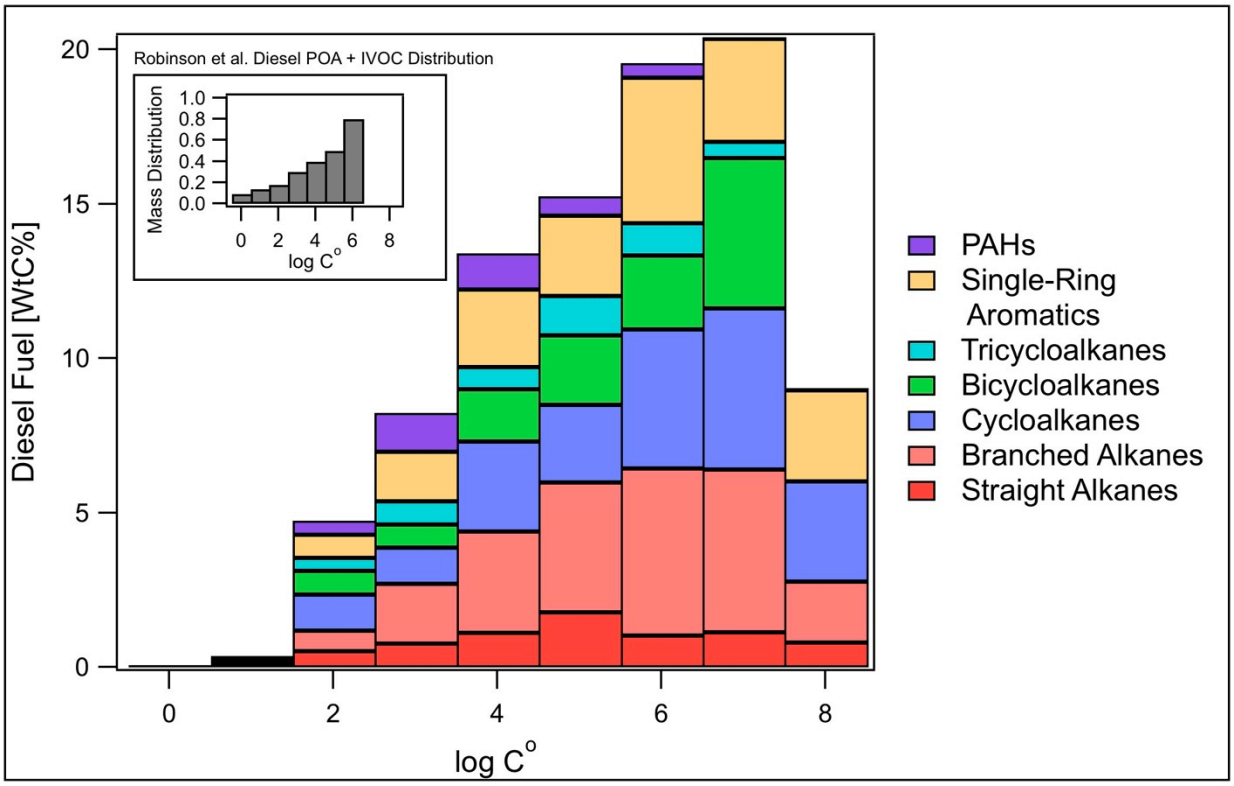

Figure S6: Volatility basis set distribution of diesel fuel broken down by chemical class. Inset shows SVOC and IVOC distribution used in current models (*28*), which does not include the $C^{\circ}=10^{7}$ μg m^{-3} and $C^{\circ}=10^{8}$ μg m^{-3} volatility bins, which contain $C_{9\text{-}11}$ aromatics. The magnitude of the $C^{\circ}=1$ μg m^{-3} and $C^{\circ}=10$ μg m^{-3} volatility bins are accurately larger in current models compared to our profile as they include primary gases and particles eminating from motor oil.

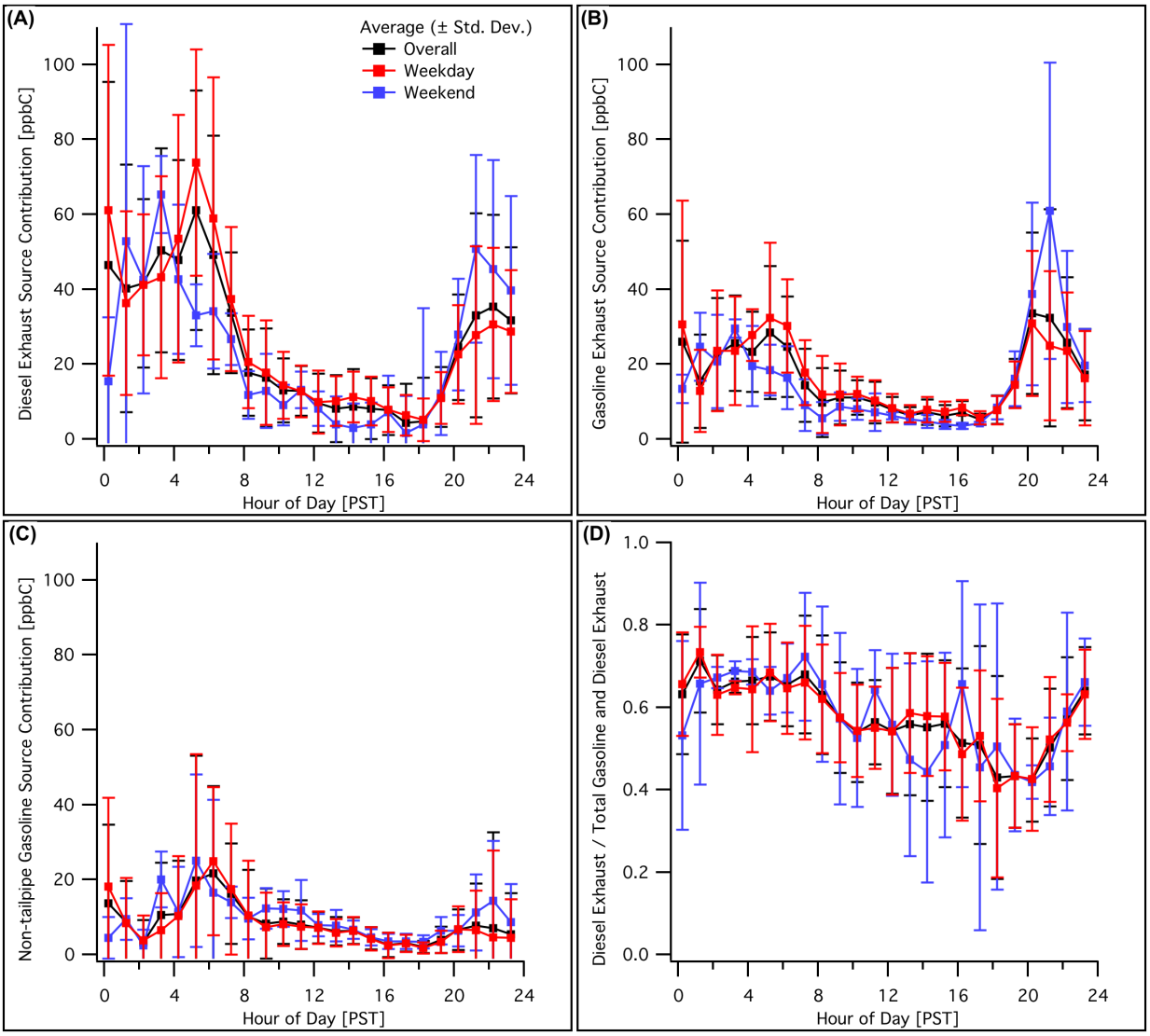

Figure S7: Weekday/weekend diurnal profiles of diesel exhaust **(A)**, gasoline exhaust **(B)**, and non-tailpipe gasoline source contributions **(C)**, and ratio of diesel to gasoline exhaust **(D)** during the early summer in Bakersfield (includes 5 weekends). The source contributions of gasoline and diesel (A-B) have greater daytime values during the week. The diesel exhaust fraction (D) shows some diurnal variablity, there is no strong weekday/weekend effect in the relative fraction of each fuel due to equivalent decreases in both gasoline and diesel. Diurnal averages for source contributions (A-C) are calculated as geometric averages, while panel (D) is an arithmatic average.

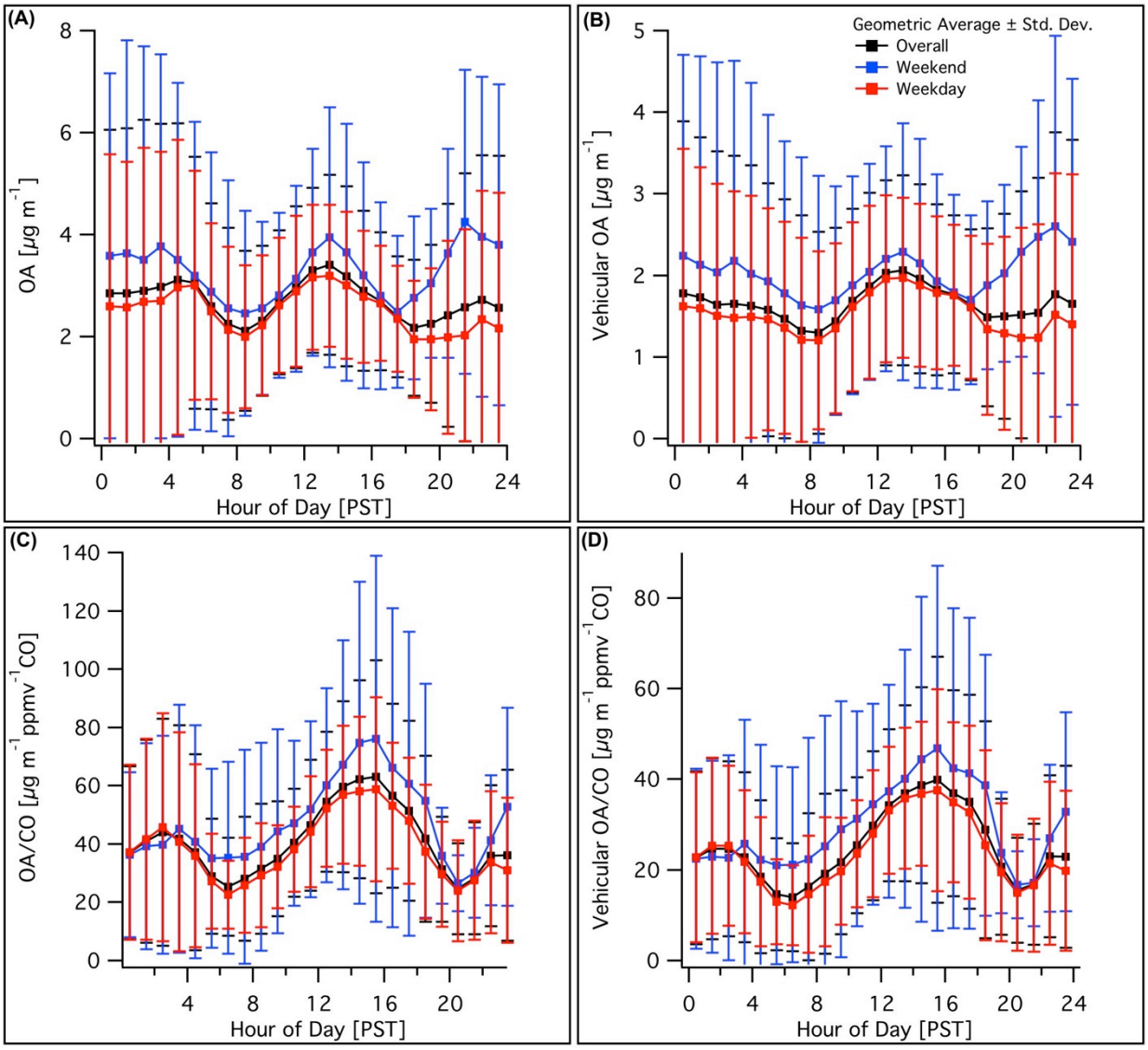

Figure S8: **(A-B)** Overall, weekday, and weekend diurnal patterns for total and vehicular organic aerosol at Bakersfield, CA during the early summer. Vehicular OA is determined from AMS positive matrix factor analysis (*4*). **(C-D)** Overall, weekday, and weekend diurnal patterns for ΔOA/ΔCO ratios for total and vehicular organic aerosol. In all cases, daytime weekend values are higher, but within the large variability observed across the 6-week campaign. Total and vehicular OA are higher over the weekend due to increased photochemical processing (as shown by increased ΔOA/ΔCO ratios) associated with decreased NO_x emissions from diesel sources and is not a function of changes in the distribution of fuel use.

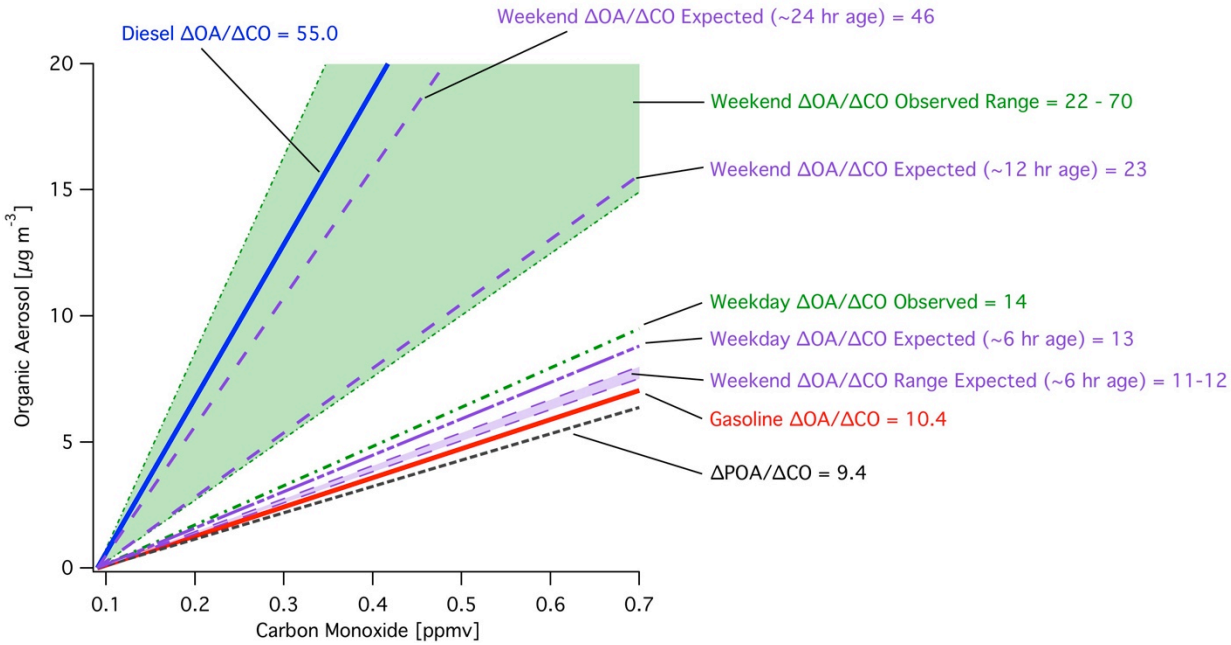

Figure S9: Weekday/weekend behavior of ΔOA/ΔCO ratios in Los Angeles, CA (Summer 2010) with best estimates for ΔOA/ΔCO ratios expected for pure gasoline and diesel emissions added to an average POA/CO value of 9.4 μg m^{-3} $ppmv^{-1}$ CO (*24*). Calculated weekday ΔOA/ΔCO slope (17% diesel) for Los Angeles agrees with observed value. Weekend values show varying degrees of aging ranging from 12 hours to 1 day based on reported photochemical ages, which roughly correspond to a 2-4x increase in ΔOA/ΔCO ratios (*36, 29, 38*). Approximate aged weekend values with 5-10% diesel use are shown and are consistent with observations. While Los Angeles is dominated by motor vehicle emissions, contributions of SOA precursors from other non-CO related sources would elevate predicted ΔOA/ΔCO ratios further.

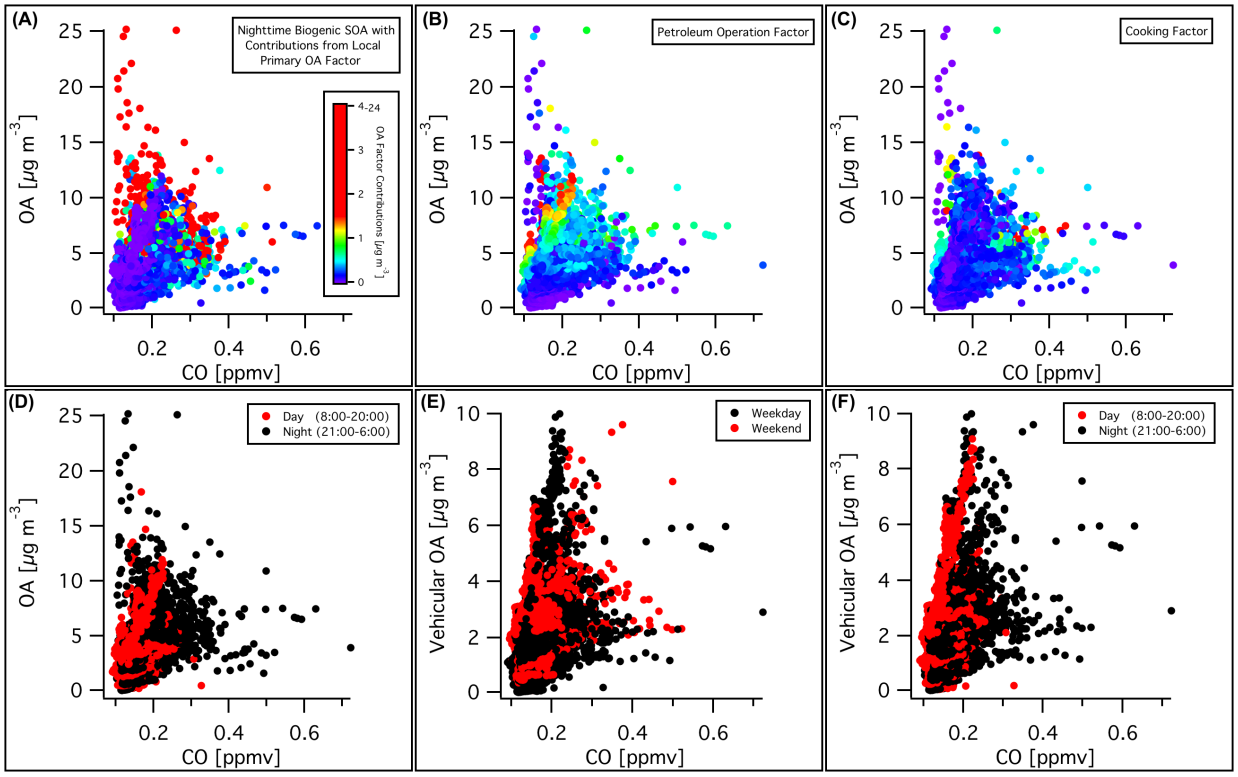

Figure S10: Observed organic aerosol vs. carbon monoxide at Bakersfield, CA during the early summer. Panels A-C show color-shaded contributions for major non-vehicular sources as determined by factor analysis of AMS data (*4*). Panel D shows day and night ratios, with increased daytime ΔOA/ΔCO slopes associated with greater aging, while nighttime values show less aged air masses and episodic contributions to OA without CO from non-vehicular sources. Panels E-F show just vehicular organic aerosol vs. carbon monoxide. Vehicular OA is determined from AMS positive matrix factor analysis (*4*). Panel E shows minor weekday/weekend differences with considerable variability and is better displayed in Fig. S8D. Panel F shows day and night ratios, with increased daytime ΔOA/ΔCO slopes associated with greater aging, while nighttime values show a mix of air mass ages.

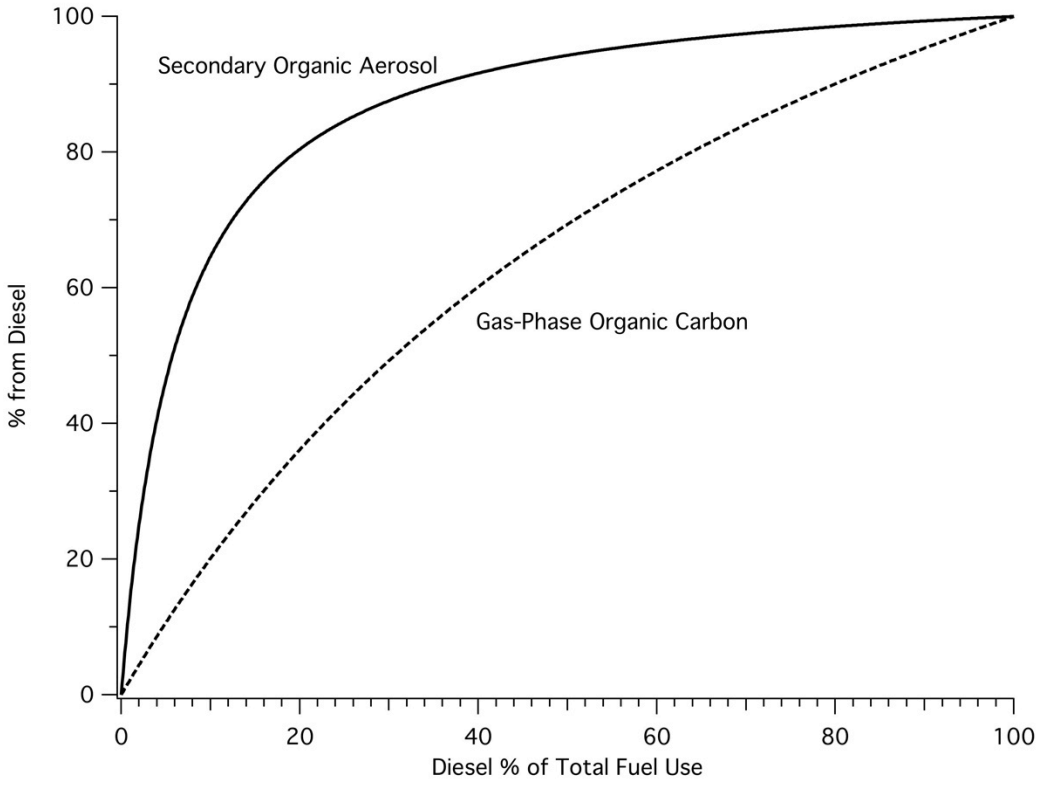

Figure S11: The percent contribution of diesel exhaust to SOA over percent diesel fuel use. The percent diesel contribution to gas-phase organic carbon is shown as well and has greater contributions from gasoline with a equivalence point at 31% diesel fuel use. The percent contribution from gasoline can be determined via the difference of diesel. The gas-phase organic carbon line does not consider contributions from non-tailpipe gasoline sources since contributions will vary depending on location and time of year.

Supplementary Tables

Table S1: Sales of on-road gasoline and diesel fuel in California and its counties (*33*)

COUNTY	Total Gas and Diesel Sales [10^6 gallons annually]	Percent Gasoline (by volume)	Percent Diesel (by volume)
ALAMEDA	772	84.2%	15.8%
ALPINE	3	89.5%	10.5%
AMADOR	24	86.8%	13.2%
BUTTE	97	85.3%	14.7%
CALAVERAS	21	89.0%	11.0%
COLUSA	43	64.6%	35.4%
CONTRA COSTA	432	89.4%	10.6%
DEL NORTE	16	77.8%	22.2%
EL DORADO	86	89.7%	10.3%
FRESNO	497	76.6%	23.4%
GLENN	40	57.7%	42.3%
HUMBOLDT	72	81.9%	18.1%
IMPERIAL	129	71.4%	28.6%
INYO	32	77.5%	22.5%
KERN	565	67.3%	32.7%
KINGS	92	71.0%	29.0%
LAKE	32	85.2%	14.8%
LASSEN	34	69.7%	30.3%
LOS ANGELES	4251	86.8%	13.2%
MADERA	102	71.0%	29.0%
MARIN	145	92.3%	7.7%
MARIPOSA	13	95.8%	4.2%
MENDOCINO	67	82.4%	17.6%
MERCED	164	73.1%	26.9%
MODOC	15	65.1%	34.9%
MONO	17	84.7%	15.3%
MONTEREY	213	79.5%	20.5%
NAPA	62	90.3%	9.7%
NEVADA	71	77.8%	22.2%
ORANGE	1415	89.3%	10.7%
PLACER	194	83.2%	16.8%
PLUMAS	23	71.9%	28.1%
RIVERSIDE	1154	78.6%	21.4%
SACRAMENTO	644	85.5%	14.5%
SAN BENITO	33	71.2%	28.8%
SAN BERNARDINO	1301	76.3%	23.7%
SAN DIEGO	1460	88.7%	11.3%
SAN FRANCISCO	171	93.9%	6.1%
SAN JOAQUIN	413	73.4%	26.6%
SAN LUIS OBISPO	161	85.4%	14.6%
SAN MATEO	336	92.3%	7.7%
SANTA BARBARA	203	86.8%	13.2%
SANTA CLARA	790	89.6%	10.4%
SANTA CRUZ	102	89.7%	10.3%
SHASTA	120	76.1%	23.9%
SIERRA	7	74.7%	25.3%
SISKIYOU	72	60.9%	39.1%
SOLANO	252	86.2%	13.8%
SONOMA	220	87.2%	12.8%
STANISLAUS	250	76.3%	23.7%
SUTTER	50	85.0%	15.0%
TEHAMA	64	71.0%	29.0%
TRINITY	13	68.8%	31.2%
TULARE	232	74.4%	25.6%
TUOLUMNE	35	85.8%	14.2%
VENTURA	364	87.2%	12.8%
YOLO	120	79.2%	20.8%
YUBA	36	86.4%	13.6%
TOTAL	**18344**	**83.5%**	**16.5%**

Table S2: Chemical class distribution of sources by total mass

	Weight Percent by mass (± St. Dev)		
Compound Class	**Diesel Fuel**	**Liquid Gasoline**	**Non-Tailpipe Gasoline**
Straight-chain Alkanes	7.3 ± 1.2	7.6 ± 0.3	19 ± 0.9
Branched Alkanes	23 ± 2.5	39 ± 0.9	58 ± 3
Cycloalkanes (Single Straight Alkyl Chain)	2.5 ± 0.2	4.2 ± 0.1	0.98 ± 0.04
Cycloalkanes (Branched or Multiple Alkyl Chain(s))	18 ± 1.8	6.0 ± 0.3	4.8 ± 0.2
Bicycloalkanes	12 ± 1.3	0	0
Tricycloalkanes	4.7 ± 0.6	0	0
Single-ring Aromatics	17.7 ± 1.6	26.7 ± 0.7	2.5 ± 0.1
Polycyclic Aromatic Compounds	3.8 ±1.6	0.29 ± 0.02	0.0003
Alkenes (Straight, Branched, & Cyclic)	0	3.5 ± 0.1	7.0 ± 0.3
Ethanol	0	10.9 ± 0.9	6.9 ± 0.6

Table S3: Summary of compounds used in source receptor modeling at Bakersfield

Master Set	Confirmation Set #1	Confirmation Set #2	Confirmation Set #3	Confirmation Set #4
n-butane	n-butane	n-butane	n-butane	n-butane
isopentane	n-pentane	isopentane	n-pentane	n-pentane
n-pentane	isopentane	2,2-dimethylbutane	2,2-dimethylbutane	isopentane
n-heptane	n-heptane	n-heptane	methylcyclopentane	toluene
isooctane	isooctane	2-methylhexane	n-heptane	isooctane
m&p-xylene	m&p-xylene	3-methylhexane	isooctane	o-xylene
o-xylene	n-nonane	m&p-xylene	m&p-xylene	n-undecane
n-nonane	n-undecane	n-nonane	n-nonane	n-dodecane
n-undecane		n-tridecane	1-ethyl-3(+4)-methylbenzene	naphthalene
n-dodecane			n-dodecane	

Table S4: Summary of compounds used in source receptor modeling at the Caldecott Tunnel

Master Set	Confirmation Set #1	Confirmation Set #2	Confirmation Set #3	Confirmation Set #4
isopentane	isopentane	n-pentane	n-pentane	n-pentane
isooctane	n-hexane	2,2-dimethylbutane	2,2-dimethylbutane	n-heptane
m&p-xylene	isooctane	n-hexane	n-hexane	n-nonane
o-xylene	m&p-xylene	3-methylpentane	3-methylpentane	1,2,3-trimethylbenzene
n-nonane	o-xylene	o-xylene	ethylcyclopentane	n-undecane
1,2,3-trimethylbenzene	n-nonane	n-nonane	methylcyclohexane	n-tridecane
1,3,5-trimethylbenzene	n-dodecane	1,2,4-trimethylbenzene	2,3-dimethylheptane	
n-propylbenzene		1-ethyl-2-methylbenzene	1-ethyl-2-methylbenzene	
n-undecane		n-tridecane	n-tridecane	
n-dodecane				

Table S5: Mass and chemical class distribution of diesel fuel (in weight percent by carbon)

Carbon Number	Straight-chain Alkanes	Branched Alkanes	Cycloalkanes (Single Straight Alkyl Chain)	Cycloalkanes (Branched or Multiple Alkyl Chain(s))	Bicycloalkanes	Tricycloalkanes	Aromatics	Polycyclic Aromatic Compounds
1	0	0	0	0	0	0	0	0
2	0	0	0	0	0	0	0	0
3	0	0	0	0	0	0	0	0
4	0	0	0	0	0	0	0	0
5	0	0	0	0	0	0	0	0
6	0	0	0	0	0	0	0	0
7	0	0	0.15	0	0	0	0.21	0
8	0.10	0.17	0.19	0.42	0	0	0.73	0
9	0.21	0.20	0.26	0.35	0	0	2.02	0
10	0.50	1.60	0.35	1.87	1.38	0.11	2.38	0.03
11	0.60	2.27	0.29	1.90	1.82	0.21	1.91	0.18
12	0.55	1.89	0.20	1.96	1.76	0.34	1.83	0.30
13	0.51	1.81	0.17	1.74	1.30	0.44	1.46	0.32
14	0.51	2.06	0.15	1.39	1.00	0.49	1.18	0.49
15	0.56	1.89	0.15	1.22	0.86	0.45	1.03	0.56
16	0.58	1.70	0.14	1.14	0.74	0.44	0.99	0.51
17	0.64	1.35	0.12	1.05	0.65	0.39	0.89	0.50
18	0.62	1.55	0.10	1.06	0.62	0.37	0.84	0.45
19	0.50	1.90	0.08	0.94	0.57	0.34	0.73	0.42
20	0.43	1.63	0.06	0.82	0.50	0.30	0.61	0.32
21	0.34	1.03	0.05	0.70	0.42	0.25	0.53	0.08
22	0.25	0.73	0.01	0.59	0.33	0.21	0.45	0.06
23	0.16	0.60	0	0.38	0.26	0.17	0.35	0
24	0.11	0.34	0	0.31	0.21	0.14	0.28	0
25	0.06	0.04	0	0.25	0.16	0.11	0.22	0

Table S6: Mass and chemical class distribution of liquid gasoline (in weight percent by carbon)

Carbon Number	Straight-chain Alkanes	Branched Alkanes	Cycloalkanes (Single Straight Alkyl Chain)	Cycloalkanes (Branched or Multiple Alkyl Chain(s))	Bicycloalkanes	Tricycloalkanes	Aromatics	Polycyclic Aromatic Compounds
1	0	0	0	0	0	0	0	0
2	0.0003	0	0	0	0	0	0	0
3	0.014	0	0	0	0	0	0	0
4	0.500	0.057	0	0	0	0	0	0
5	2.84	7.83	0.475	0	0	0	0	0
6	1.84	8.51	3.75	0	0	0	0.750	0
7	1.39	7.60	1.76	1.89	0	0	7.59	0
8	0.621	10.89	0.214	1.78	0	0	9.69	0
9	0.278	3.33	0.043	0.536	0	0	7.74	0
10	0.116	1.20	0	0.126	0	0	2.63	0.130
11	0.063	0.516	0	0	0	0	0.558	0.127
12	0.017	0.040	0	0	0	0	0.060	0.048
13	0.008	0	0	0	0	0	0	0.016
14	0.004	0.007	0	0	0	0	0.001	0
15	0.004	0.006	0	0	0	0	0	0.002
16	0	0	0	0	0	0	0	0.0004
17	0	0	0	0	0	0	0	0
18	0	0	0	0	0	0	0	0
19	0	0	0	0	0	0	0	0
20	0	0	0	0	0	0	0	0
21	0	0	0	0	0	0	0	0
22	0	0	0	0	0	0	0	0
23	0	0	0	0	0	0	0	0
24	0	0	0	0	0	0	0	0
25	0	0	0	0	0	0	0	0

Table S7: Mass and chemical class distribution of non-tailpipe gasoline (in weight percent by carbon)

Carbon Number	Straight-chain Alkanes	Branched Alkanes	Cycloalkanes (Single Straight Alkyl Chain)	Cycloalkanes (Branched or Multiple Alkyl Chain(s))	Bicycloalkanes	Tricycloalkanes	Aromatics	Polycyclic Aromatic Compounds
1	0	0	0	0	0	0	0	0
2	0.0987	0	0	0	0	0	0	0
3	0.690	0	0	0	0	0	0	0
4	6.54	1.07	0	0	0	0	0	0
5	10.3	38.4	1.07	0	0	0	0	0
6	1.97	13.4	3.35	0	0	0	0.506	0
7	0.137	3.89	0.562	0.774	0	0	1.52	0
8	0.0616	2.59	0.0194	0.257	0	0	0.564	0
9	0.0085	0.262	0.0014	0	0	0	0.139	0
10	0.0012	0	0	0.0003	0	0	0.0085	0.0002
11	0.0002	0	0	0	0	0	0.0001	0
12	0	0	0	0	0	0	0	0
13	0	0	0	0	0	0	0	0
14	0	0	0	0	0	0	0	0
15	0	0	0	0	0	0	0	0
16	0	0	0	0	0	0	0	0
17	0	0	0	0	0	0	0	0
18	0	0	0	0	0	0	0	0
19	0	0	0	0	0	0	0	0
20	0	0	0	0	0	0	0	0
21	0	0	0	0	0	0	0	0
22	0	0	0	0	0	0	0	0
23	0	0	0	0	0	0	0	0
24	0	0	0	0	0	0	0	0
25	0	0	0	0	0	0	0	0

Table S8: Average high-NO_x SOA yields with uncertainties (± st. dev) constructed from scenarios and Monte Carlo analysis

Carbon Number	Straight-chain Alkanes	Branched Alkanes	Cycloalkanes (Single Straight Alkyl Chain)	Cycloalkanes (Branched or Multiple Alkyl Chain(s))	Bicycloalkanes	Tricycloalkanes	Aromatics	Polycyclic Aromatic Compounds
1	--	--	--	--	--	--	--	--
2	--	--	--	--	--	--	--	--
3	--	--	--	--	--	--	--	--
4	--	--	--	--	--	--	--	--
5	--	--	--	--	--	--	--	--
6	--	--	0.0004 ± 0.0003	--	--	--	0.14	--
7	--	--	0.0007 ± 0.0006	0.0001 ± 0.0001	--	--	0.083	--
8	0.0006	0.0001	0.0015 ± 0.0011	0.0002 ± 0.0002	--	--	0.048	--
9	0.0012	0.0002	0.0031 ± 0.0020	0.0005 ± 0.0003	0.0005 ± 0.0002	--	0.077 ± 0.057	--
10	0.0026	0.0004	0.0059 ± 0.0039	0.0010 ± 0.0006	0.0010 ± 0.0005	--	0.12 ± 0.08	0.17 ± 0.09
11	0.0053	0.0008	0.010 ± 0.006	0.0018 ± 0.0011	0.0018 ± 0.0008	--	0.15 ± 0.11	0.23 ± 0.11
12	0.010	0.0017	0.016 ± 0.010	0.0034 ± 0.0022	0.0031 ± 0.0015	0.0032 ± 0.0015	0.19 ± 0.16	0.28 ± 0.15
13	0.019	0.0035	0.026 ± 0.016	0.0062 ± 0.0042	0.0056 ± 0.0029	0.0057 ± 0.0030	0.26 ± 0.27	0.40 ± 0.23
14	0.033	0.0070	0.041 ± 0.026	0.011 ± 0.008	0.0097 ± 0.0056	0.0098 ± 0.0057	0.33 ± 0.38	0.49 ± 0.31
15	0.055	0.013	0.064 ± 0.042	0.019 ± 0.014	0.016 ± 0.010	0.017 ± 0.010	0.39 ± 0.45	0.62 ± 0.32
16	0.089	0.024	0.099 ± 0.071	0.031 ± 0.024	0.026 ± 0.017	0.027 ± 0.018	0.43 ± 0.47	0.70 ± 0.35
17	0.14	0.042	0.16 ± 0.11	0.053 ± 0.039	0.044 ± 0.028	0.045 ± 0.028	0.46 ± 0.48	0.75 ± 0.37
18	0.23	0.073	0.24 ± 0.17	0.088 ± 0.065	0.072 ± 0.045	0.073 ± 0.045	0.51 ± 0.47	0.79 ± 0.40
19	0.37	0.12	0.36 ± 0.23	0.14 ± 0.10	0.12 ± 0.07	0.12 ± 0.07	0.56 ± 0.48	0.82 ± 0.42
20	0.56	0.20	0.50 ± 0.26	0.22 ± 0.15	0.19 ± 0.12	0.19 ± 0.12	0.61 ± 0.50	0.82 ± 0.42
21	0.77	0.32	0.66 ± 0.27	0.33 ± 0.19	0.29 ± 0.17	0.30 ± 0.18	0.65 ± 0.52	0.82 ± 0.42
22	0.96	0.47	0.82 ± 0.26	0.45 ± 0.23	0.43 ± 0.24	0.43 ± 0.24	0.67 ± 0.54	0.82 ± 0.42
23	1.08	0.61	0.94 ± 0.23	0.57 ± 0.25	0.56 ± 0.28	0.57 ± 0.28	0.68 ± 0.55	0.82 ± 0.42
24	1.14	0.70	1.03 ± 0.20	0.67 ± 0.25	0.66 ± 0.29	0.67 ± 0.30	0.68 ± 0.55	0.82 ± 0.42
25	1.16	0.75	1.09 ± 0.17	0.73 ± 0.23	0.74 ± 0.28	0.74 ± 0.28	0.68 ± 0.55	0.82 ± 0.42

Table S9: Compound specific liquid gasoline speciation for California in Summer 2010

	Weight percentage in fuel [% weight by carbon (± St. Dev)]					Molar percentage in fuel [% mol (± St. Dev)]				
Compound	**Statewide**	**Bakersfield**	**Berkeley**	**Pasadena**	**Sacramento**	**Statewide**	**Bakersfield**	**Berkeley**	**Pasadena**	**Sacramento**
ethane	0.000±0.000	0.001±0.000	0.000±0.000	0.000±0.000	0.000±0.000	0.001±0.000	0.004±0.001	0.000±0.000	0.001±0.000	0.000±0.000
propane	0.014±0.001	0.030±0.003	0.006±0.002	0.006±0.001	0.012±0.003	0.027±0.002	0.060±0.006	0.012±0.003	0.011±0.002	0.024±0.006
n-butane	0.500±0.038	0.692±0.049	0.420±0.074	0.478±0.098	0.411±0.074	0.747±0.057	1.025±0.073	0.626±0.110	0.722±0.148	0.615±0.110
n-pentane	2.839±0.220	3.920±0.207	2.487±0.484	2.582±0.533	2.366±0.459	3.376±0.261	4.635±0.247	2.957±0.574	3.080±0.634	2.830±0.548
n-hexane	1.837±0.156	2.117±0.037	1.715±0.351	1.841±0.386	1.674±0.341	1.821±0.155	2.085±0.037	1.698±0.347	1.832±0.383	1.668±0.340
n-heptane	1.385±0.116	1.538±0.026	1.652±0.329	1.093±0.214	1.257±0.248	1.177±0.099	1.299±0.022	1.403±0.279	0.933±0.182	1.074±0.211
n-octane	0.621±0.052	0.690±0.015	0.710±0.141	0.493±0.097	0.593±0.119	0.462±0.039	0.510±0.011	0.527±0.105	0.368±0.072	0.444±0.089
n-nonane	0.278±0.024	0.303±0.012	0.298±0.061	0.237±0.047	0.275±0.056	0.184±0.016	0.199±0.008	0.197±0.040	0.158±0.031	0.182±0.037
n-decane	0.116±0.011	0.100±0.003	0.099±0.020	0.147±0.030	0.117±0.023	0.069±0.006	0.059±0.002	0.059±0.012	0.088±0.018	0.070±0.014
n-undecane	0.063±0.007	0.034±0.002	0.054±0.012	0.098±0.022	0.065±0.013	0.034±0.004	0.018±0.001	0.029±0.006	0.054±0.012	0.036±0.007
n-dodecane	0.017±0.003	0.004±0.000	0.010±0.002	0.045±0.011	0.011±0.003	0.009±0.001	0.002±0.000	0.005±0.001	0.022±0.005	0.006±0.001
n-tridecane	0.008±0.001	0.002±0.000	0.002±0.000	0.025±0.005	0.004±0.001	0.004±0.001	0.001±0.000	0.001±0.000	0.012±0.003	0.002±0.000
n-tetradecane	0.004±0.001	0.001±0.000	0.001±0.000	0.011±0.002	0.002±0.000	0.002±0.000	0.000±0.000	0.000±0.000	0.005±0.001	0.001±0.000
n-pentadecane	0.004±0.001	0.002±0.000	0.003±0.001	0.007±0.002	0.003±0.000	0.002±0.000	0.001±0.000	0.001±0.000	0.003±0.001	0.001±0.000
2-methylpropane	0.057±0.006	0.085±0.009	0.043±0.011	0.078±0.018	0.023±0.004	0.085±0.009	0.125±0.014	0.064±0.017	0.119±0.027	0.034±0.006
2-methylbutane	7.821±0.646	7.166±0.192	8.426±1.555	7.475±1.393	8.216±1.508	9.321±0.770	8.470±0.219	10.032±1.849	8.946±1.661	9.838±1.803
2,2-dimethylpropane	0.008±0.001	0.009±0.001	0.007±0.001	0.007±0.002	0.008±0.001	0.009±0.001	0.011±0.001	0.009±0.002	0.009±0.002	0.010±0.002
2-methylpentane	3.858±0.344	3.283±0.246	4.323±0.832	3.922±0.776	3.906±0.736	3.829±0.341	3.231±0.238	4.287±0.824	3.904±0.769	3.895±0.733
3-methylpentane	2.412±0.212	2.097±0.135	2.664±0.511	2.408±0.474	2.479±0.466	2.394±0.210	2.064±0.131	2.642±0.505	2.399±0.470	2.473±0.464
2,2-dimethylbutane	0.902±0.106	0.585±0.107	1.303±0.304	0.728±0.201	0.991±0.186	0.894±0.105	0.575±0.104	1.291±0.300	0.721±0.199	0.989±0.185
2,3-dimethylbutane	1.341±0.109	1.196±0.064	1.327±0.237	1.418±0.254	1.423±0.256	1.333±0.109	1.178±0.062	1.318±0.235	1.417±0.253	1.421±0.255
2-methylhexane	1.339±0.137	1.164±0.078	1.813±0.386	1.090±0.266	1.288±0.270	1.136±0.116	0.981±0.065	1.538±0.328	0.925±0.225	1.100±0.230
3-methylhexane	1.981±0.174	1.883±0.053	2.368±0.474	1.850±0.359	1.823±0.355	1.685±0.148	1.590±0.044	2.011±0.402	1.579±0.305	1.557±0.303
3-ethylpentane	0.087±0.011	0.108±0.012	0.142±0.036	0.054±0.019	0.045±0.016	0.074±0.010	0.091±0.010	0.120±0.031	0.045±0.016	0.038±0.014
2,2-dimethylpentane	0.113±0.010	0.129±0.002	0.121±0.027	0.113±0.024	0.089±0.017	0.096±0.008	0.109±0.002	0.103±0.023	0.096±0.020	0.076±0.014
2,3-dimethylpentane	2.720±0.218	3.048±0.124	1.999±0.348	3.581±0.671	2.251±0.418	2.324±0.188	2.579±0.107	1.704±0.296	3.086±0.580	1.927±0.358
2,4-dimethylpentane	1.200±0.093	1.292±0.051	0.874±0.148	1.516±0.269	1.116±0.204	1.025±0.080	1.093±0.044	0.745±0.126	1.304±0.232	0.956±0.174
3,3-Dimethylpentane	0.112±0.010	0.133±0.002	0.111±0.029	0.112±0.023	0.093±0.018	0.095±0.009	0.112±0.001	0.094±0.025	0.096±0.019	0.080±0.015
2,2,3-Trimethylbutane	0.044±0.003	0.044±0.000	0.042±0.007	0.044±0.008	0.044±0.008	0.037±0.003	0.037±0.000	0.036±0.006	0.038±0.007	0.038±0.007
2-Methylheptane	0.940±0.078	0.990±0.013	0.976±0.191	0.913±0.176	0.882±0.171	0.700±0.058	0.731±0.010	0.726±0.141	0.683±0.132	0.660±0.128
3-Methylheptane	1.014±0.083	1.115±0.015	1.089±0.213	0.917±0.180	0.936±0.181	0.754±0.062	0.824±0.011	0.809±0.158	0.684±0.134	0.700±0.135
4-Methylheptane	0.427±0.034	0.456±0.005	0.443±0.085	0.399±0.076	0.409±0.077	0.318±0.026	0.337±0.004	0.330±0.063	0.299±0.056	0.306±0.058
2,2-dimethylhexane	0.059±0.005	0.080±0.004	0.068±0.015	0.045±0.009	0.045±0.008	0.044±0.004	0.059±0.003	0.050±0.011	0.033±0.007	0.033±0.006
2,4-dimethylhexane	0.622±0.047	0.630±0.011	0.575±0.099	0.638±0.112	0.645±0.114	0.464±0.035	0.466±0.008	0.429±0.074	0.479±0.084	0.483±0.086
2,5-dimethylhexane	0.604±0.046	0.599±0.012	0.544±0.092	0.585±0.101	0.688±0.121	0.451±0.034	0.443±0.009	0.406±0.069	0.439±0.075	0.516±0.091
3,3-dimethylhexane	0.070±0.006	0.097±0.005	0.078±0.016	0.050±0.010	0.054±0.010	0.052±0.004	0.072±0.004	0.058±0.012	0.037±0.007	0.041±0.008
2-Me-3-Et-pentane	0.572±0.043	0.577±0.011	0.503±0.086	0.596±0.104	0.611±0.109	0.427±0.032	0.427±0.009	0.375±0.064	0.448±0.078	0.458±0.081
2,2,3-triMe-pentane	0.167±0.014	0.152±0.005	0.146±0.026	0.145±0.025	0.226±0.040	0.125±0.010	0.113±0.004	0.109±0.019	0.109±0.019	0.170±0.030
2,2,4-triMe-pentane	3.639±0.293	3.171±0.123	2.871±0.496	4.106±0.706	4.406±0.786	2.724±0.220	2.346±0.090	2.148±0.371	3.094±0.532	3.306±0.590
2,3,3-triMe-pentane	1.374±0.112	1.261±0.042	1.168±0.205	1.161±0.202	1.904±0.340	1.026±0.084	0.934±0.031	0.873±0.153	0.871±0.152	1.428±0.255
2,3,4-triMe-pentane	1.405±0.111	1.330±0.043	1.153±0.195	1.325±0.227	1.810±0.324	1.050±0.083	0.985±0.032	0.862±0.146	0.998±0.171	1.357±0.243
2,2,5-trimethylhexane	0.894±0.083	0.896±0.041	0.874±0.205	0.656±0.117	1.148±0.228	0.594±0.055	0.590±0.028	0.582±0.137	0.438±0.078	0.767±0.152
2,3,5-trimethylhexane	0.183±0.016	0.194±0.008	0.174±0.038	0.141±0.025	0.225±0.043	0.122±0.010	0.128±0.005	0.116±0.025	0.094±0.017	0.150±0.028
2,4,4-trimethylhexane	0.089±0.008	0.072±0.003	0.072±0.014	0.109±0.021	0.104±0.019	0.059±0.005	0.047±0.002	0.048±0.009	0.073±0.014	0.069±0.013
2,4-dimethylheptane	0.115±0.009	0.144±0.007	0.118±0.023	0.090±0.018	0.105±0.019	0.076±0.006	0.095±0.004	0.078±0.015	0.060±0.012	0.070±0.013
2,6-dimethylheptane	0.186±0.018	0.165±0.003	0.168±0.035	0.227±0.050	0.184±0.036	0.123±0.012	0.108±0.002	0.111±0.023	0.152±0.033	0.122±0.024
2,5-dimethylheptane	0.009±0.001	0.010±0.000	0.010±0.002	0.008±0.002	0.010±0.002	0.006±0.001	0.006±0.000	0.006±0.001	0.005±0.001	0.007±0.001

3,5-dimethylheptane	0.391±0.031	0.448±0.016	0.360±0.069	0.383±0.073	0.375±0.071	0.259±0.021	0.294±0.010	0.238±0.046	0.255±0.049	0.249±0.047
2,3-dimethylheptane	0.121±0.009	0.130±0.004	0.119±0.022	0.108±0.020	0.129±0.023	0.080±0.006	0.085±0.003	0.079±0.014	0.071±0.013	0.086±0.016
3,4-dimethylheptane	0.058±0.005	0.057±0.001	0.053±0.010	0.063±0.013	0.060±0.011	0.038±0.003	0.037±0.001	0.035±0.007	0.042±0.008	0.040±0.007
3,3-dimethylheptane	0.039±0.004	0.029±0.001	0.028±0.006	0.059±0.013	0.039±0.008	0.026±0.003	0.019±0.001	0.019±0.004	0.040±0.009	0.026±0.005
4,4-dimethylheptane	0.030±0.003	0.024±0.002	0.022±0.004	0.047±0.010	0.027±0.006	0.020±0.002	0.016±0.001	0.014±0.003	0.032±0.007	0.018±0.004
2-methyloctane	0.323±0.027	0.343±0.007	0.313±0.063	0.322±0.063	0.314±0.063	0.214±0.018	0.225±0.005	0.207±0.042	0.214±0.042	0.209±0.042
3-methyloctane	0.400±0.033	0.437±0.014	0.382±0.076	0.389±0.074	0.393±0.076	0.265±0.022	0.287±0.009	0.253±0.050	0.259±0.049	0.261±0.050
4-methyloctane	0.274±0.023	0.312±0.011	0.269±0.054	0.260±0.051	0.257±0.051	0.182±0.015	0.205±0.007	0.178±0.036	0.173±0.034	0.171±0.034
3-ethylheptane	0.090±0.008	0.098±0.003	0.092±0.019	0.078±0.017	0.094±0.019	0.060±0.005	0.064±0.002	0.061±0.012	0.051±0.011	0.062±0.013
4-ethylheptane	0.054±0.004	0.064±0.003	0.053±0.010	0.048±0.009	0.051±0.010	0.036±0.003	0.043±0.002	0.035±0.007	0.032±0.006	0.034±0.007
2,2-dimethylheptane	0.024±0.002	0.040±0.003	0.024±0.005	0.015±0.003	0.017±0.003	0.016±0.001	0.026±0.002	0.016±0.003	0.010±0.002	0.011±0.002
3-Me-4-Et-hexane	0.029±0.002	0.037±0.002	0.030±0.006	0.020±0.004	0.028±0.005	0.019±0.001	0.024±0.001	0.020±0.004	0.013±0.003	0.019±0.003
2,2,3-trimethylhexane	0.020±0.003	0.047±0.005	0.022±0.009	0.000±0.000	0.012±0.004	0.013±0.002	0.031±0.003	0.014±0.006	0.000±0.000	0.008±0.002
2-methylnonane	0.111±0.010	0.101±0.002	0.105±0.022	0.120±0.025	0.119±0.025	0.066±0.006	0.060±0.001	0.062±0.013	0.072±0.015	0.071±0.015
3-methylnonane	0.110±0.010	0.108±0.004	0.104±0.022	0.114±0.023	0.113±0.023	0.065±0.006	0.064±0.002	0.062±0.013	0.068±0.014	0.068±0.014
4-methylnonane	0.145±0.015	0.207±0.006	0.116±0.030	0.074±0.023	0.182±0.046	0.086±0.009	0.123±0.004	0.069±0.018	0.044±0.014	0.109±0.027
3-ethyloctane	0.004±0.001	0.000±0.000	0.001±0.001	0.010±0.003	0.005±0.002	0.003±0.000	0.000±0.000	0.001±0.000	0.006±0.002	0.003±0.001
4-ethyloctane	0.048±0.004	0.044±0.002	0.043±0.008	0.054±0.011	0.050±0.010	0.029±0.003	0.026±0.001	0.026±0.005	0.033±0.006	0.030±0.006
2,2-dimethyloctane	0.055±0.005	0.057±0.003	0.050±0.010	0.058±0.012	0.055±0.011	0.033±0.003	0.034±0.002	0.030±0.006	0.035±0.007	0.033±0.007
2,3-dimethyloctane	0.042±0.004	0.038±0.002	0.035±0.007	0.053±0.012	0.040±0.008	0.025±0.003	0.022±0.001	0.021±0.004	0.032±0.008	0.024±0.005
2,6-dimethyloctane	0.019±0.003	0.004±0.001	0.011±0.004	0.037±0.010	0.024±0.006	0.011±0.002	0.002±0.001	0.006±0.002	0.022±0.006	0.014±0.004
4,4-dimethyloctane	0.022±0.002	0.021±0.001	0.020±0.004	0.026±0.005	0.023±0.005	0.013±0.001	0.012±0.000	0.012±0.002	0.015±0.003	0.014±0.003
2-methyldecane	0.046±0.004	0.053±0.002	0.031±0.006	0.043±0.008	0.059±0.011	0.025±0.002	0.029±0.001	0.017±0.003	0.024±0.004	0.032±0.006
3-methyldecane	0.033±0.004	0.020±0.001	0.030±0.008	0.048±0.011	0.036±0.008	0.018±0.002	0.010±0.001	0.016±0.004	0.026±0.006	0.020±0.004
2,6-dimethylnonane	0.025±0.004	0.012±0.001	0.018±0.004	0.047±0.012	0.024±0.005	0.014±0.002	0.007±0.000	0.010±0.002	0.026±0.007	0.013±0.003
C-11 Isoparaffins	0.012±0.001	0.009±0.000	0.010±0.002	0.017±0.003	0.013±0.002	0.006±0.001	0.005±0.000	0.005±0.001	0.009±0.002	0.007±0.001
C-11 Isoparaf alky	0.026±0.003	0.019±0.001	0.018±0.004	0.041±0.010	0.026±0.006	0.014±0.002	0.011±0.001	0.010±0.002	0.022±0.006	0.014±0.003
223-triMethylheptane	0.068±0.006	0.070±0.003	0.062±0.012	0.070±0.014	0.069±0.014	0.041±0.003	0.042±0.002	0.037±0.007	0.042±0.008	0.041±0.008
224-triMe-heptane	0.031±0.002	0.029±0.001	0.026±0.005	0.030±0.005	0.039±0.007	0.019±0.001	0.017±0.001	0.016±0.003	0.018±0.003	0.023±0.004
225-triMe-heptane	0.067±0.007	0.046±0.010	0.067±0.014	0.085±0.017	0.069±0.013	0.040±0.004	0.027±0.006	0.040±0.008	0.051±0.011	0.041±0.008
236-triMe-heptane	0.077±0.006	0.082±0.004	0.058±0.010	0.088±0.016	0.079±0.014	0.046±0.004	0.049±0.002	0.035±0.006	0.053±0.009	0.047±0.008
244-triMe-heptane	0.152±0.019	0.093±0.007	0.124±0.029	0.235±0.058	0.157±0.039	0.091±0.011	0.055±0.004	0.074±0.017	0.142±0.035	0.094±0.023
245-triMe-heptane	0.029±0.002	0.026±0.001	0.021±0.004	0.036±0.007	0.030±0.005	0.017±0.001	0.016±0.001	0.013±0.002	0.022±0.004	0.018±0.003
246-triMe-heptane	0.026±0.003	0.022±0.000	0.020±0.004	0.035±0.008	0.028±0.005	0.016±0.002	0.013±0.000	0.012±0.002	0.021±0.005	0.017±0.003
255-triMe-heptane	0.120±0.010	0.116±0.005	0.089±0.015	0.147±0.027	0.128±0.023	0.072±0.006	0.069±0.003	0.053±0.009	0.088±0.016	0.077±0.014
335-triMe-heptane	0.000±0.000	0.000±0.000	0.000±0.000	0.001±0.000	0.000±0.000	0.000±0.000	0.000±0.000	0.000±0.000	0.000±0.000	0.000±0.000
22466pentMe-heptane	0.008±0.002	0.000±0.000	0.005±0.002	0.019±0.006	0.007±0.002	0.004±0.001	0.000±0.000	0.003±0.001	0.010±0.003	0.004±0.001
C-10 Isoparaffin O	0.027±0.003	0.019±0.001	0.016±0.003	0.047±0.010	0.027±0.005	0.016±0.002	0.011±0.000	0.010±0.002	0.029±0.006	0.016±0.003
2-Me-3-Et-heptane	0.047±0.006	0.018±0.004	0.049±0.010	0.066±0.017	0.057±0.012	0.028±0.004	0.011±0.002	0.029±0.006	0.040±0.011	0.034±0.007
2,6-diMe-hendecane	0.007±0.001	0.005±0.000	0.006±0.001	0.012±0.002	0.006±0.001	0.004±0.000	0.002±0.000	0.003±0.001	0.006±0.001	0.003±0.001
2,6,10triM-hendecane	0.007±0.001	0.004±0.000	0.004±0.001	0.014±0.003	0.007±0.001	0.004±0.000	0.002±0.000	0.002±0.000	0.007±0.001	0.003±0.001
2,6,10triMe-dodecane	0.006±0.001	0.001±0.000	0.005±0.001	0.011±0.002	0.005±0.001	0.003±0.000	0.000±0.000	0.002±0.001	0.005±0.001	0.002±0.000
C-9 Naphthenes	0.047±0.004	0.047±0.001	0.045±0.009	0.047±0.009	0.050±0.009	0.031±0.003	0.031±0.001	0.029±0.006	0.031±0.006	0.033±0.006
Cyclopentane	0.475±0.037	0.615±0.028	0.466±0.092	0.385±0.079	0.432±0.081	0.565±0.044	0.727±0.033	0.554±0.109	0.459±0.094	0.518±0.097
Methylcyclopentane	2.669±0.220	3.037±0.051	2.734±0.550	2.470±0.491	2.435±0.482	2.648±0.219	2.992±0.052	2.708±0.544	2.463±0.488	2.428±0.480
Ethylcyclopentane	0.332±0.029	0.369±0.009	0.299±0.063	0.346±0.070	0.314±0.064	0.283±0.024	0.312±0.007	0.254±0.054	0.297±0.060	0.269±0.055
1T2-diMecyclopentane	0.617±0.050	0.986±0.079	0.529±0.118	0.483±0.101	0.470±0.096	0.525±0.042	0.833±0.067	0.450±0.100	0.414±0.087	0.402±0.082
1C3-diMecyclopentane	0.679±0.058	0.814±0.031	0.655±0.146	0.638±0.128	0.610±0.124	0.578±0.050	0.687±0.026	0.557±0.124	0.547±0.110	0.521±0.106
1T3-diMecyclopentane	0.592±0.050	0.741±0.032	0.558±0.124	0.555±0.112	0.515±0.105	0.504±0.043	0.626±0.027	0.474±0.105	0.475±0.096	0.440±0.090
Propylcyclopentane	0.024±0.002	0.024±0.001	0.018±0.004	0.029±0.006	0.023±0.005	0.018±0.002	0.018±0.000	0.013±0.003	0.022±0.005	0.018±0.003

112-triMeCyPentane	0.007±0.001	0.006±0.001	0.005±0.001	0.011±0.002	0.006±0.001	0.005±0.001	0.004±0.000	0.004±0.001	0.008±0.002	0.005±0.001
113-triMeCyPentane	0.146±0.012	0.204±0.010	0.111±0.023	0.154±0.032	0.117±0.024	0.109±0.009	0.151±0.007	0.083±0.017	0.116±0.024	0.087±0.018
1C2C3-triMeCypentane	0.004±0.000	0.003±0.000	0.003±0.001	0.005±0.001	0.004±0.001	0.003±0.000	0.002±0.000	0.002±0.001	0.004±0.001	0.003±0.001
1C2T3-triMeCyPentane	0.013±0.001	0.016±0.000	0.013±0.003	0.013±0.003	0.011±0.002	0.010±0.001	0.012±0.000	0.009±0.002	0.010±0.002	0.009±0.002
1T2C3-triMeCyPentane	0.149±0.012	0.221±0.015	0.104±0.022	0.156±0.034	0.113±0.023	0.111±0.009	0.164±0.011	0.078±0.016	0.117±0.026	0.084±0.017
1C2C4-triMeCyPentane	0.005±0.001	0.004±0.001	0.003±0.001	0.008±0.002	0.003±0.001	0.003±0.000	0.002±0.000	0.002±0.001	0.006±0.001	0.003±0.001
1T2C4-triMeCyPentane	0.239±0.021	0.268±0.007	0.189±0.040	0.288±0.060	0.211±0.044	0.178±0.016	0.198±0.005	0.141±0.030	0.216±0.045	0.158±0.033
Cyclohexane	1.076±0.100	1.147±0.044	1.313±0.289	0.820±0.178	1.024±0.210	1.066±0.099	1.130±0.044	1.299±0.285	0.815±0.177	1.021±0.209
Methylcyclohexane	1.424±0.123	1.542±0.028	1.361±0.284	1.473±0.299	1.322±0.267	1.212±0.105	1.302±0.023	1.157±0.241	1.262±0.256	1.129±0.228
Ethylcyclohexane	0.191±0.022	0.125±0.011	0.134±0.032	0.312±0.070	0.192±0.043	0.142±0.017	0.092±0.008	0.100±0.024	0.235±0.053	0.144±0.032
1,1-diMecyclohexane	0.031±0.003	0.041±0.002	0.026±0.006	0.031±0.007	0.026±0.005	0.023±0.002	0.030±0.002	0.019±0.004	0.023±0.005	0.019±0.004
1C2-diMecyclohexane	0.060±0.006	0.045±0.002	0.047±0.011	0.089±0.020	0.062±0.013	0.045±0.005	0.033±0.002	0.035±0.008	0.067±0.015	0.046±0.010
1T2-diMecyclohexane	0.121±0.012	0.113±0.005	0.094±0.019	0.164±0.035	0.111±0.022	0.090±0.009	0.083±0.004	0.070±0.014	0.123±0.027	0.083±0.016
1C3-diMecyclohexane	0.259±0.027	0.220±0.014	0.204±0.044	0.375±0.082	0.239±0.050	0.193±0.020	0.163±0.010	0.151±0.033	0.281±0.062	0.178±0.037
1T3-diMecyclohexane	0.208±0.022	0.157±0.011	0.161±0.036	0.311±0.066	0.204±0.042	0.155±0.016	0.115±0.008	0.120±0.027	0.233±0.050	0.152±0.032
1C4-diMecyclohexane	0.051±0.005	0.043±0.004	0.032±0.007	0.085±0.018	0.046±0.009	0.038±0.004	0.032±0.003	0.024±0.005	0.064±0.014	0.034±0.007
Propylcyclohexane	0.043±0.005	0.027±0.001	0.032±0.007	0.069±0.017	0.044±0.010	0.029±0.003	0.018±0.000	0.021±0.005	0.046±0.011	0.029±0.006
iso-Bu-Cyclohexane	0.004±0.000	0.003±0.000	0.004±0.001	0.004±0.001	0.006±0.001	0.003±0.000	0.002±0.000	0.002±0.001	0.003±0.001	0.004±0.001
sec-Bu-Cyclohexane	0.017±0.002	0.011±0.000	0.014±0.003	0.023±0.005	0.019±0.004	0.010±0.001	0.007±0.000	0.008±0.002	0.014±0.003	0.011±0.002
113-t4-tetraMeCyPent	0.113±0.011	0.108±0.002	0.090±0.020	0.143±0.030	0.111±0.023	0.075±0.007	0.071±0.001	0.060±0.014	0.096±0.020	0.074±0.015
1Me-1EtCyclopentane	0.100±0.010	0.109±0.004	0.072±0.017	0.136±0.031	0.082±0.020	0.074±0.008	0.080±0.003	0.053±0.013	0.103±0.023	0.061±0.015
1Me-C2EtCyclopentane	0.055±0.006	0.040±0.002	0.050±0.012	0.069±0.014	0.063±0.013	0.041±0.004	0.030±0.001	0.037±0.009	0.052±0.011	0.047±0.010
1MeC3EtCyclopentane	0.165±0.016	0.143±0.005	0.135±0.031	0.219±0.046	0.165±0.035	0.123±0.012	0.106±0.003	0.100±0.023	0.165±0.034	0.123±0.026
1-M-t-3-Et Cycpentane	0.164±0.016	0.149±0.005	0.126±0.028	0.223±0.045	0.161±0.033	0.123±0.012	0.110±0.004	0.093±0.020	0.167±0.034	0.120±0.024
1MeC3Etcyclohexane	0.082±0.008	0.095±0.004	0.055±0.011	0.086±0.018	0.091±0.022	0.054±0.005	0.063±0.003	0.037±0.008	0.057±0.012	0.061±0.015
1MeC4EtCyclohexane	0.011±0.001	0.007±0.001	0.009±0.002	0.015±0.003	0.013±0.002	0.007±0.001	0.005±0.000	0.006±0.001	0.010±0.002	0.009±0.002
1MeT4Etcyclohexane	0.032±0.003	0.025±0.000	0.026±0.006	0.044±0.010	0.034±0.007	0.022±0.002	0.016±0.000	0.017±0.004	0.030±0.007	0.023±0.005
113-triMecyclohexane	0.048±0.004	0.045±0.001	0.043±0.009	0.056±0.011	0.048±0.009	0.032±0.003	0.030±0.000	0.029±0.006	0.037±0.007	0.032±0.006
1C2C3-triMeCyhexane	0.000±0.000	0.000±0.000	0.000±0.000	0.000±0.000	0.000±0.000	0.000±0.000	0.000±0.000	0.000±0.000	0.000±0.000	0.000±0.000
1C2T3-triMeCyhexane	0.023±0.002	0.021±0.002	0.018±0.004	0.029±0.006	0.023±0.005	0.015±0.001	0.014±0.001	0.012±0.003	0.019±0.004	0.015±0.003
1C3T5-triMeCyhexane	0.142±0.015	0.105±0.004	0.106±0.022	0.215±0.047	0.144±0.028	0.095±0.010	0.069±0.003	0.070±0.014	0.144±0.032	0.096±0.018
1-M-t2-PropCyHexane	0.062±0.006	0.049±0.002	0.042±0.007	0.089±0.017	0.069±0.012	0.037±0.003	0.029±0.001	0.025±0.004	0.053±0.010	0.041±0.007
C-9 Naphthene A	0.013±0.001	0.010±0.001	0.009±0.002	0.019±0.004	0.014±0.003	0.008±0.001	0.006±0.001	0.006±0.002	0.013±0.003	0.009±0.002
C-9 Naphthene B	0.011±0.001	0.011±0.000	0.008±0.002	0.014±0.003	0.011±0.002	0.007±0.001	0.007±0.000	0.005±0.001	0.009±0.002	0.007±0.001
C-9 Naphthene I	0.014±0.002	0.012±0.003	0.014±0.004	0.004±0.001	0.025±0.005	0.009±0.001	0.008±0.002	0.009±0.002	0.003±0.001	0.017±0.003
C-10 Cyclohexane AA	0.014±0.002	0.003±0.001	0.009±0.003	0.029±0.008	0.013±0.003	0.009±0.002	0.002±0.001	0.006±0.002	0.019±0.005	0.009±0.002
C-10 Cyclohexane BB	0.027±0.004	0.013±0.001	0.017±0.004	0.054±0.016	0.025±0.005	0.016±0.003	0.008±0.000	0.010±0.002	0.032±0.009	0.015±0.003
2MePropylCyclohexane	0.001±0.001	0.000±0.000	0.000±0.000	0.005±0.003	0.000±0.000	0.001±0.000	0.000±0.000	0.000±0.000	0.003±0.002	0.000±0.000
Benzene	0.750±0.063	0.800±0.017	0.725±0.145	0.805±0.154	0.669±0.134	0.744±0.062	0.788±0.017	0.719±0.143	0.804±0.153	0.667±0.133
Toluene	7.523±0.596	9.344±0.470	8.219±1.614	5.710±1.100	6.818±1.280	6.397±0.506	7.904±0.400	6.980±1.368	4.874±0.935	5.829±1.093
Ethylbenzene	1.433±0.124	1.280±0.041	1.677±0.324	1.302±0.251	1.475±0.278	1.067±0.092	0.946±0.030	1.246±0.240	0.973±0.187	1.103±0.208
o-Xylene	2.209±0.186	2.148±0.027	2.455±0.474	1.984±0.382	2.251±0.423	1.645±0.138	1.588±0.020	1.825±0.352	1.483±0.284	1.684±0.316
m-Xylene	4.881±0.409	4.831±0.069	5.533±1.077	4.191±0.804	4.969±0.933	3.633±0.305	3.571±0.053	4.113±0.800	3.132±0.598	3.717±0.698
p-Xylene	1.168±0.094	1.196±0.010	1.228±0.232	1.082±0.203	1.165±0.216	0.869±0.070	0.884±0.008	0.913±0.173	0.809±0.151	0.871±0.162
Cumene	0.097±0.009	0.090±0.004	0.114±0.022	0.088±0.018	0.096±0.018	0.064±0.006	0.059±0.002	0.076±0.015	0.058±0.012	0.064±0.012
1-Me-2-Et-benzene	0.545±0.046	0.519±0.011	0.609±0.118	0.494±0.096	0.556±0.106	0.360±0.031	0.341±0.007	0.403±0.078	0.328±0.064	0.370±0.070
1-Me-3-Et-benzene	1.575±0.133	1.501±0.015	1.739±0.337	1.434±0.274	1.626±0.309	1.042±0.088	0.986±0.010	1.149±0.223	0.953±0.181	1.081±0.205
1-Me-4-Et-benzene	0.681±0.057	0.667±0.006	0.748±0.145	0.614±0.118	0.695±0.132	0.451±0.038	0.438±0.004	0.494±0.096	0.408±0.078	0.462±0.087
123-triMe-benzene	0.587±0.049	0.581±0.012	0.606±0.117	0.575±0.111	0.586±0.112	0.388±0.032	0.382±0.007	0.400±0.077	0.382±0.073	0.389±0.074
124-TriMe-benzene	2.629±0.213	2.824±0.044	2.705±0.522	2.417±0.463	2.568±0.485	1.739±0.141	1.856±0.029	1.787±0.344	1.606±0.307	1.708±0.322

135-triMe-benzene	0.800±0.065	0.881±0.028	0.836±0.163	0.704±0.133	0.781±0.148	0.530±0.043	0.579±0.019	0.552±0.108	0.468±0.088	0.519±0.098
Butylbenzene	0.071±0.008	0.027±0.008	0.084±0.019	0.077±0.017	0.095±0.020	0.042±0.005	0.016±0.005	0.050±0.011	0.047±0.010	0.057±0.012
Isobutylbenzene	0.085±0.007	0.071±0.002	0.072±0.012	0.112±0.021	0.087±0.016	0.051±0.004	0.042±0.001	0.043±0.007	0.068±0.013	0.052±0.009
Sec-butylbenzene	0.042±0.004	0.029±0.002	0.050±0.010	0.036±0.008	0.051±0.011	0.025±0.002	0.017±0.001	0.030±0.006	0.022±0.005	0.031±0.006
T-butylbenzene	0.006±0.003	0.000±0.000	0.000±0.000	0.024±0.012	0.000±0.000	0.004±0.002	0.000±0.000	0.000±0.000	0.015±0.007	0.000±0.000
o-Cymene	0.019±0.002	0.012±0.001	0.016±0.003	0.033±0.007	0.014±0.003	0.011±0.001	0.007±0.001	0.010±0.002	0.020±0.005	0.008±0.002
m-Cymene	0.066±0.006	0.046±0.004	0.071±0.014	0.075±0.014	0.073±0.014	0.040±0.004	0.027±0.003	0.043±0.008	0.045±0.009	0.044±0.008
p-Cymene	0.020±0.002	0.014±0.001	0.021±0.004	0.022±0.004	0.022±0.004	0.012±0.001	0.008±0.001	0.013±0.003	0.013±0.003	0.013±0.003
1234-tetMe-benzene	0.071±0.006	0.068±0.002	0.063±0.013	0.084±0.016	0.067±0.013	0.042±0.004	0.041±0.001	0.038±0.007	0.050±0.009	0.040±0.007
1235-tetMe-benzene	0.230±0.019	0.226±0.004	0.229±0.044	0.249±0.047	0.214±0.040	0.137±0.011	0.134±0.002	0.137±0.026	0.149±0.028	0.128±0.024
1245-tetMe-benzene	0.170±0.014	0.168±0.003	0.173±0.033	0.178±0.033	0.159±0.030	0.101±0.008	0.099±0.002	0.103±0.020	0.107±0.020	0.095±0.018
Pentamethylbenzene	0.015±0.001	0.012±0.000	0.011±0.002	0.023±0.004	0.012±0.002	0.008±0.001	0.007±0.000	0.006±0.001	0.013±0.002	0.007±0.001
Propylbenzene	0.499±0.043	0.453±0.008	0.557±0.109	0.488±0.093	0.498±0.096	0.330±0.029	0.297±0.005	0.368±0.072	0.325±0.062	0.331±0.064
1,3-diethylbenzene	0.108±0.010	0.081±0.004	0.120±0.024	0.113±0.021	0.117±0.023	0.064±0.006	0.048±0.002	0.071±0.014	0.068±0.013	0.070±0.014
1-Me-3-Pr-benzene	0.291±0.026	0.238±0.008	0.321±0.063	0.298±0.057	0.307±0.060	0.174±0.016	0.141±0.005	0.191±0.037	0.179±0.034	0.184±0.036
1-Me-4-Pr-benzene	0.182±0.016	0.172±0.003	0.197±0.039	0.186±0.035	0.175±0.033	0.109±0.009	0.102±0.002	0.117±0.023	0.111±0.021	0.104±0.020
Indan	0.274±0.024	0.255±0.006	0.278±0.055	0.265±0.050	0.298±0.059	0.181±0.016	0.167±0.004	0.184±0.037	0.176±0.033	0.198±0.039
1,4-diethylbenzene	0.329±0.029	0.279±0.005	0.349±0.068	0.347±0.066	0.341±0.065	0.196±0.017	0.165±0.003	0.208±0.040	0.208±0.039	0.204±0.039
1-Me-2-Pr-benzene	0.099±0.009	0.077±0.004	0.106±0.021	0.113±0.022	0.100±0.019	0.059±0.005	0.045±0.002	0.063±0.012	0.068±0.013	0.060±0.011
14-diMe2Et-benzene	0.237±0.022	0.187±0.006	0.253±0.051	0.255±0.049	0.253±0.050	0.141±0.013	0.110±0.003	0.151±0.030	0.153±0.029	0.151±0.030
13-diMe4Et-benzene	0.193±0.017	0.160±0.004	0.207±0.041	0.201±0.038	0.203±0.039	0.115±0.010	0.095±0.002	0.123±0.024	0.120±0.023	0.122±0.023
12-diMe4Et-benzene	0.297±0.026	0.256±0.005	0.326±0.064	0.305±0.058	0.302±0.058	0.177±0.015	0.151±0.003	0.194±0.038	0.182±0.034	0.180±0.035
13-diMe2Et-benzene	0.026±0.002	0.020±0.001	0.025±0.005	0.033±0.007	0.027±0.005	0.016±0.001	0.012±0.001	0.015±0.003	0.020±0.004	0.016±0.003
Indene	0.035±0.003	0.027±0.001	0.027±0.005	0.051±0.011	0.035±0.007	0.023±0.002	0.018±0.001	0.018±0.003	0.035±0.007	0.023±0.004
12-diMe3Et-benzene	0.087±0.008	0.065±0.003	0.091±0.018	0.104±0.020	0.089±0.017	0.052±0.005	0.039±0.002	0.054±0.011	0.062±0.012	0.053±0.010
1-Me35diEt-benzene	0.032±0.003	0.018±0.001	0.030±0.007	0.047±0.010	0.033±0.007	0.017±0.002	0.010±0.001	0.017±0.004	0.026±0.005	0.018±0.004
1-Phenyl-2Me butane	0.031±0.003	0.021±0.001	0.030±0.005	0.040±0.008	0.035±0.006	0.017±0.002	0.011±0.001	0.016±0.003	0.022±0.004	0.019±0.003
1-Phenyl-3Me butane	0.014±0.001	0.011±0.000	0.010±0.002	0.019±0.004	0.016±0.003	0.008±0.001	0.006±0.000	0.006±0.001	0.010±0.002	0.009±0.002
124-triMe-5Etbenzene	0.026±0.002	0.022±0.001	0.022±0.004	0.036±0.007	0.025±0.005	0.014±0.001	0.012±0.000	0.012±0.002	0.020±0.004	0.013±0.003
123-triMe-5Etbenzene	0.024±0.003	0.015±0.000	0.018±0.004	0.045±0.009	0.018±0.004	0.013±0.001	0.008±0.000	0.010±0.002	0.025±0.005	0.010±0.002
124-triMe-3Etbenzene	0.006±0.001	0.003±0.000	0.004±0.001	0.011±0.002	0.006±0.001	0.003±0.000	0.002±0.000	0.002±0.000	0.006±0.001	0.003±0.001
12-diMe-3Pr-benzene	0.040±0.004	0.029±0.001	0.039±0.008	0.054±0.011	0.038±0.008	0.022±0.002	0.015±0.000	0.021±0.005	0.030±0.006	0.021±0.004
135-triMe-2Etbenzene	0.026±0.002	0.022±0.001	0.022±0.004	0.030±0.005	0.029±0.005	0.014±0.001	0.012±0.000	0.012±0.002	0.016±0.003	0.016±0.003
Tetralin	0.010±0.002	0.001±0.000	0.001±0.000	0.027±0.009	0.011±0.004	0.006±0.001	0.000±0.000	0.001±0.000	0.016±0.005	0.007±0.002
1-Me-3Bu-benzene	0.054±0.006	0.034±0.002	0.054±0.011	0.079±0.018	0.048±0.010	0.029±0.003	0.018±0.001	0.029±0.006	0.043±0.010	0.026±0.005
12-diMe-4Pr-benzene	0.055±0.005	0.045±0.002	0.044±0.008	0.069±0.012	0.061±0.011	0.033±0.003	0.027±0.001	0.026±0.005	0.041±0.007	0.036±0.006
125-triMe-3Etbenzene	0.027±0.003	0.020±0.001	0.024±0.005	0.039±0.007	0.024±0.005	0.016±0.002	0.012±0.000	0.014±0.003	0.023±0.004	0.014±0.003
123-triMe4Et-benzene	0.004±0.001	0.002±0.000	0.003±0.001	0.009±0.003	0.004±0.001	0.003±0.000	0.001±0.000	0.002±0.000	0.006±0.002	0.002±0.000
C-11 Aromatic K	0.017±0.002	0.013±0.001	0.013±0.002	0.026±0.005	0.017±0.003	0.011±0.001	0.008±0.000	0.008±0.001	0.016±0.003	0.010±0.002
Cis-hydrindane	0.015±0.001	0.014±0.001	0.013±0.003	0.017±0.004	0.016±0.003	0.010±0.001	0.009±0.000	0.009±0.002	0.012±0.002	0.010±0.002
C-7 cyclopentene A	0.036±0.004	0.026±0.003	0.019±0.005	0.064±0.013	0.034±0.007	0.030±0.003	0.022±0.002	0.016±0.004	0.055±0.011	0.029±0.006
C-7 cyclopentene B	0.034±0.004	0.025±0.003	0.018±0.005	0.062±0.013	0.033±0.007	0.029±0.003	0.021±0.002	0.015±0.004	0.053±0.011	0.028±0.006
C-11 Aromatic E	0.059±0.006	0.032±0.002	0.057±0.012	0.086±0.018	0.061±0.013	0.033±0.003	0.018±0.001	0.032±0.007	0.048±0.010	0.033±0.007
C-12 Aromatic A	0.002±0.000	0.003±0.000	0.001±0.000	0.003±0.002	0.001±0.000	0.001±0.000	0.001±0.000	0.000±0.000	0.002±0.001	0.001±0.000
C-12 Aromatic E	0.001±0.000	0.000±0.000	0.001±0.000	0.004±0.002	0.000±0.000	0.001±0.000	0.000±0.000	0.000±0.000	0.002±0.001	0.000±0.000
C-12 Aromatic F	0.005±0.001	0.003±0.000	0.003±0.001	0.011±0.002	0.004±0.001	0.003±0.000	0.001±0.000	0.002±0.000	0.006±0.001	0.002±0.000
Octylbenzene	0.001±0.000	0.000±0.000	0.000±0.000	0.001±0.000	0.001±0.000	0.000±0.000	0.000±0.000	0.000±0.000	0.000±0.000	0.000±0.000
1-Methylindane	0.101±0.010	0.068±0.003	0.097±0.020	0.136±0.028	0.101±0.020	0.060±0.006	0.040±0.002	0.058±0.012	0.081±0.017	0.061±0.012
2-Methylindane	0.151±0.015	0.102±0.004	0.149±0.030	0.202±0.041	0.151±0.031	0.090±0.009	0.061±0.002	0.089±0.018	0.122±0.025	0.090±0.018
4-Methylindane	0.002±0.000	0.002±0.001	0.004±0.001	0.000±0.000	0.002±0.001	0.001±0.000	0.001±0.001	0.003±0.001	0.000±0.000	0.001±0.001

Dimethylindane A	0.017±0.002	0.011±0.000	0.013±0.002	0.031±0.006	0.014±0.003	0.009±0.001	0.006±0.000	0.007±0.001	0.017±0.003	0.008±0.001
Dimethylindane B	0.029±0.004	0.012±0.001	0.021±0.005	0.056±0.012	0.025±0.005	0.016±0.002	0.006±0.000	0.012±0.003	0.031±0.007	0.014±0.003
Dimethylindane C	0.016±0.002	0.006±0.000	0.011±0.003	0.034±0.008	0.014±0.003	0.009±0.001	0.003±0.000	0.006±0.001	0.019±0.004	0.007±0.002
Dimethylindane E	0.020±0.003	0.009±0.000	0.013±0.003	0.040±0.009	0.017±0.004	0.011±0.001	0.004±0.000	0.007±0.002	0.022±0.005	0.009±0.002
Dimethylindane F	0.030±0.003	0.017±0.001	0.021±0.004	0.057±0.012	0.024±0.005	0.016±0.002	0.009±0.000	0.012±0.002	0.031±0.006	0.013±0.002
Dimethylindane G	0.021±0.003	0.009±0.001	0.011±0.002	0.055±0.011	0.011±0.002	0.012±0.002	0.005±0.000	0.006±0.001	0.030±0.006	0.006±0.001
C-11 Indane H	0.012±0.002	0.006±0.000	0.008±0.002	0.029±0.006	0.008±0.002	0.007±0.001	0.003±0.000	0.004±0.001	0.016±0.003	0.004±0.001
Biphenyl	0.005±0.001	0.002±0.000	0.004±0.001	0.007±0.002	0.007±0.001	0.003±0.000	0.001±0.000	0.002±0.000	0.003±0.001	0.004±0.001
Naphthalene	0.130±0.013	0.073±0.005	0.140±0.029	0.179±0.035	0.129±0.026	0.078±0.008	0.043±0.003	0.083±0.017	0.108±0.021	0.077±0.016
1-Methylnaphthalene	0.038±0.004	0.022±0.001	0.028±0.006	0.069±0.014	0.032±0.006	0.021±0.002	0.012±0.001	0.015±0.004	0.037±0.007	0.017±0.003
2-Methylnaphthalene	0.090±0.010	0.047±0.002	0.075±0.016	0.168±0.034	0.069±0.013	0.049±0.005	0.025±0.001	0.041±0.008	0.092±0.019	0.038±0.007
12-DiMe-naphthalene	0.003±0.000	0.002±0.000	0.002±0.001	0.006±0.001	0.003±0.001	0.002±0.000	0.001±0.000	0.001±0.000	0.003±0.001	0.001±0.000
13-DiMe-naphthalene	0.014±0.002	0.008±0.000	0.012±0.003	0.025±0.005	0.011±0.002	0.007±0.001	0.004±0.000	0.006±0.001	0.013±0.003	0.006±0.001
14-DiMe-naphthalene	0.000±0.000	0.000±0.000	0.001±0.000	0.001±0.000	0.001±0.000	0.000±0.000	0.000±0.000	0.000±0.000	0.000±0.000	0.000±0.000
15-DiMe-naphthalene	0.001±0.000	0.000±0.000	0.000±0.000	0.002±0.000	0.001±0.000	0.000±0.000	0.000±0.000	0.000±0.000	0.001±0.000	0.000±0.000
16-DiMe-naphthalene	0.008±0.001	0.005±0.000	0.006±0.001	0.014±0.003	0.007±0.001	0.004±0.000	0.002±0.000	0.003±0.001	0.007±0.001	0.003±0.001
17-DiMe-naphthalene	0.000±0.000	0.000±0.000	0.000±0.000	0.000±0.000	0.000±0.000	0.000±0.000	0.000±0.000	0.000±0.000	0.000±0.000	0.000±0.000
18-DiMe-naphthalene	0.000±0.000	0.000±0.000	0.000±0.000	0.001±0.000	0.000±0.000	0.000±0.000	0.000±0.000	0.000±0.000	0.000±0.000	0.000±0.000
23-DiMe-naphthalene	0.007±0.001	0.004±0.000	0.006±0.001	0.012±0.003	0.006±0.001	0.003±0.000	0.002±0.000	0.003±0.001	0.006±0.001	0.003±0.001
26-DiMe-naphthalene	0.002±0.000	0.002±0.000	0.001±0.000	0.003±0.001	0.001±0.000	0.001±0.000	0.001±0.000	0.000±0.000	0.002±0.000	0.001±0.000
27-DiMe-naphthalene	0.001±0.000	0.001±0.000	0.001±0.000	0.002±0.000	0.002±0.001	0.001±0.000	0.001±0.000	0.000±0.000	0.001±0.000	0.001±0.000
1-Ethylnaphthalene	0.003±0.000	0.002±0.000	0.001±0.000	0.006±0.001	0.003±0.001	0.002±0.000	0.001±0.000	0.001±0.000	0.003±0.001	0.002±0.000
2-Ethylnaphthalene	0.006±0.001	0.003±0.000	0.006±0.001	0.011±0.002	0.004±0.001	0.003±0.000	0.001±0.000	0.003±0.001	0.005±0.001	0.002±0.000
Acenaphthylene	0.000±0.000	0.000±0.000	0.000±0.000	0.000±0.000	0.000±0.000	0.000±0.000	0.000±0.000	0.000±0.000	0.000±0.000	0.000±0.000
Acenaphthene	0.001±0.000	0.001±0.000	0.000±0.000	0.001±0.000	0.001±0.000	0.000±0.000	0.000±0.000	0.000±0.000	0.000±0.000	0.000±0.000
Ethanol	6.925±0.549	7.038±0.031	6.854±1.261	6.929±1.277	6.877±1.267	20.638±1.639	20.808±0.084	20.396±3.745	20.763±3.819	20.584±3.787
Propene	0.000±0.000	0.000±0.000	0.000±0.000	0.001±0.000	0.000±0.000	0.001±0.000	0.001±0.000	0.000±0.000	0.002±0.000	0.001±0.000
1-butene	0.005±0.001	0.003±0.000	0.003±0.001	0.009±0.002	0.004±0.001	0.007±0.001	0.005±0.000	0.005±0.001	0.013±0.003	0.006±0.001
Cis-2-butene	0.027±0.004	0.017±0.002	0.015±0.005	0.055±0.013	0.020±0.005	0.040±0.005	0.025±0.002	0.022±0.007	0.084±0.019	0.029±0.007
Trans-2-butene	0.025±0.003	0.015±0.001	0.018±0.005	0.044±0.010	0.022±0.005	0.037±0.005	0.022±0.002	0.026±0.008	0.067±0.015	0.033±0.008
2-methylpropene	0.003±0.000	0.002±0.000	0.002±0.001	0.006±0.001	0.003±0.001	0.005±0.001	0.003±0.000	0.003±0.001	0.009±0.002	0.004±0.001
1-pentene	0.102±0.012	0.061±0.007	0.075±0.023	0.168±0.033	0.103±0.023	0.122±0.014	0.072±0.009	0.089±0.027	0.203±0.040	0.124±0.027
Cis-2-pentene	0.161±0.018	0.097±0.011	0.121±0.032	0.261±0.051	0.164±0.036	0.192±0.021	0.114±0.013	0.144±0.038	0.314±0.061	0.197±0.043
trans-2-pentene	0.310±0.035	0.177±0.021	0.252±0.066	0.473±0.092	0.339±0.077	0.371±0.041	0.209±0.025	0.300±0.078	0.569±0.111	0.405±0.092
2-methyl-1-butene	0.200±0.023	0.113±0.015	0.154±0.045	0.324±0.064	0.208±0.046	0.239±0.028	0.134±0.018	0.183±0.053	0.391±0.078	0.249±0.055
3-methyl-1-butene	0.029±0.004	0.016±0.003	0.024±0.009	0.045±0.009	0.031±0.007	0.034±0.004	0.018±0.003	0.028±0.010	0.054±0.011	0.037±0.009
2-methyl-2-butene	0.447±0.049	0.243±0.028	0.386±0.097	0.665±0.130	0.494±0.109	0.534±0.059	0.287±0.033	0.459±0.115	0.800±0.157	0.591±0.130
1-hexene	0.037±0.004	0.029±0.003	0.024±0.005	0.063±0.012	0.031±0.006	0.037±0.004	0.028±0.003	0.024±0.005	0.063±0.012	0.031±0.006
Cis-2-hexene	0.074±0.007	0.058±0.006	0.053±0.011	0.100±0.019	0.086±0.015	0.074±0.007	0.057±0.006	0.053±0.011	0.100±0.019	0.086±0.015
Trans-2-hexene	0.171±0.016	0.131±0.017	0.135±0.030	0.178±0.033	0.238±0.044	0.170±0.016	0.130±0.017	0.135±0.030	0.178±0.033	0.238±0.045
Cis-3-hexene	0.097±0.009	0.076±0.009	0.071±0.015	0.123±0.023	0.117±0.021	0.097±0.009	0.075±0.008	0.071±0.015	0.123±0.023	0.118±0.021
2-Me-1-pentene	0.099±0.009	0.075±0.008	0.077±0.017	0.126±0.024	0.118±0.021	0.099±0.009	0.074±0.008	0.077±0.016	0.127±0.024	0.118±0.021
4-methyl-1-pentene	0.044±0.004	0.031±0.003	0.033±0.007	0.066±0.013	0.046±0.008	0.044±0.004	0.031±0.003	0.033±0.007	0.066±0.013	0.046±0.008
2-methyl-2-pentene	0.324±0.037	0.246±0.047	0.293±0.075	0.207±0.039	0.548±0.112	0.322±0.037	0.243±0.047	0.291±0.075	0.207±0.039	0.548±0.112
C-3Me-2-pentene	0.073±0.008	0.054±0.006	0.048±0.012	0.123±0.023	0.067±0.014	0.073±0.007	0.053±0.006	0.047±0.012	0.123±0.023	0.067±0.014
T-3Me-2-pentene	0.104±0.012	0.062±0.013	0.061±0.019	0.196±0.037	0.096±0.022	0.103±0.012	0.061±0.013	0.061±0.019	0.196±0.037	0.096±0.022
C-4Me-2-pentene	0.016±0.002	0.010±0.002	0.013±0.004	0.011±0.003	0.030±0.008	0.016±0.002	0.010±0.002	0.013±0.004	0.011±0.003	0.030±0.008
T-4Me-2-pentene	0.148±0.018	0.108±0.024	0.138±0.037	0.077±0.015	0.269±0.057	0.147±0.018	0.107±0.023	0.137±0.037	0.077±0.015	0.269±0.057
2-Et-1-butene	0.026±0.003	0.020±0.002	0.017±0.004	0.046±0.009	0.022±0.004	0.026±0.003	0.020±0.002	0.017±0.004	0.047±0.009	0.022±0.004
2,3-dimethyl-1-butene	0.037±0.003	0.026±0.003	0.030±0.007	0.043±0.008	0.048±0.009	0.037±0.003	0.025±0.003	0.030±0.007	0.043±0.008	0.048±0.009

3,3-dimethylbutene	0.003±0.000	0.002±0.000	0.002±0.001	0.005±0.001	0.003±0.001	0.003±0.000	0.002±0.000	0.002±0.001	0.005±0.001	0.003±0.001
2,3-dimethyl-2-butene	0.053±0.005	0.039±0.006	0.044±0.010	0.050±0.009	0.078±0.015	0.053±0.005	0.039±0.006	0.044±0.010	0.050±0.009	0.078±0.015
Nonenes	0.009±0.001	0.012±0.000	0.008±0.002	0.009±0.002	0.007±0.002	0.006±0.000	0.008±0.000	0.005±0.001	0.006±0.001	0.005±0.001
Undecenes	0.001±0.000	0.000±0.000	0.000±0.000	0.000±0.000	0.003±0.001	0.001±0.000	0.000±0.000	0.000±0.000	0.000±0.000	0.002±0.001
Tridecenes	0.001±0.000	0.001±0.000	0.001±0.000	0.001±0.001	0.000±0.000	0.000±0.000	0.000±0.000	0.000±0.000	0.001±0.000	0.000±0.000
Tetradecenes	0.002±0.000	0.002±0.000	0.001±0.000	0.002±0.000	0.002±0.000	0.001±0.000	0.000±0.000	0.000±0.000	0.001±0.000	0.001±0.000
C-1,3-pentadiene	0.003±0.000	0.002±0.000	0.003±0.001	0.005±0.001	0.003±0.001	0.004±0.000	0.002±0.000	0.003±0.001	0.006±0.001	0.004±0.001
T-1,3-pentadiene	0.006±0.001	0.004±0.000	0.005±0.001	0.009±0.002	0.006±0.001	0.007±0.001	0.004±0.000	0.006±0.002	0.011±0.002	0.008±0.002
2-Me-1,3-butadiene	0.006±0.001	0.004±0.000	0.005±0.002	0.009±0.002	0.007±0.001	0.007±0.001	0.004±0.000	0.006±0.002	0.011±0.002	0.008±0.002
T-1Me-1,3-pentadiene	0.000±0.000	0.000±0.000	0.000±0.000	0.000±0.000	0.000±0.000	0.000±0.000	0.000±0.000	0.000±0.000	0.000±0.000	0.000±0.000
1,7-Octadiene	0.001±0.000	0.001±0.000	0.001±0.000	0.003±0.001	0.001±0.000	0.001±0.000	0.001±0.000	0.001±0.000	0.002±0.000	0.001±0.000
Cyclopentadiene	0.004±0.000	0.002±0.000	0.003±0.001	0.007±0.001	0.004±0.001	0.005±0.001	0.003±0.000	0.003±0.001	0.008±0.002	0.005±0.001
1-Me-cyclopentadiene	0.006±0.002	0.000±0.000	0.011±0.004	0.011±0.005	0.000±0.000	0.005±0.002	0.000±0.000	0.011±0.004	0.011±0.005	0.000±0.000
Octadiene A	0.029±0.003	0.020±0.002	0.020±0.005	0.041±0.008	0.034±0.007	0.021±0.002	0.014±0.002	0.015±0.004	0.031±0.006	0.025±0.005
23-diMe-1-pentene	0.009±0.001	0.007±0.001	0.006±0.001	0.017±0.003	0.007±0.001	0.008±0.001	0.006±0.001	0.005±0.001	0.014±0.003	0.006±0.001
24-dime-1-pentene	0.006±0.001	0.005±0.001	0.003±0.001	0.012±0.002	0.004±0.001	0.005±0.001	0.004±0.001	0.003±0.001	0.010±0.002	0.003±0.001
33-DiMe-1-pentene	0.002±0.000	0.002±0.000	0.002±0.000	0.004±0.001	0.002±0.000	0.002±0.000	0.002±0.000	0.001±0.000	0.004±0.001	0.002±0.000
3,4-Dimethyl-2-Pentene	0.000±0.000	0.000±0.000	0.001±0.000	0.000±0.000	0.000±0.000	0.000±0.000	0.000±0.000	0.001±0.000	0.000±0.000	0.000±0.000
44-diMe-1-pentene	0.009±0.001	0.004±0.001	0.005±0.001	0.024±0.005	0.003±0.001	0.008±0.001	0.003±0.001	0.004±0.001	0.021±0.004	0.003±0.001
23-diMe-2-pentene	0.037±0.004	0.028±0.004	0.025±0.006	0.061±0.011	0.036±0.008	0.032±0.003	0.024±0.003	0.021±0.005	0.052±0.010	0.031±0.006
24Dimethyl-2-Pentene	0.002±0.000	0.002±0.000	0.001±0.000	0.004±0.001	0.001±0.000	0.002±0.000	0.001±0.000	0.001±0.000	0.004±0.001	0.001±0.000
34-diMe-c2-pentene	0.009±0.001	0.007±0.001	0.007±0.002	0.015±0.003	0.009±0.002	0.008±0.001	0.006±0.001	0.006±0.001	0.013±0.002	0.008±0.002
44-diMe-c2-pentene	0.004±0.000	0.003±0.000	0.002±0.000	0.008±0.002	0.003±0.001	0.004±0.000	0.003±0.000	0.002±0.000	0.007±0.001	0.003±0.001
3-Et-1-pentene	0.000±0.000	0.000±0.000	0.000±0.000	0.001±0.000	0.000±0.000	0.000±0.000	0.000±0.000	0.000±0.000	0.000±0.000	0.000±0.000
3-Et-2-pentene	0.075±0.008	0.055±0.007	0.046±0.011	0.128±0.025	0.070±0.014	0.064±0.007	0.046±0.006	0.040±0.010	0.110±0.021	0.060±0.012
2-Me-1-hexene	0.020±0.002	0.016±0.002	0.012±0.003	0.036±0.007	0.015±0.003	0.017±0.002	0.014±0.002	0.011±0.003	0.031±0.006	0.013±0.003
3-Me-1-hexene	0.003±0.000	0.002±0.000	0.002±0.001	0.006±0.001	0.002±0.001	0.003±0.000	0.002±0.000	0.002±0.000	0.005±0.001	0.002±0.000
5-Me-1-hexene	0.012±0.001	0.010±0.001	0.008±0.002	0.021±0.004	0.010±0.002	0.011±0.001	0.008±0.001	0.007±0.002	0.018±0.003	0.009±0.002
2-Me-2-hexene	0.041±0.004	0.031±0.004	0.027±0.007	0.065±0.012	0.038±0.008	0.035±0.004	0.026±0.003	0.023±0.006	0.056±0.010	0.033±0.007
5-Me-t2-hexene	0.000±0.000	0.000±0.000	0.000±0.000	0.001±0.000	0.000±0.000	0.000±0.000	0.000±0.000	0.000±0.000	0.001±0.000	0.000±0.000
2-Me-t3-hexene	0.020±0.002	0.016±0.002	0.012±0.003	0.037±0.007	0.015±0.003	0.017±0.002	0.013±0.002	0.011±0.003	0.032±0.006	0.013±0.003
3-Me-c3-hexene	0.028±0.003	0.021±0.003	0.019±0.005	0.045±0.009	0.027±0.006	0.024±0.002	0.018±0.002	0.016±0.004	0.039±0.007	0.023±0.005
3-Me-t3-hexene	0.017±0.002	0.013±0.002	0.012±0.003	0.028±0.005	0.016±0.003	0.015±0.002	0.011±0.001	0.010±0.003	0.024±0.005	0.013±0.003
1-Heptene	0.019±0.002	0.015±0.003	0.010±0.003	0.033±0.007	0.016±0.004	0.016±0.002	0.013±0.003	0.008±0.003	0.028±0.006	0.014±0.003
Cis-2-heptene	0.000±0.000	0.000±0.000	0.000±0.000	0.001±0.000	0.000±0.000	0.000±0.000	0.000±0.000	0.000±0.000	0.001±0.000	0.000±0.000
Trans-2-heptene	0.002±0.000	0.005±0.001	0.000±0.000	0.001±0.000	0.000±0.000	0.001±0.000	0.004±0.000	0.000±0.000	0.001±0.000	0.000±0.000
T3-Heptene	0.025±0.003	0.015±0.004	0.012±0.004	0.051±0.009	0.022±0.005	0.021±0.003	0.013±0.003	0.011±0.004	0.043±0.008	0.019±0.004
C2-Octene	0.015±0.001	0.011±0.002	0.012±0.003	0.015±0.003	0.021±0.004	0.011±0.001	0.008±0.001	0.009±0.002	0.011±0.002	0.016±0.003
C4-Octene	0.001±0.000	0.002±0.001	0.001±0.001	0.002±0.001	0.000±0.000	0.001±0.000	0.001±0.001	0.001±0.001	0.002±0.001	0.000±0.000
25-Dimethyl-1-hexene	0.000±0.000	0.000±0.000	0.000±0.000	0.001±0.000	0.000±0.000	0.000±0.000	0.000±0.000	0.000±0.000	0.001±0.000	0.000±0.000
4-M-1-Heptene	0.058±0.005	0.075±0.003	0.041±0.008	0.065±0.013	0.050±0.010	0.042±0.003	0.055±0.003	0.030±0.006	0.048±0.010	0.037±0.007
t-4-M-2-Heptene	0.001±0.000	0.001±0.000	0.002±0.000	0.001±0.000	0.002±0.000	0.001±0.000	0.001±0.000	0.001±0.000	0.001±0.000	0.002±0.000
C-2-m-3-heptene	0.137±0.014	0.114±0.009	0.107±0.023	0.202±0.043	0.126±0.026	0.102±0.011	0.084±0.006	0.079±0.017	0.151±0.033	0.095±0.019
c-6-M-2-Heptene	0.002±0.000	0.002±0.000	0.002±0.000	0.004±0.001	0.002±0.000	0.002±0.000	0.001±0.000	0.001±0.000	0.003±0.001	0.002±0.000
t-6-M-2-Heptene	0.001±0.001	0.000±0.000	0.000±0.000	0.000±0.000	0.004±0.002	0.001±0.000	0.000±0.000	0.000±0.000	0.000±0.000	0.003±0.002
2-Methyl-2-heptene	0.042±0.004	0.034±0.001	0.032±0.007	0.058±0.012	0.043±0.009	0.031±0.003	0.025±0.001	0.023±0.005	0.043±0.009	0.032±0.007
2235TetMethylhexane	0.000±0.000	0.000±0.000	0.001±0.000	0.000±0.000	0.000±0.000	0.000±0.000	0.000±0.000	0.000±0.000	0.000±0.000	0.000±0.000
C-7 Olefin A	0.006±0.001	0.005±0.001	0.003±0.001	0.011±0.002	0.004±0.001	0.005±0.001	0.004±0.001	0.003±0.001	0.010±0.002	0.003±0.001
C-7 Olefin B	0.001±0.000	0.001±0.000	0.000±0.000	0.002±0.000	0.001±0.000	0.001±0.000	0.001±0.000	0.000±0.000	0.001±0.000	0.000±0.000
C-7 Olefin D	0.002±0.000	0.002±0.000	0.001±0.000	0.004±0.001	0.001±0.000	0.002±0.000	0.001±0.000	0.001±0.000	0.004±0.001	0.001±0.000

Octene B	0.003±0.000	0.002±0.000	0.002±0.000	0.005±0.001	0.003±0.001	0.002±0.000	0.002±0.000	0.001±0.000	0.004±0.001	0.003±0.001
Octene C	0.006±0.001	0.004±0.000	0.003±0.001	0.012±0.002	0.005±0.001	0.005±0.001	0.003±0.000	0.002±0.001	0.009±0.002	0.003±0.001
Octene D	0.008±0.001	0.006±0.001	0.004±0.001	0.016±0.003	0.007±0.001	0.006±0.001	0.004±0.001	0.003±0.001	0.012±0.003	0.005±0.001
Octene F	0.001±0.000	0.001±0.000	0.000±0.000	0.005±0.001	0.000±0.000	0.001±0.000	0.000±0.000	0.000±0.000	0.004±0.001	0.000±0.000
Octene G	0.001±0.000	0.001±0.000	0.001±0.000	0.002±0.000	0.001±0.000	0.001±0.000	0.001±0.000	0.001±0.000	0.002±0.000	0.001±0.000
Octene H	0.007±0.001	0.006±0.001	0.005±0.001	0.012±0.002	0.007±0.001	0.006±0.001	0.004±0.000	0.004±0.001	0.009±0.002	0.006±0.001
Octene I	0.011±0.001	0.008±0.001	0.008±0.002	0.016±0.003	0.010±0.002	0.008±0.001	0.006±0.001	0.006±0.001	0.012±0.002	0.008±0.002
C-8 Olefin K	0.013±0.001	0.024±0.002	0.008±0.002	0.012±0.003	0.008±0.002	0.009±0.001	0.017±0.001	0.006±0.001	0.009±0.002	0.006±0.001
C-8 Olefin M	0.027±0.003	0.021±0.002	0.022±0.005	0.034±0.007	0.031±0.006	0.020±0.002	0.015±0.001	0.016±0.004	0.025±0.005	0.022±0.005
44DiMe2neopen1pentene	0.001±0.001	0.000±0.000	0.002±0.001	0.004±0.002	0.000±0.000	0.001±0.000	0.000±0.000	0.001±0.000	0.002±0.001	0.000±0.000
22466PentaMe3heptene	0.000±0.000	0.000±0.000	0.001±0.001	0.000±0.000	0.000±0.000	0.000±0.000	0.000±0.000	0.001±0.000	0.000±0.000	0.000±0.000
T-2-T-4-hexadiene	0.005±0.001	0.004±0.000	0.003±0.001	0.010±0.002	0.004±0.001	0.004±0.000	0.003±0.000	0.002±0.000	0.009±0.002	0.003±0.001
Cyclopentene	0.065±0.007	0.041±0.004	0.042±0.011	0.114±0.023	0.063±0.013	0.078±0.009	0.048±0.005	0.050±0.013	0.138±0.028	0.076±0.016
1-Me-cyclopentene	0.143±0.016	0.105±0.012	0.074±0.020	0.262±0.052	0.133±0.027	0.126±0.014	0.091±0.010	0.065±0.018	0.231±0.046	0.116±0.024
3-Me-cyclopentene	0.036±0.004	0.026±0.003	0.020±0.005	0.072±0.014	0.027±0.005	0.032±0.004	0.023±0.003	0.017±0.004	0.064±0.013	0.024±0.005
Sum of Unclassified Compounds	2.589±0.007	1.417±0.000	1.540±0.003	3.174±0.014	2.113±0.006	1.433±0.002	0.782±0.000	0.849±0.001	1.755±0.004	1.174±0.002

Note: Compounds for which an exact isomer could not be determined are denoted and differentiated by a CAPITAL suffix.

Table S10: Compound specific diesel fuel speciation for California in Summer 2010

	Weight percentage in fuel [% weight by carbon (± St. Dev)]				
Compound	**Statewide**	**Bakersfield**	**Berkeley**	**Pasadena**	**Sacramento**
n-octane	0.104±0.069	0.046±0.003	0.057±0.045	0.180±0.071	0.132±0.035
n-nonane	0.209±0.111	0.120±0.031	0.125±0.095	0.330±0.095	0.263±0.012
n-decane	0.444±0.169	0.353±0.066	0.315±0.228	0.588±0.122	0.519±0.098
n-undecane	0.581±0.183	0.456±0.039	0.573±0.312	0.695±0.168	0.602±0.114
n-dodecane	0.478±0.115	0.364±0.032	0.520±0.167	0.565±0.094	0.466±0.033
n-tridecane	0.440±0.091	0.337±0.029	0.469±0.102	0.517±0.091	0.436±0.005
n-tetradecane	0.439±0.081	0.322±0.020	0.503±0.021	0.493±0.018	0.437±0.061
n-pentadecane	0.524±0.106	0.414±0.033	0.560±0.076	0.605±0.104	0.518±0.121
n-hexadecane	0.552±0.162	0.395±0.041	0.588±0.090	0.645±0.188	0.579±0.216
n-heptadecane	0.628±0.189	0.542±0.102	0.659±0.131	0.646±0.257	0.665±0.297
n-octadecane	0.556±0.161	0.507±0.083	0.600±0.117	0.543±0.243	0.576±0.236
n-nonadecane	0.400±0.182	0.215±0.028	0.506±0.130	0.413±0.217	0.464±0.209
n-eicosane	0.386±0.175	0.233±0.021	0.511±0.128	0.351±0.215	0.450±0.197
2-5-dimethylhexane	0.009±0.004	0.012±0.002	0.005±0.004	0.009±0.002	0.010±0.003
2-4-dimethylhexane	0.006±0.002	0.005±0.002	0.004±0.002	0.006±0.002	0.007±0.003
2-methylheptane	0.057±0.021	0.047±0.008	0.038±0.030	0.075±0.007	0.067±0.013
4-methylheptane	0.017±0.008	0.012±0.003	0.012±0.010	0.023±0.007	0.023±0.004
3-methylheptane	0.052±0.022	0.034±0.003	0.036±0.026	0.070±0.010	0.068±0.014
2,6-dimethylheptane	0.051±0.026	0.032±0.004	0.028±0.021	0.078±0.022	0.063±0.005
3-5-dimethylheptane	0.028±0.015	0.014±0.002	0.019±0.011	0.040±0.012	0.041±0.011
2,3-dimethyheptane	0.013±0.005	0.012±0.002	0.007±0.005	0.017±0.003	0.017±0.001
4&2-methyloctane	0.056±0.031	0.024±0.005	0.037±0.024	0.081±0.018	0.084±0.012
3-methyloctane+3-ethylheptane	0.079±0.039	0.038±0.007	0.054±0.038	0.117±0.011	0.108±0.005
C10 Branched alkanes A	0.057±0.020	0.043±0.008	0.040±0.015	0.067±0.020	0.076±0.010
2-6-dimethyloctane	0.035±0.016	0.029±0.006	0.023±0.018	0.045±0.018	0.042±0.016
C10 Branch alkanes B	0.316±0.118	0.206±0.032	0.243±0.092	0.405±0.113	0.408±0.054
C11 Branched Alkanes A	0.046±0.014	0.030±0.002	0.050±0.006	0.049±0.022	0.054±0.002
C11 Branched Alkanes B	0.018±0.008	0.007±0.002	0.017±0.005	0.024±0.005	0.023±0.002
dimethylundecane A	0.174±0.067	0.225±0.012	0.176±0.083	0.163±0.088	0.133±0.055
dimethyundecane B	0.129±0.049	0.191±0.009	0.120±0.048	0.111±0.046	0.093±0.024
methylcyclohexane	0.127±0.050	0.156±0.025	0.067±0.050	0.142±0.031	0.141±0.048
Ethylcyclopentane	0.025±0.010	0.029±0.008	0.016±0.011	0.032±0.010	0.025±0.007
n-propylcyclopentane	0.031±0.016	0.018±0.002	0.018±0.011	0.051±0.014	0.036±0.002

ethylcyclohexane	0.157±0.068	0.111±0.021	0.088±0.053	0.221±0.045	0.207±0.017
propylcyclohexane	0.256±0.095	0.270±0.047	0.147±0.053	0.312±0.112	0.294±0.083
cumene	0.029±0.009	0.036±0.005	0.022±0.017	0.030±0.001	0.029±0.004
n-propyl_benzene	0.090±0.020	0.092±0.017	0.069±0.021	0.099±0.019	0.101±0.012
1-ethyl-4(and3)-methylbenzene	0.389±0.091	0.348±0.049	0.339±0.107	0.452±0.131	0.415±0.029
1-3-5-trimethylbenzene	0.150±0.045	0.197±0.027	0.114±0.057	0.145±0.034	0.145±0.022
1-ethyl-2-methylbenzene	0.136±0.023	0.129±0.018	0.128±0.035	0.149±0.029	0.137±0.015
1-2-4-trimethylbenzene	0.699±0.222	0.984±0.111	0.589±0.255	0.605±0.122	0.617±0.120
1-ethenyl-2-(or3)-methylbenzene	0.019±0.009	0.020±0.002	0.020±0.015	0.021±0.012	0.015±0.002
isobutylbenzene	0.009±0.003	0.012±0.002	0.008±0.003	0.007±0.002	0.010±0.003
m-cymene	0.040±0.015	0.054±0.007	0.035±0.028	0.037±0.006	0.035±0.007
p-cymene	0.039±0.021	0.065±0.007	0.029±0.026	0.031±0.010	0.030±0.011
m-diethylbenzene	0.589±0.244	0.588±0.047	0.693±0.504	0.545±0.171	0.531±0.130
1-methyl-3-n-propylbenzene	0.267±0.076	0.279±0.024	0.287±0.144	0.267±0.088	0.233±0.014
indan	0.142±0.060	0.152±0.015	0.150±0.104	0.152±0.083	0.112±0.013
p-diethylbenzene	0.415±0.172	0.417±0.034	0.487±0.357	0.383±0.120	0.374±0.088
n-butylbenzene	0.132±0.053	0.103±0.014	0.146±0.093	0.150±0.066	0.128±0.013
o-diethylbenzene	0.034±0.006	0.038±0.002	0.037±0.009	0.033±0.002	0.028±0.001
1-methyl-2-n-propylbenzene	0.071±0.018	0.076±0.007	0.083±0.030	0.062±0.016	0.063±0.009
1,4-dimethyl-2-ethylbenzene	0.162±0.047	0.164±0.022	0.204±0.078	0.149±0.027	0.130±0.022
1,3-dimethyl-4-ethylbenzene	0.164±0.046	0.203±0.017	0.182±0.071	0.145±0.025	0.127±0.023
1,2-dimethyl-4-ethylbenzene	0.108±0.040	0.116±0.007	0.130±0.080	0.098±0.023	0.088±0.015
Trans-1-butenylbenzene	0.009±0.003	0.012±0.002	0.009±0.004	0.008±0.002	0.007±0.002
1,3-dimethyl-2-ethylbenzene	0.071±0.030	0.096±0.007	0.075±0.057	0.057±0.006	0.055±0.003
1,2-dimethyl-3-ethylbenzene	0.052±0.016	0.069±0.004	0.058±0.022	0.042±0.005	0.040±0.006
1-2-4-5-tetramethylbenzene	0.078±0.038	0.108±0.014	0.086±0.069	0.061±0.017	0.057±0.017
1-2-3-5-tetramethylbenzene	0.114±0.046	0.160±0.014	0.126±0.066	0.087±0.022	0.082±0.020
C11 Aromatics A	0.020±0.007	0.026±0.005	0.023±0.012	0.017±0.002	0.016±0.002
1-methylindan	0.113±0.072	0.085±0.015	0.171±0.131	0.114±0.060	0.083±0.009
C11 Aromatics B	0.010±0.003	0.015±0.001	0.010±0.003	0.008±0.002	0.008±0.001
1-2-3-4-tetramethylbenzene	0.183±0.084	0.301±0.012	0.190±0.073	0.122±0.016	0.119±0.021
2-methylindan	0.217±0.092	0.215±0.018	0.289±0.168	0.200±0.069	0.164±0.010
toluene	0.214±0.102	0.252±0.043	0.106±0.074	0.242±0.122	0.256±0.108
ethylbenzene	0.093±0.043	0.063±0.010	0.061±0.033	0.132±0.044	0.115±0.033
m&p-xylene	0.475±0.154	0.467±0.069	0.321±0.158	0.575±0.186	0.538±0.098
o-xylene	0.164±0.056	0.151±0.021	0.107±0.040	0.202±0.070	0.195±0.038

123-trimethylbenzene	0.286±0.178	0.564±0.075	0.189±0.090	0.190±0.040	0.199±0.060
dimethylnaphthalenes	0.182±0.167	0.456±0.007	0.125±0.021	0.067±0.015	0.082±0.010
trimethylnapthalenes	0.153±0.134	0.370±0.007	0.112±0.030	0.056±0.022	0.073±0.012
naphthalene	0.045±0.037	0.103±0.017	0.034±0.010	0.022±0.007	0.020±0.003
2-methylnaphthalene	0.124±0.120	0.319±0.029	0.082±0.032	0.046±0.019	0.050±0.009
1-methylnaphthalene	0.066±0.062	0.166±0.013	0.046±0.013	0.024±0.008	0.027±0.005
C9 Cycloalkene A	0.052±0.026	0.065±0.007	0.028±0.007	0.047±0.026	0.068±0.039
ctc-1-2-4-trimethylcyclopentane	0.016±0.006	0.023±0.004	0.009±0.005	0.017±0.002	0.016±0.002
ctc-1,2,3-trimethylcyclopentane	0.040±0.020	0.066±0.014	0.018±0.013	0.041±0.014	0.036±0.007
ctt-1-2-4-trimethylcyclopentane	0.010±0.004	0.012±0.001	0.006±0.003	0.013±0.005	0.010±0.001
cis-1,3 & 1,1-dimethylcyclohexane	0.099±0.043	0.072±0.010	0.054±0.036	0.135±0.027	0.135±0.010
trans-1-2-dimethylcyclohexane	0.118±0.048	0.100±0.010	0.060±0.041	0.154±0.027	0.157±0.013
trans-1-3-dimethylcyclohexane	0.078±0.034	0.050±0.005	0.049±0.030	0.112±0.024	0.100±0.006
isopropylcyclopentane	0.010±0.006	0.007±0.001	0.006±0.003	0.017±0.007	0.011±0.001
ccc-1-3-5-trimethylcyclohexane	0.052±0.048	0.020±0.003	0.025±0.014	0.065±0.045	0.100±0.066
cis-1-2-dimethylcyclohexane	0.049±0.025	0.030±0.005	0.029±0.015	0.078±0.024	0.060±0.011
1-1-3-trimethylcyclohexane	0.096±0.047	0.128±0.018	0.043±0.029	0.105±0.050	0.109±0.050
1-1-4-trimethylcyclohexane	0.027±0.011	0.020±0.002	0.018±0.007	0.031±0.004	0.040±0.010
ctt-1,2,4-trimethylcyclohexane	0.018±0.013	0.011±0.001	0.010±0.004	0.018±0.009	0.031±0.018
ctc-1-2-4-trimetylcyclohexane	0.099±0.057	0.091±0.014	0.056±0.022	0.102±0.046	0.149±0.091
C9 cycloalkanes A	0.008±0.003	0.007±0.001	0.005±0.001	0.011±0.004	0.010±0.001
methyl-ethylcyclohexane isomer A	0.010±0.004	0.011±0.002	0.008±0.002	0.010±0.007	0.012±0.005
isopropylcyclohexane	0.039±0.014	0.052±0.007	0.022±0.009	0.041±0.011	0.041±0.012
C10 cyclohexanes A	0.126±0.050	0.129±0.014	0.094±0.014	0.134±0.073	0.148±0.075

Note: This list only comprises a fraction of compounds in diesel. Compounds for which an exact isomer could not be determined are denoted and differentiated by a CAPITAL suffix.

Table S11: Compound specific non-tailpipe gasoline speciation for California in Summer 2010

	Weight percentage in fuel [% weight by carbon (± St. Dev)]					Molar percentage in fuel [% mol (± St. Dev)]				
Compound	**Statewide**	**Bakersfield**	**Berkeley**	**Pasadena**	**Sacramento**	**Statewide**	**Bakersfield**	**Berkeley**	**Pasadena**	**Sacramento**
ethane	0.099±0.011	0.310±0.042	0.015±0.006	0.069±0.014	0.000±0.000	0.235±0.026	0.735±0.099	0.037±0.015	0.169±0.033	0.000±0.000
propane	0.690±0.059	1.534±0.156	0.315±0.088	0.287±0.063	0.624±0.143	1.105±0.095	2.430±0.242	0.511±0.141	0.461±0.100	1.020±0.234
n-butane	6.542±0.499	8.944±0.646	5.472±0.961	6.326±1.301	5.426±0.973	7.929±0.603	10.652±0.740	6.734±1.182	7.652±1.561	6.676±1.197
n-pentane	10.313±0.801	14.100±0.768	9.068±1.766	9.362±1.924	8.723±1.690	10.060±0.787	13.484±0.685	8.950±1.746	9.210±1.899	8.595±1.666
n-hexane	1.970±0.168	2.245±0.044	1.837±0.374	1.976±0.413	1.823±0.372	1.605±0.138	1.797±0.030	1.511±0.308	1.617±0.338	1.497±0.306
n-heptane	0.137±0.012	0.150±0.003	0.164±0.033	0.108±0.021	0.126±0.025	0.096±0.008	0.103±0.002	0.116±0.023	0.075±0.015	0.088±0.017
n-octane	0.062±0.005	0.067±0.002	0.071±0.014	0.049±0.010	0.059±0.012	0.038±0.003	0.040±0.001	0.044±0.009	0.030±0.006	0.037±0.007
n-nonane	0.008±0.001	0.009±0.000	0.009±0.002	0.007±0.001	0.008±0.002	0.005±0.000	0.005±0.000	0.005±0.001	0.004±0.001	0.005±0.001
n-decane	0.001±0.000	0.001±0.000	0.001±0.000	0.001±0.000	0.001±0.000	0.001±0.000	0.000±0.000	0.000±0.000	0.001±0.000	0.001±0.000
2-methylpropane	1.072±0.111	1.569±0.176	0.807±0.212	1.484±0.341	0.428±0.076	1.293±0.134	1.859±0.206	0.994±0.260	1.791±0.408	0.527±0.094
2-methylbutane	38.367±3.173	34.577±0.809	41.426±7.644	36.647±6.790	40.817±7.477	37.582±3.129	33.334±0.935	40.855±7.546	35.930±6.675	40.209±7.370
2,2-dimethylpropane	0.072±0.006	0.083±0.005	0.066±0.012	0.066±0.014	0.074±0.013	0.071±0.006	0.080±0.004	0.065±0.012	0.065±0.014	0.073±0.013
2-methylpentane	5.814±0.519	4.856±0.345	6.545±1.260	5.893±1.158	5.961±1.121	4.756±0.427	3.923±0.298	5.384±1.038	4.821±0.950	4.895±0.921
3-methylpentane	3.247±0.286	2.774±0.169	3.598±0.688	3.235±0.633	3.381±0.634	2.655±0.235	2.238±0.147	2.960±0.567	2.646±0.519	2.776±0.521
2,2-dimethylbutane	2.051±0.241	1.295±0.232	3.006±0.703	1.628±0.448	2.276±0.426	1.688±0.199	1.060±0.194	2.483±0.582	1.341±0.370	1.869±0.350
2,3-dimethylbutane	2.247±0.183	1.967±0.099	2.231±0.399	2.377±0.425	2.413±0.433	1.834±0.151	1.583±0.087	1.835±0.329	1.937±0.347	1.980±0.356
2-methylhexane	0.625±0.064	0.535±0.034	0.852±0.182	0.504±0.122	0.610±0.128	0.439±0.045	0.370±0.026	0.601±0.129	0.356±0.087	0.430±0.090
3-methylhexane	0.867±0.076	0.811±0.020	1.042±0.209	0.808±0.156	0.808±0.157	0.607±0.054	0.559±0.017	0.735±0.148	0.566±0.110	0.568±0.111
3-ethylpentane	0.036±0.005	0.044±0.005	0.059±0.015	0.022±0.008	0.019±0.007	0.025±0.003	0.030±0.003	0.042±0.011	0.015±0.006	0.013±0.005
2,2-dimethylpentane	0.085±0.008	0.095±0.001	0.092±0.021	0.084±0.017	0.068±0.013	0.059±0.005	0.065±0.001	0.065±0.015	0.059±0.012	0.048±0.009
2,3-dimethylpentane	1.338±0.108	1.474±0.061	0.985±0.171	1.775±0.334	1.118±0.208	0.929±0.075	1.007±0.040	0.693±0.121	1.229±0.230	0.786±0.146
2,4-dimethylpentane	0.844±0.066	0.894±0.036	0.615±0.104	1.075±0.191	0.794±0.145	0.587±0.046	0.612±0.024	0.432±0.073	0.746±0.132	0.558±0.102
3,3-Dimethylpentane	0.066±0.006	0.077±0.001	0.066±0.018	0.066±0.013	0.056±0.010	0.046±0.004	0.053±0.001	0.047±0.013	0.046±0.009	0.039±0.007
2,2,3-Trimethylbutane	0.032±0.002	0.032±0.000	0.031±0.006	0.032±0.006	0.032±0.006	0.022±0.002	0.022±0.000	0.022±0.004	0.022±0.004	0.023±0.004
2-Methylheptane	0.137±0.011	0.142±0.002	0.143±0.028	0.133±0.026	0.130±0.025	0.084±0.007	0.085±0.001	0.088±0.017	0.081±0.016	0.080±0.016
3-methylheptane	0.140±0.012	0.152±0.002	0.151±0.030	0.127±0.025	0.131±0.025	0.086±0.007	0.091±0.001	0.093±0.018	0.078±0.015	0.081±0.016
4-Methylheptane	0.062±0.005	0.066±0.001	0.065±0.012	0.058±0.011	0.060±0.011	0.038±0.003	0.039±0.000	0.040±0.008	0.036±0.007	0.037±0.007
2,2-dimethylhexane	0.014±0.001	0.019±0.001	0.016±0.004	0.011±0.002	0.011±0.002	0.009±0.001	0.011±0.001	0.010±0.002	0.007±0.001	0.007±0.001
2,4-dimethylhexane	0.135±0.010	0.134±0.003	0.125±0.022	0.139±0.024	0.141±0.025	0.082±0.006	0.081±0.001	0.077±0.013	0.085±0.015	0.087±0.015
2,5-dimethylhexane	0.131±0.010	0.128±0.003	0.118±0.020	0.127±0.022	0.151±0.026	0.080±0.006	0.076±0.001	0.073±0.012	0.078±0.013	0.093±0.016
3,3-dimethylhexane	0.014±0.001	0.020±0.001	0.016±0.003	0.010±0.002	0.011±0.002	0.009±0.001	0.012±0.001	0.010±0.002	0.006±0.001	0.007±0.001
2-Me-3-Et-pentane	0.097±0.007	0.097±0.002	0.086±0.015	0.102±0.018	0.105±0.019	0.059±0.005	0.058±0.001	0.053±0.009	0.062±0.011	0.065±0.012
2,2,3-triMe-pentane	0.038±0.003	0.034±0.001	0.033±0.006	0.033±0.006	0.052±0.009	0.023±0.002	0.020±0.001	0.020±0.004	0.020±0.004	0.032±0.006
2,2,4-triMe-pentane	1.287±0.104	1.101±0.042	1.013±0.175	1.465±0.252	1.571±0.280	0.785±0.064	0.658±0.024	0.624±0.108	0.893±0.154	0.967±0.172
2,3,3-triMe-pentane	0.265±0.022	0.240±0.008	0.224±0.039	0.224±0.039	0.371±0.066	0.162±0.013	0.144±0.005	0.138±0.024	0.137±0.024	0.229±0.041
2,3,4-triMe-pentane	0.271±0.022	0.253±0.008	0.222±0.038	0.257±0.044	0.353±0.063	0.165±0.013	0.151±0.005	0.137±0.023	0.157±0.027	0.217±0.039
2,2,5-trimethylhexane	0.106±0.010	0.105±0.005	0.104±0.024	0.078±0.014	0.138±0.027	0.058±0.005	0.056±0.002	0.057±0.013	0.042±0.008	0.075±0.015
2,3,5-trimethylhexane	0.022±0.002	0.023±0.001	0.021±0.004	0.017±0.003	0.027±0.005	0.012±0.001	0.012±0.000	0.011±0.002	0.009±0.002	0.015±0.003
2,4,4-trimethylhexane	0.011±0.001	0.008±0.000	0.008±0.002	0.013±0.003	0.012±0.002	0.006±0.001	0.004±0.000	0.005±0.001	0.007±0.001	0.007±0.001
2,4-dimethylheptane	0.009±0.001	0.011±0.001	0.009±0.002	0.007±0.001	0.008±0.002	0.005±0.000	0.006±0.000	0.005±0.001	0.004±0.001	0.005±0.001
2,6-dimethylheptane	0.015±0.001	0.013±0.000	0.013±0.003	0.018±0.004	0.015±0.003	0.008±0.001	0.007±0.000	0.007±0.001	0.010±0.002	0.008±0.002
3,5-dimethylheptane	0.031±0.002	0.035±0.001	0.028±0.005	0.030±0.006	0.030±0.006	0.017±0.001	0.018±0.001	0.015±0.003	0.016±0.003	0.016±0.003
2,3-dimethylheptane	0.009±0.001	0.010±0.000	0.009±0.002	0.008±0.002	0.010±0.002	0.005±0.000	0.005±0.000	0.005±0.001	0.005±0.001	0.006±0.001
3,4-dimethylheptane	0.005±0.000	0.004±0.000	0.004±0.001	0.005±0.001	0.005±0.001	0.002±0.000	0.002±0.000	0.002±0.000	0.003±0.001	0.003±0.000
3,3-dimethylheptane	0.003±0.000	0.002±0.000	0.002±0.000	0.005±0.001	0.003±0.001	0.002±0.000	0.001±0.000	0.001±0.000	0.003±0.001	0.002±0.000
4,4-dimethylheptane	0.002±0.000	0.002±0.000	0.002±0.000	0.004±0.001	0.002±0.000	0.001±0.000	0.001±0.000	0.001±0.000	0.002±0.000	0.001±0.000
2-methyloctane	0.015±0.001	0.016±0.000	0.014±0.003	0.015±0.003	0.015±0.003	0.008±0.001	0.008±0.000	0.008±0.002	0.008±0.002	0.008±0.002

3-methyloctane	0.018±0.002	0.020±0.001	0.018±0.003	0.018±0.003	0.018±0.004	0.010±0.001	0.011±0.000	0.010±0.002	0.010±0.002	0.010±0.002
4-methyloctane	0.013±0.001	0.014±0.001	0.012±0.002	0.012±0.002	0.012±0.002	0.007±0.001	0.008±0.000	0.007±0.001	0.007±0.001	0.007±0.001
2,2-dimethylheptane	0.002±0.000	0.003±0.000	0.002±0.000	0.001±0.000	0.001±0.000	0.001±0.000	0.002±0.000	0.001±0.000	0.001±0.000	0.001±0.000
2,2,3-trimethylhexane	0.002±0.000	0.004±0.000	0.002±0.001	0.000±0.000	0.001±0.000	0.001±0.000	0.002±0.000	0.001±0.000	0.000±0.000	0.001±0.000
Cyclopentane	1.070±0.084	1.371±0.065	1.056±0.209	0.864±0.177	0.988±0.186	1.044±0.083	1.312±0.057	1.043±0.207	0.850±0.174	0.973±0.183
Methylcyclopentane	2.602±0.216	2.923±0.055	2.669±0.536	2.409±0.477	2.408±0.477	2.119±0.177	2.339±0.036	2.194±0.441	1.967±0.390	1.977±0.391
Ethylcyclopentane	0.095±0.008	0.104±0.003	0.084±0.018	0.099±0.020	0.091±0.019	0.066±0.006	0.071±0.001	0.059±0.012	0.069±0.014	0.064±0.013
1T2-diMecyclopentane	0.279±0.023	0.441±0.036	0.239±0.053	0.219±0.046	0.216±0.044	0.193±0.016	0.300±0.023	0.168±0.037	0.153±0.032	0.152±0.031
1C3-diMecyclopentane	0.228±0.020	0.270±0.011	0.220±0.049	0.215±0.043	0.208±0.042	0.159±0.014	0.185±0.007	0.154±0.034	0.150±0.030	0.146±0.030
1T3-diMecyclopentane	0.268±0.023	0.331±0.015	0.252±0.056	0.251±0.051	0.236±0.048	0.186±0.016	0.226±0.009	0.177±0.039	0.175±0.035	0.166±0.034
Propylcyclopentane	0.002±0.000	0.002±0.000	0.002±0.000	0.003±0.001	0.002±0.000	0.001±0.000	0.001±0.000	0.001±0.000	0.002±0.000	0.001±0.000
112-triMeCyPentane	0.001±0.000	0.001±0.000	0.001±0.000	0.002±0.000	0.001±0.000	0.001±0.000	0.001±0.000	0.001±0.000	0.001±0.000	0.001±0.000
113-triMeCyPentane	0.041±0.003	0.057±0.003	0.031±0.006	0.044±0.009	0.034±0.007	0.025±0.002	0.034±0.002	0.019±0.004	0.027±0.006	0.021±0.004
1C2T3-triMeCyPentane	0.003±0.000	0.004±0.000	0.003±0.001	0.003±0.001	0.003±0.001	0.002±0.000	0.002±0.000	0.002±0.000	0.002±0.000	0.002±0.000
1T2C3-triMeCyPentane	0.034±0.003	0.051±0.004	0.024±0.005	0.036±0.008	0.027±0.005	0.021±0.002	0.030±0.002	0.015±0.003	0.022±0.005	0.016±0.003
1T2C4-triMeCyPentane	0.055±0.005	0.061±0.002	0.044±0.009	0.067±0.014	0.050±0.010	0.034±0.003	0.037±0.001	0.027±0.006	0.041±0.008	0.031±0.006
Cyclohexane	0.747±0.070	0.787±0.031	0.915±0.202	0.567±0.122	0.722±0.148	0.611±0.058	0.632±0.027	0.754±0.167	0.465±0.101	0.593±0.122
Methylcyclohexane	0.468±0.041	0.500±0.009	0.445±0.092	0.486±0.099	0.441±0.089	0.326±0.028	0.343±0.005	0.313±0.065	0.339±0.069	0.310±0.063
Ethylcyclohexane	0.017±0.002	0.011±0.001	0.012±0.003	0.029±0.006	0.018±0.004	0.011±0.001	0.007±0.001	0.007±0.002	0.017±0.004	0.011±0.002
1,1-diMecyclohexane	0.005±0.000	0.006±0.000	0.004±0.001	0.005±0.001	0.004±0.001	0.003±0.000	0.004±0.000	0.003±0.001	0.003±0.001	0.003±0.001
1C2-diMecyclohexane	0.006±0.001	0.004±0.000	0.004±0.001	0.009±0.002	0.006±0.001	0.004±0.000	0.003±0.000	0.003±0.001	0.005±0.001	0.004±0.001
1T2-diMecyclohexane	0.017±0.002	0.015±0.001	0.013±0.003	0.023±0.005	0.016±0.003	0.010±0.001	0.009±0.000	0.008±0.002	0.014±0.003	0.010±0.002
1C3-diMecyclohexane	0.040±0.004	0.033±0.002	0.031±0.007	0.057±0.013	0.037±0.008	0.024±0.002	0.020±0.001	0.019±0.004	0.035±0.008	0.023±0.005
1T3-diMecyclohexane	0.032±0.003	0.024±0.002	0.024±0.005	0.048±0.010	0.032±0.007	0.020±0.002	0.014±0.001	0.015±0.003	0.029±0.006	0.020±0.004
1C4-diMecyclohexane	0.007±0.001	0.006±0.000	0.004±0.001	0.011±0.002	0.006±0.001	0.004±0.000	0.003±0.000	0.003±0.001	0.007±0.001	0.004±0.001
Propylcyclohexane	0.001±0.000	0.001±0.000	0.001±0.000	0.002±0.001	0.001±0.000	0.001±0.000	0.000±0.000	0.001±0.000	0.001±0.000	0.001±0.000
1Me-1EtCyclopentane	0.014±0.001	0.015±0.001	0.010±0.002	0.019±0.004	0.012±0.003	0.009±0.001	0.009±0.000	0.006±0.001	0.012±0.003	0.007±0.002
Benzene	0.506±0.042	0.532±0.012	0.491±0.098	0.544±0.103	0.457±0.091	0.412±0.035	0.426±0.008	0.404±0.081	0.445±0.085	0.375±0.075
Toluene	1.521±0.121	1.878±0.099	1.665±0.328	1.149±0.220	1.393±0.261	1.061±0.085	1.286±0.066	1.174±0.232	0.806±0.155	0.980±0.184
Ethylbenzene	0.097±0.008	0.086±0.003	0.114±0.022	0.088±0.017	0.102±0.019	0.060±0.005	0.052±0.002	0.071±0.014	0.054±0.010	0.062±0.012
o-Xylene	0.104±0.009	0.100±0.001	0.116±0.022	0.094±0.018	0.108±0.020	0.064±0.005	0.060±0.001	0.072±0.014	0.057±0.011	0.066±0.012
m-Xylene	0.289±0.024	0.282±0.005	0.329±0.064	0.248±0.047	0.298±0.056	0.177±0.015	0.169±0.003	0.203±0.040	0.152±0.029	0.183±0.034
p-Xylene	0.073±0.006	0.073±0.001	0.077±0.015	0.067±0.013	0.073±0.014	0.044±0.004	0.044±0.000	0.047±0.009	0.041±0.008	0.045±0.008
Cumene	0.003±0.000	0.003±0.000	0.004±0.001	0.003±0.001	0.003±0.001	0.002±0.000	0.002±0.000	0.002±0.000	0.002±0.000	0.002±0.000
1-Me-2-Et-benzene	0.010±0.001	0.010±0.000	0.012±0.002	0.009±0.002	0.011±0.002	0.006±0.000	0.005±0.000	0.006±0.001	0.005±0.001	0.006±0.001
1-Me-3-Et-benzene	0.035±0.003	0.033±0.000	0.039±0.008	0.032±0.006	0.037±0.007	0.019±0.002	0.018±0.000	0.021±0.004	0.017±0.003	0.020±0.004
1-Me-4-Et-benzene	0.015±0.001	0.014±0.000	0.016±0.003	0.013±0.003	0.015±0.003	0.008±0.001	0.008±0.000	0.009±0.002	0.007±0.001	0.008±0.002
123-triMe-benzene	0.007±0.001	0.007±0.000	0.007±0.001	0.007±0.001	0.007±0.001	0.004±0.000	0.004±0.000	0.004±0.001	0.004±0.001	0.004±0.001
124-TriMe-benzene	0.041±0.003	0.043±0.001	0.042±0.008	0.038±0.007	0.040±0.008	0.022±0.002	0.023±0.000	0.023±0.004	0.020±0.004	0.022±0.004
135-triMe-benzene	0.015±0.001	0.016±0.001	0.016±0.003	0.013±0.002	0.015±0.003	0.008±0.001	0.009±0.000	0.009±0.002	0.007±0.001	0.008±0.002
Propylbenzene	0.012±0.001	0.011±0.000	0.014±0.003	0.012±0.002	0.012±0.002	0.007±0.001	0.006±0.000	0.008±0.001	0.007±0.001	0.007±0.001
1,4-diethylbenzene	0.002±0.000	0.002±0.000	0.003±0.001	0.003±0.000	0.003±0.000	0.001±0.000	0.001±0.000	0.001±0.000	0.001±0.000	0.001±0.000
Ethanol	4.387±0.351	4.363±0.014	4.392±0.810	4.374±0.805	4.421±0.815	10.726±0.863	10.485±0.035	10.831±2.000	10.701±1.973	10.885±2.008
Propene	0.029±0.004	0.031±0.002	0.012±0.004	0.047±0.014	0.025±0.006	0.046±0.006	0.049±0.004	0.020±0.006	0.076±0.022	0.041±0.010
1-butene	0.077±0.010	0.052±0.004	0.048±0.014	0.142±0.033	0.067±0.016	0.094±0.012	0.062±0.005	0.059±0.017	0.173±0.040	0.082±0.019
Cis-2-butene	0.307±0.041	0.192±0.018	0.168±0.051	0.643±0.147	0.227±0.054	0.374±0.050	0.233±0.023	0.206±0.062	0.779±0.176	0.279±0.066
2-methylpropene	0.052±0.007	0.033±0.002	0.033±0.009	0.096±0.023	0.048±0.011	0.063±0.008	0.039±0.003	0.040±0.011	0.116±0.028	0.059±0.013
1-pentene	0.461±0.053	0.271±0.033	0.329±0.100	0.769±0.153	0.475±0.106	0.451±0.052	0.264±0.033	0.324±0.098	0.750±0.149	0.468±0.104
Cis-2-pentene	0.568±0.063	0.335±0.038	0.419±0.108	0.930±0.182	0.589±0.130	0.556±0.061	0.325±0.038	0.412±0.106	0.907±0.177	0.580±0.128
trans-2-pentene	1.118±0.125	0.626±0.075	0.889±0.229	1.718±0.336	1.239±0.281	1.095±0.123	0.609±0.075	0.875±0.226	1.676±0.327	1.219±0.277

2-methyl-1-butene	0.871±0.101	0.484±0.064	0.653±0.187	1.428±0.284	0.920±0.205	0.853±0.098	0.471±0.064	0.642±0.183	1.392±0.276	0.906±0.202
3-methyl-1-butene	0.185±0.024	0.097±0.017	0.147±0.054	0.292±0.060	0.203±0.047	0.181±0.023	0.095±0.017	0.144±0.053	0.284±0.058	0.200±0.047
2-methyl-2-butene	1.959±0.217	1.044±0.121	1.659±0.414	2.939±0.577	2.196±0.485	1.919±0.213	1.014±0.121	1.634±0.407	2.866±0.561	2.163±0.477
1-hexene	0.049±0.005	0.037±0.004	0.032±0.007	0.084±0.016	0.041±0.008	0.040±0.004	0.030±0.003	0.026±0.006	0.068±0.013	0.034±0.006
Cis-2-hexene	0.079±0.007	0.061±0.006	0.056±0.012	0.107±0.020	0.093±0.017	0.065±0.006	0.049±0.005	0.046±0.010	0.087±0.016	0.076±0.014
Trans-2-hexene	0.188±0.018	0.143±0.019	0.148±0.033	0.197±0.037	0.266±0.050	0.154±0.015	0.116±0.016	0.120±0.027	0.161±0.030	0.218±0.041
Cis-3-hexene	0.114±0.010	0.087±0.010	0.083±0.018	0.145±0.027	0.140±0.025	0.093±0.009	0.071±0.008	0.068±0.015	0.118±0.022	0.114±0.021
2-Me-1-pentene	0.111±0.010	0.082±0.009	0.086±0.018	0.143±0.027	0.135±0.024	0.091±0.008	0.067±0.008	0.070±0.015	0.116±0.022	0.110±0.020
4-methyl-1-pentene	0.050±0.005	0.034±0.003	0.037±0.008	0.075±0.014	0.053±0.009	0.041±0.004	0.028±0.003	0.030±0.007	0.061±0.012	0.043±0.008
2-methyl-2-pentene	0.363±0.042	0.273±0.053	0.323±0.083	0.234±0.044	0.624±0.127	0.296±0.034	0.222±0.043	0.263±0.067	0.190±0.036	0.510±0.104
C-3Me-2-pentene	0.082±0.008	0.059±0.006	0.053±0.014	0.138±0.026	0.076±0.016	0.067±0.007	0.048±0.005	0.044±0.011	0.112±0.021	0.062±0.013
T-3Me-2-pentene	0.103±0.012	0.060±0.013	0.061±0.019	0.196±0.037	0.097±0.022	0.084±0.010	0.049±0.011	0.050±0.016	0.159±0.030	0.080±0.018
C-4Me-2-pentene	0.028±0.004	0.018±0.004	0.022±0.008	0.019±0.005	0.053±0.014	0.023±0.003	0.015±0.003	0.018±0.006	0.015±0.004	0.044±0.011
T-4Me-2-pentene	0.235±0.029	0.169±0.037	0.214±0.057	0.123±0.023	0.432±0.091	0.191±0.024	0.138±0.030	0.174±0.046	0.100±0.019	0.354±0.074
2,3-dimethyl-1-butene	0.066±0.006	0.046±0.006	0.053±0.012	0.078±0.015	0.087±0.016	0.054±0.005	0.037±0.005	0.044±0.009	0.063±0.012	0.071±0.013
3,3-dimethylbutene	0.009±0.001	0.006±0.001	0.007±0.002	0.015±0.003	0.008±0.002	0.007±0.001	0.005±0.000	0.005±0.001	0.012±0.002	0.007±0.001
2,3-dimethyl-2-butene	0.047±0.005	0.034±0.005	0.039±0.009	0.045±0.008	0.070±0.013	0.038±0.004	0.028±0.004	0.032±0.007	0.036±0.007	0.057±0.011
C-1,3-pentadiene	0.009±0.001	0.006±0.001	0.007±0.002	0.015±0.003	0.009±0.002	0.009±0.001	0.006±0.001	0.007±0.002	0.014±0.003	0.009±0.002
T-1,3-pentadiene	0.017±0.002	0.010±0.001	0.014±0.004	0.027±0.005	0.019±0.004	0.017±0.002	0.010±0.001	0.013±0.004	0.026±0.005	0.019±0.004
2-Me-1,3-butadiene	0.024±0.003	0.014±0.002	0.020±0.006	0.036±0.007	0.027±0.006	0.024±0.003	0.014±0.002	0.019±0.006	0.035±0.007	0.026±0.006
1-Heptene	0.007±0.001	0.006±0.001	0.004±0.001	0.013±0.003	0.006±0.001	0.005±0.001	0.004±0.001	0.003±0.001	0.009±0.002	0.005±0.001
Trans-2-heptene	0.001±0.000	0.002±0.000	0.000±0.000	0.000±0.000	0.000±0.000	0.000±0.000	0.001±0.000	0.000±0.000	0.000±0.000	0.000±0.000
T3-Heptene	0.010±0.001	0.006±0.001	0.005±0.002	0.020±0.004	0.009±0.002	0.007±0.001	0.004±0.001	0.004±0.001	0.014±0.003	0.006±0.001
C2-Octene	0.002±0.000	0.001±0.000	0.001±0.000	0.002±0.000	0.002±0.000	0.001±0.000	0.001±0.000	0.001±0.000	0.001±0.000	0.002±0.000
Cyclopentene	0.177±0.020	0.109±0.011	0.112±0.028	0.312±0.064	0.174±0.036	0.173±0.019	0.105±0.011	0.110±0.028	0.304±0.062	0.171±0.036